Politecnico di Milano
Department of Energy

SuperGrid Institute

Master of Science Degree in Electrical Engineering-Smart Grids

Master's Degree Dissertation

AC to DC Converters for Medium Voltage Direct Current Networks with Integrated Renewable Energy Sources

Academic Supervisor:
Prof. Roberto PERINI

Industrial Supervisors:
Dr. Juan PAEZ
Dr. Piotr DWORAKOWSKI

Candidate:
Ali KHONYA

Academic Year 2020 – 2021

[Pagina lasciata intenzionalmente vuota/Page intentionally left blank]

Acknowledgment

I joined SuperGrid Institute when all the world was fighting with Covid-19. Despite, many problems including pandemie and serious finincial problems, I was very motivated to come to France and do this challenge. But my motivation was not the only factor. Another reason for insiting on doing this work was an appreciation to all the people who always supported me. I worked at SuperGrid Institute almost everyday form 8 AM to 8 PM to have an excellent outcome. I am always inspired by Nikola Tesla. Based on some sources, during his trip from Europe to the USA, most of his money was stolen on the boat ride over and he had only 4 cents (equivalent to 1.07 $ in 2021) in his pocket upon arriving there. Moreover, we know all the problems he faced in his life such as stealing his ideas. However, nothing stopped him to revolutionize electrical engineering.

I am very grateful to my industrial supervisors at SupeGrid Institute, Dr. Juan Paez and Dr. Piotr Dworakowski. They are intelligent, experienced, and always full of ideas. Since the beginning, their support was wonderful and they spent a lot of their time to help me extend my knowledge. I also wish to thank my academic supervisor, Prof. Perini for accepting my request to be my supervisor and for increasing my motivation in power electronics.

I am also very grateful to my colleagues at the Politecnico di Milano, Arastoo H. Salimi and Miad Ahmadi who always motivated me. Moreover, Many thanks to my colleagues at the SuperGrid Institue in power electronics and converter program. In these months, I learned a lot from them and they always were available to help me.

To my beloved Golnaz: my deepest gratitude. Your encouragement when the times got rough are much appreciated and duly noted. In these months, the biggest issue that I had was being far from you, however you always encouraged me significantly. I appreciate a lot my parents and sister. I never forget your continuous supports since when I was a kid. Also, to my aunts and uncles: I am very fortunate to have you as my family. Moreover, to my mother-in-law: thank you so much for always being motivating.

Finally, this work was fully dedicated to my grandfather (R.I.P.) who passed away last year. Since when I was born, he always encouraged, motivated and supported me. He is one of the strongest reasons for all of my accomplishments. I never forget you, grandfather and I always do my best to make you proud.

Abstract

The negative impacts of the increase in the temperature of the world has motivated all the sectors to move towards sustainability and energy transition. As a consequence, reduction of using fossil fuels and Increasing use of natural resources to generate electricity is essential. The higher interest in electric vehicles and higher investment on renewable energy sources integration into the electrical networks have been the a part of the response of the energy sector to this need. Hence, in the future, the consumption and generation of electricity will be significantly higher.

Due to the limited capacity of the current Alternating Current (AC) networks, an extension in the capacity of the electrical networks will be required. This can be done by implementing a parallel layer in Direct Current (DC) to the AC networks. The advantages of DC transmission allow us to accelerate energy transition more efficiently and economically. In the high voltage (HV) ranges, HVDC networks have been implemented but in medium voltage ranges, it has been mostly handled by AC. With increasing in the DC loads such as electric vehicles and interest in integrating renewable sources in this level of voltage, MVDC networks could be a feasible choice.

To interconnect the existing AC networks and the future DC networks, AC to DC conversion is needed. An in-depth study on MV AC-DC converters is necessary. In this work, a state-of-the-art review on the industrial MV AC-DC converters is done. With this review, the recommended topologies for different voltage and power ranges are proposed. Then, the trends related to MVDC networks in literature are studied. This shows the potential applications and interests related to MVDC in the researchers' insights.

In the next chapter, DC faults on MV AC-DC converter is studied. To analyze this phenomenon, a study case of an MV converter with power rating of 20 MW and DC voltage of ±10 kV is considered. The results of state-of-the-art review are beneficial to choose 3-Level Neutral Point Clamped (3-L NPC) as the recommended topology for these ratings. There are few publications on the study of faults on 2-level converters. But there is no research on fault on 3-L NPC topology. Hence, this study is very essential since 3-L NPC is a promising topology for MV converters. First, this problem is analyzed theoretically and then using MATLAB SimPowerSystem, it is verified. It is seen that fault is a serious problem for the converter diodes. This constraint and the effective parameters are analyzed deeply.

In the final chapter, an issue with the integration of renewable energy sources into the MVDC networks is analyzed. This phenomenon is an over-voltage that happens as a consequence of blocking AC-DC converters in an MVDC network with integrated renewable energy sources. It is noticed that this problem also exists in HV levels but in medium voltage ranges, it is relatively higher. A state-space model is proposed to analyze this problem in the networks with any number of renewable energy sources with less computational effort. Finally, a solution to limit this problem is proposed.

Keywords: MVDC, Fault, NPC, RES Integration

Astratta

L'impatto negativo dell'aumento della temperatura mondialeha motivato tutti i settori a muoversi verso la sostenibilità e la transizione energetica. Di conseguenza, la riduzione dell'uso di combustibili fossili e l'aumento dell'uso di risorse rinnovabiliper generare elettricità è essenziale. Il maggiore interesse per i veicoli elettrici e i maggiori investimenti sull'integrazione delle fonti di energia rinnovabile nelle reti elettriche rappresentano una parte della risposta del settore energetico a questa necessità. Di conseguenza l'entitá del consumo e della generazione é costretta a subire un aumento sostanziale negli anni a venire.

A causa della capacità limitata delle attuali reti a corrente alternata (AC), sarà necessaria un'estensione della capacità delle reti elettriche. Questo può essere fatto implementando uno strato in corrente continua (DC) parallelo alle reti AC. I vantaggi della trasmissione in CC permettono di accelerare la transizione energetica in modo più efficiente ed economico. Nelle gamme di alta tensione (HV), le reti HVDC sono giá state implementate a livello globale, ma nelle gamme di media tensione, la trasmissione energetica principalmente gestita in AC. Con l'aumento dei carichi DC come i veicoli elettrici e l'interesse ad integrare le fonti rinnovabili in questo livello di tensione, le reti MVDC potrebbero essere una scelta interessante.

Per interconnettere le reti AC esistenti e le future reti DC, è necessaria una conversione da AC a DC e viceversa. Conseguentemente, é necessario uno studio approfondito sui convertitori MV AC-DC. In questo lavoro, é presentata una revisione dello stato dell'arte sui convertitori industriali MV AC-DC. In seguito, vengono proposte le topologie suggerite secondo i diversi range di tensione e potenza. Infine, vengono studiate le tendenze relative alle reti MVDC in letteratura. Questo mostra le potenziali applicazioni e gli interessi legati alla MVDC nelle intuizioni dei ricercatori.

Questo lavoro affronta anche lo studio dei guasti DC nelle reti MVDC e viene analizzato l'impatto sul convertitore AC-DC. Per analizzare questo fenomeno, viene considerato il caso di un convertitore MV con una potenza di 20 MW e una tensione DC di ±10 kV. La topologia del convertitore analizzato è un convertitore NPC (Natural Point Clamped) a 3 livelli. In primo luogo, questo problema é analizzato teoricamente e successivamente é sviluppato un modello di simulazione grazie aMATLAB SimPowerSystem. Cio' che risulta di estremo interesse é l'individuazione di una situazione critica per i diodi del convertitori durante il tmepo di guasto. La valutazione e lo studio di questo fenomeno sono presentati in questa tesi insieme alla quantifcazione ed identificazione dei parametri principali coinvolti in tale condizione di funzionamento.

Infine, vengono analizzate le sovratensioni transitorie nelle reti MVDC. Questo transitorio avviene come conseguenza del blocco dei convertitori AC-DC in una rete MVDC con fonti di energia rinnovabili integrate. Si nota che questo problema esiste anche nei livelli HV, ma nelle applicazioni di media tensione, è relativamente più alto. Infine, viene proposto un modello state-space per analizzare questo problema nelle reti con qualsiasi numero di fonti di energia rinnovabile ed una soluzione per limitare la sovratensione.

Parole chiave: MVDC, guasto, NPC, integrazione FER

Table of Contents

Chapter 1

Introduction

1.1. Sustainability and Energy Transition Acceleration by DC Networks

In the recent years, human activity is increasing the amount of CO2 (Carbon Dioxide) in the atmosphere and this has resulted in significant and harmful impacts, from stronger, more frequent storms, to drought, sea level rise, and extinction [1][2]. The parameter CO2E is the amount of carbon dioxide required to produce an equivalent amount of warming. Burning natural gas for electricity releases between 0.27 and 0.91 kg of carbon dioxide equivalent per kilowatt-hour (CO2E/kWh). Coal also emits between 0.64 and 1.63 kg of CO2E/kWh [3].

These high amounts of CO2 emission by conventional electricity generators have motivated the energy sector to introduce a new type of energy sources which are more sustainable with the environment [1]. These sources which are used to produce electricity from natural clean sources which stand against using fossil fuels are called renewable energy sources. Wind, solar, hydroelectric, and geothermal are the most important renewable energy sources [4]. In terms of CO2 emission, wind is responsible for only 0.009 to 0.018 kg of CO2E/kWh on a life-cycle basis; solar 0.032 to 0.091 kg of CO2E/kWh, geothermal 0.045 to 0.091 kg of CO2E/kWh, and hydroelectric between 0.045 and 0.227 kg of CO2E/kWh [3]. Between these sources, currently, hydro power is the most popular source and due to the reducing trend of Levelized Cost of Energy (LCOE) of wind and solar power [4] [5], they are becoming more popular. Moreover, there are incentives on the production of renewable energy by governments that motivate also for an energy transition [6]. Overall, economical aspects of renewable sources (higher rate of return, lower costs, and the governmental incentives) is the other effective parameter which has made them attractive for energy suppliers [3] [7].

Due to the above-mentioned facts, currently, there is a trend in the world which is called “energy transition” and it refers to the global shift from conventional fossil fuel-based energy sources to renewable energy sources [8]. In the recent decades, the integration of renewable energy sources into the networks has been one of the most popular subject of multiple industrial or research works. Several issues have been addressed but there are plenty of other issues which must be analyzed to accelerate the energy transition. The ultimate goal is to develop a 100% Renewable Energy Sources) RES-based energy production by electrification of the energy sectors to decrease CO2 emissions [9].

The trend of generating/consuming electricity is changing very fast and ‘the future is electric’ [10]. As can be seen, nowadays, in the car industry, manufacturers are replacing traditional cars with electric vehicles (expected growth of 40.7% by 2027) [11], the interest in the rooftop mounted PV systems has been significantly increased (74% of the installed PV generation capacity in the U.S. in 2008) [12], there are higher number of investors on the renewable energy sources [13], and generally speaking, low-carbon applications is a top subject for industrial and research works. These are all representing the more intensive using of electricity in the near future. But the current energy networks are not capable of this energy transition and the capacity of the networks must be increased [14]. Moreover, the expansion of RES requires the improvements in the electric networks. Hence, there are two solutions, traditional way with improving current AC networks (for example by installing new lines) or the modern way by adding a new layer to the existing networks – the direct current (DC) -network [15].

To accelerate energy transition, DC networks will be needed [15] and to interconnect the current AC networks and the DC networks, AC to DC converters are needed. AC-DC converters are well-known in the low-voltage applications for example their usage in electric vehicles charging infrastructures, household electricity generation by PV panels, motor drives and traction drives. Additionally, in the high-voltage applications in for example for integration of wind power plants, AC-DC converters have been very popular [16][17][18][19]. But there has been limited applications of MVDC networks until now (for example on ships [20]) and this voltage range has been supplied mostly by AC system. Therefore, taking into account the potential importance of MVDC networks for the future of electrical systems, the AC-DC converters in the medium-voltage applications need an in-depth study.

In this master's thesis work, the main objective is analysis of AC-DC converters which can be used in the networks with the integrated renewable energy sources (RES) in medium voltage level.

1.2. Scope of the work

The first chapter is allocated to the importance of DC transmission system and its advantages over AC systems. The topologies and structures for implementing DC networks are studied. In the next two chapters, a state-of-the-art review on industrial work and literature related to MVDC technologies are explained. From this work, the design recommendations for medium-voltage converters will be identified and the analysis of literature will help detect the potential applications of MVDC networks. In chapter 5, one of the common issues which an AC-DC converter faces will be studied. DC faults are the phenomena which AC-DC converters must be able of deal with, so this problem will be analyzed and verified in a study case by simulation in MATLAB Simulink using SimPowerSystems tool. The design of study case used to analyze MVDC networks faults is based in the results of state-of-the-art review in chapters 3 and 4. Finally, an over-voltage problem which occurs in MVDC networks will be studied; the reasons will be explained in detail, it will be simulated considering a study case in MATLAB SimPowerSystem. To analyze this phenomenon with less computational effort, a mathematical model based on state-space modelling is proposed and as a benefit of this model, a possible solution is analyzed. Finally, conclusions and novelties of this work are shown in final chapter and some interesting perspectives are proposed.

Chapter 2

DC Transmission System

2.1. Background – The War of Currents

Direct current was produced in 1800 by Italian physicist Alessandro Volta's battery, his Voltaic pile [21]. French physicist André-Marie Ampère conjectured that current travelled in one direction from positive potential to negative potential [21]. The wide spread use of low voltage direct current for indoor electric lighting in business and homes after inventor Thomas Edison launched his incandescent bulb based electric "utility" in 1882 [21] [22]. The direct current and Thomas Edison were the winners of the electricity market until Nikola Tesla, arrives in the USA.

At that time, Tesla could receive a patent for his alternating current (AC) induction motor, then George Westinghouse, inventor and industrialist, bought Tesla's patents and commercialized it [23]. By raising attentions in AC system, a battle between Thomas Edison and Nikola Tesla on the AC and DC currents occurred which was named "The War of Currents".

Despite all the efforts of Edison, because of the significant advantages of alternating current over direct current in using transformers to raise and lower voltages to allow much longer transmission distances, direct current was replaced over the next few decades by alternating current in power delivery. The war of currents is still present but today, DC networks are more like a complement for AC networks rather than a rival. As it was mentioned before, DC networks will be useful for increasing capacity of the existing networks to have a faster and smoother energy transition and there are unbeatable benefits for DC networks representing the necessity of these networks for the future of electrical systems. These benefits are explained in the next section. The goal of this work is to enable such DC systems in medium-voltage level as there have been a lot of works in high-voltage and low-voltage applications of DC networks.

2.2. DC Transmission Advantages over AC Transmission

It was explained that to accelerate energy transition, a parallel layer in DC will be needed. In this section, the advantages of DC networks over AC networks are explained. The major differences between DC and AC networks are explained in following.

Due to the changing in amplitude of AC current, the reactive elements of the network consumes a part of the apparent power as reactive power. This causes a reduction in power factor (PF). While in DC transmission, due to the constant amplitude of current, no reactive power will be lost in the reactive elements of the network, so the power factor is always unity (PF=1).

In addition to the DC resistance of the conductors, there is an equivalent AC resistance which refers to the tendency of current to pass through the surface (skin) of conductor. This is called 'Skin Effect' which occurs due to the changing magnetic field around conductors with AC current [24]. This phenomena makes the current density higher in the outer layer of conductor. As a consequent, the efficient cross-section area of conductor decreases and the total resistance of the conductor slightly increases [25]. With DC, there is a magnetic field around the conductor as well but since it is not changing, the flow of current through the whole cross-section is uniform so the DC current in the

core of inductor is the same as the outer surface. Therefore, there is no Skin Effect and loss due to this phenomena in the conductors with DC current [25].

This is also the same for a similar so called 'Proximity Effect' phenomena. When two conductors are close, their magnetic fields interact with each other. Due to this interaction, the currents flowing through the conductors are affected. With AC, due to the changing magnetic field, the current is not uniformly distributed and this causes the increment in the effective resistance and consequently higher loss. While in DC, current is distributed uniformly, so this effect is absent [26].

DC transmission requires fewer conductors than AC transmission - 2 conductors per DC circuit whereas three conductors per 3 phase AC circuit. DC lines have the ability of transmitting the same power with two conductors as AC lines with three conductors [27]. As a consequent, DC transmission requires fewer infrastructure and this is also another reason to reduce the costs [27]. Moreover, the land coverage of DC transmission system and the associated cost are less [27] [29]. This will reduce the visual impact and save the land for future extension of the network.

Overall from costs point of view, considering the costs of transmission infrastructure and converter station, a so called 'Break-even Distance' parameter can be considered. This parameter presents the distance which costs of AC and DC transmission for a project based on voltage/power requirements become equal. For distances shorter than break-even distance, AC is a more economical choice and in opposite, for transmitting power to a distance more that break-even distance, DC should be preferred. Figure 1 shows the costs of DC and AC transmission system and the visual definition of break-even distance [27] [31]. This figure shows that in high distances, DC is a preferable solution. Depending on different parameters such as country-specific cost elements, interest rate, losses, etc., break-even distance is in the range of 500-800 kilometers (km) for the HVDC transmission when using overhead lines [27] [32] and around 100 km when using cables. In [22], a list of some of HVDC projects since 1954 is presented which shows the distances considering voltage/power requirements where the DC transmission was preferred. For medium voltage ranges, DC can be also a cost-effective choice, and due to the lower voltage/power for MVDC networks, the break-even distance will be probably shorter in the range of tens of kilometers.

For losses, it is very similar to the costs comparison. A figure like Figure 1 is present for the comparison of losses between DC and AC transmissions, however the break-even distance for losses can be longer than break-even distance for costs [27]. For medium voltage ranges, to find the break-even distance from losses point of view based on the voltage/power requirements, an analysis is done in [36]. It presents that for this range, the break-even distance considering losses is in the range of less than 10 km and some tens of kilometers depending on the voltage and power ratings [36].

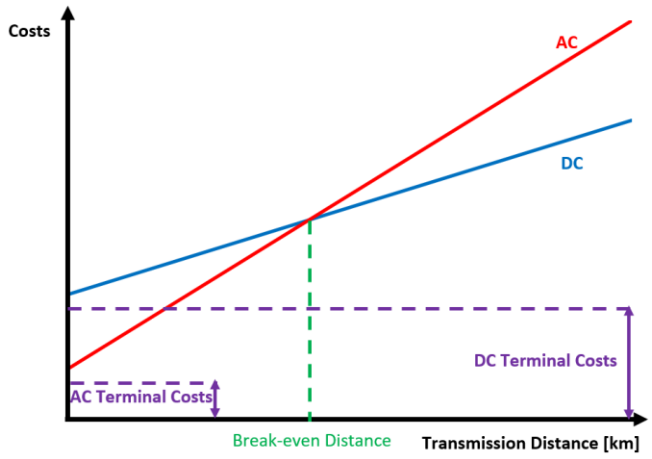

Figure 1 : Investment Costs Comparison between DC and AC

There are some other advantages which are offered by DC systems such as more controllability, stability, non-existence of Ferranti effect, and no physical restriction limiting distance [22] [27] [31]. However, there are some drawbacks related to DC transmission such as high costs of converters and complexity of multi-terminal network implementation [27], and also the challenges related to DC protection systems [28].

Due to the advantages of DC transmission system, in 1954, high-voltage direct current transmission was developed commercially with mercury-arc valves-based converters in Gotland I HVDC project in Sweden [22], and is now a feasible option instead of long-distance high voltage alternating current systems [27] [29].

Currently, the number of DC distribution systems is very few and there are almost no DC distribution systems in operation and only high voltage DC transmission systems or low voltage DC pilot projects exist. It is expected that in the near future, the LVDC distribution systems will be more focused and implemented [51]. This is also the same for MVDC distribution systems. In the near future, with increasing use of DC power in for example increasing electric vehicles, and large-scale integration of renewable energy sources into the networks, it is expected to focus more on DC networks. Therefore, the use of DC energy networks will not be limited to only point to point power transmission and the DC networks will play a vital role in the future of electrical networks [51].

2.3. The Motivation to Study MVDC Networks

In previous section, the advantages of DC transmission to AC transmission were explained. These advantages can include all the voltage levels including medium voltage. The importance of DC transmission is significant for the energy transition. Thus, there have been multiple HVDC projects [22]. At significantly lower power and voltage levels, MVDC networks seem to offer promising advantages for a decentralized application [52]. But the medium voltage level has been mostly handled by AC so far and for distribution system, it is still mostly a research topic [51] [52]. For the networks of the future, there may be potential interests in the MVDC networks [51]. In [51], a survey is presented which shows the increasing interest in growth of DC loads (electric vehicles charging stations for example) and then interconnecting distributed generation (DG) and energy storages. It can be observed that MVDC networks are capable of providing this access more efficiently and also, developing MVDC networks with wind energy, development of electric vehicles, and DC load market demand are the additional driving forces [51][54]. Moreover, recently, there has been an interest in integrating offshore wind farms with MVDC networks [30]. The schematic of current electrical networks is shown in Figure 2 and it is expected that by operating medium voltage level in DC, the schematic of electrical networks will become like Figure 3.

Now, despite the strong motivations behind MVDC networks in the distribution level, their use may make operational, safety, and reliability issues including reverse power flow in radial distribution networks or uncontrolled power flow in meshed distribution networks [51], and difficulties associated to the protection of those systems. This shows the necessity of this study.

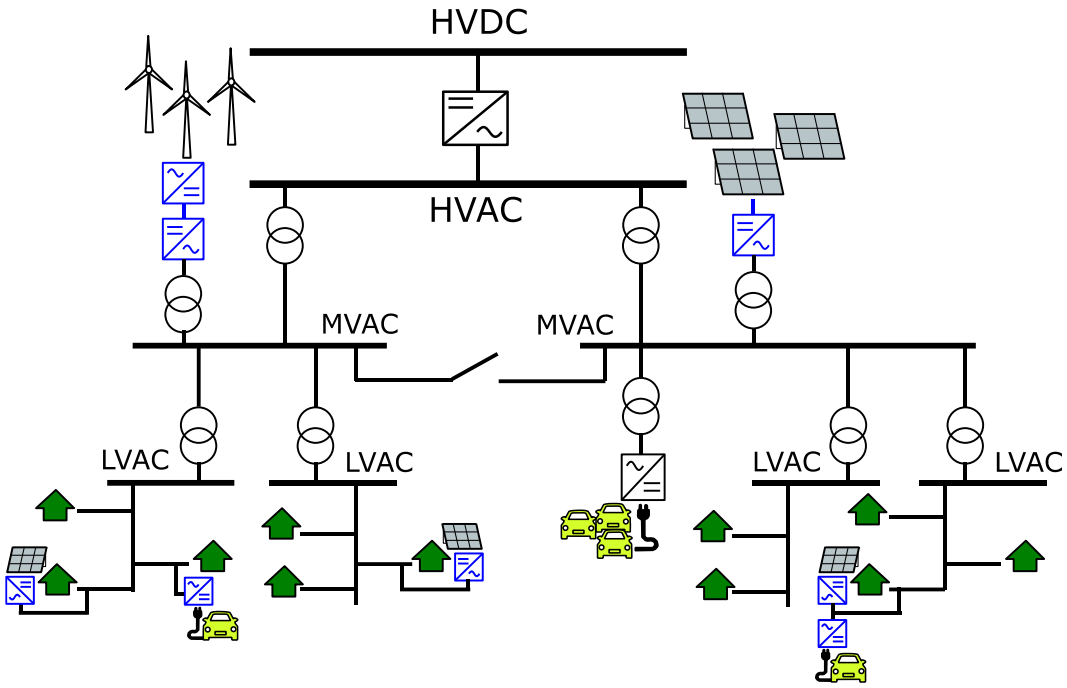

Figure 2 : The Current Electrical Grids with MVAC Networks

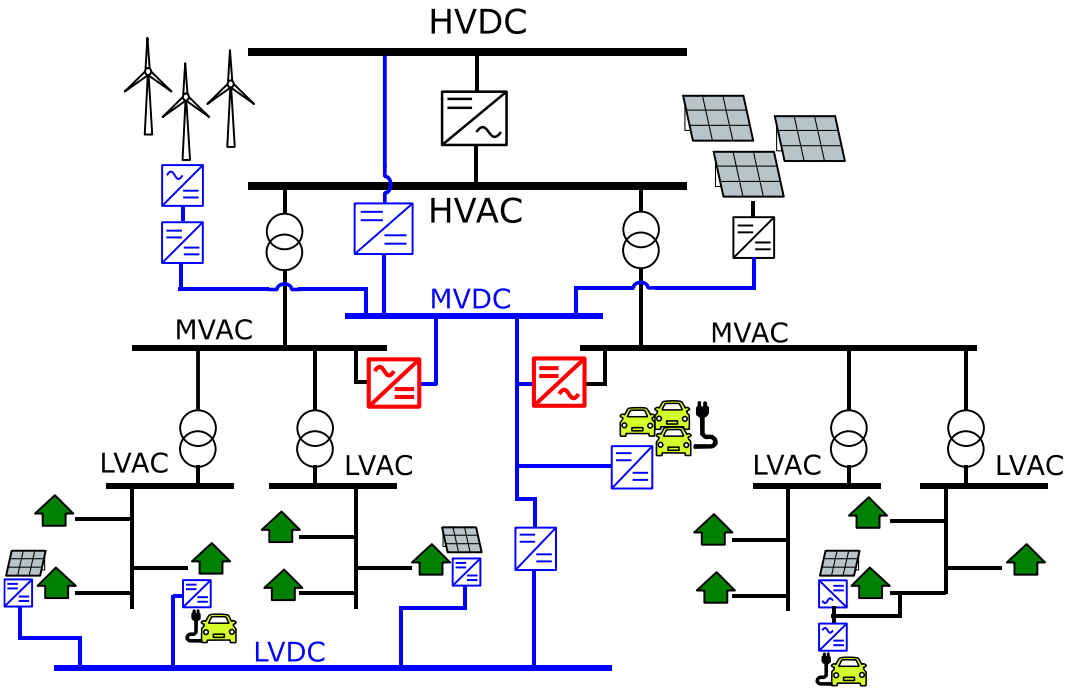

Figure 3 : The Future of Electrical Grids with MVDC Networks

2.4. Architectures of DC Networks

There are different architectures to transmit power in the DC systems. In each architecture, the connection between two points in the network can have different schemes. In the following, first, the general architectures are explained and then, the different line schemes between points are described in Section 2.5.

Mainly, there are two structures for the DC networks: radial structure and meshed structure [51].

2.4.1. Radial Structure

In this structure, there is only one path between two nodes (DC or AC). The DC side may be supplied by renewable energy sources or other DC or AC networks through power converters. This structure is shown in Figure 4. Point to point transmission which has been used in particularly HVDC networks is the basic radial structure.

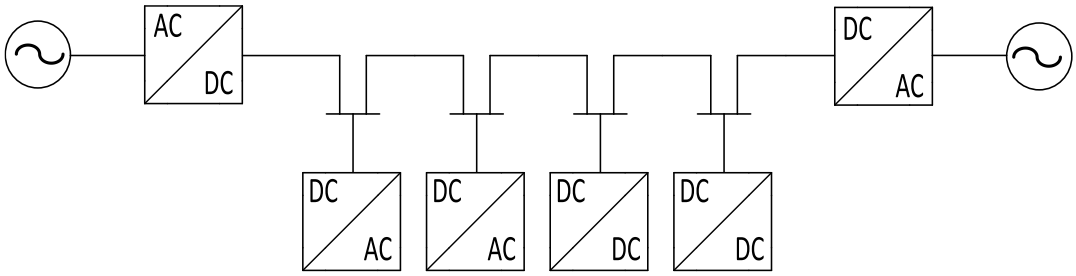

Figure 4 : The Radial Structure of the DC Networks

2.4.2. Meshed Structure

In a meshed structure, there are two or more paths between two nodes of the structure (DC or AC). This structure is more reliable than the radial structure as losing one line will not necessarily impose losing the supply of AC grid. Figure 5 illustrates this structure.

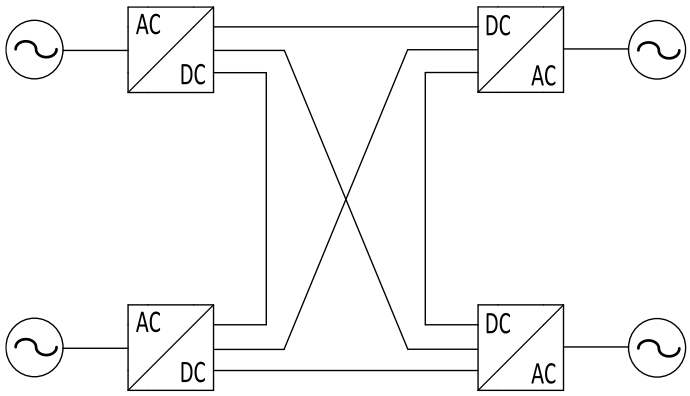

Figure 5 : The Meshed Structure of the DC Networks

2.5. Line Topologies

For DC transmission, there are some line configurations and choosing a scheme depends on various factors such as voltage and power rating, the reliability requirements, cost of the project, and the specific defined regulations for each project [34]. The differences between these transmission schemes are based on the grounding, and configuration of DC poles. These topologies have been used in the HVDC transmission but they can be potentially used for MVDC voltage levels [51]. The main topologies are explained in following [34] [35].

2.5.1. Asymmetrical Monopole

In this scheme, DC line is supplied form two side by an AC-DC converter which is connected to an AC grid. One pole (positive pole) is rated at the nominal DC voltage and the negative pole (returning path) of the converters are grounded. This earthing can be done by simply connecting the negative pole to the ground at the terminal of converters which is shown in Figure 6 or this can be done by a using a metallic return connected to ground. The latter is shown in Figure 7 and in this approach, the metallic return will have a lower voltage specification compared to the main DC line.

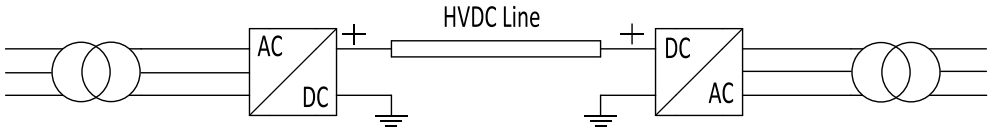

Figure 6 : The Asymmetrical Monopole Scheme with Solid Earthing Return

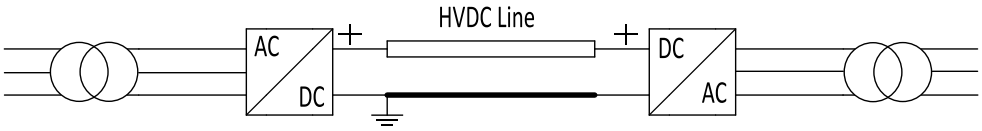

Figure 7 : The Asymmetrical Monopole Scheme with Metallic Earthing Return

2.5.2. Symmetrical Monopole

In this scheme the voltage is shared between both of the DC poles and these poles will be isolated from the ground. So, this configuration includes two DC lines for two poles and these DC lines have the same insulation constraints. This scheme is shown in Figure 8.

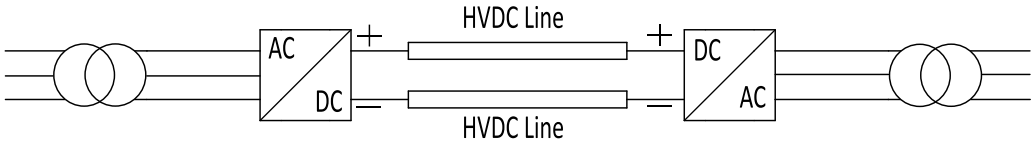

Figure 8 : The Symmetrical Monopole Scheme

2.5.3. Bipolar

This scheme is a combination of two asymmetrical monopoles. One DC pole of the two converter stations is connected to each other and for the other DC pole, it can be directly connected to earth or using a metallic return similar to the asymmetrical monopole scheme. Both bipolar configurations are shown Figure 9 in and Figure 10, respectively.

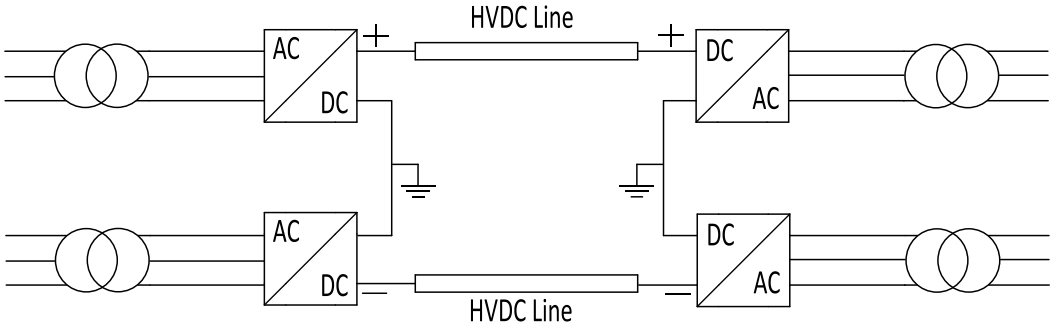

Figure 9 : The Bipolar Scheme with Solid Earthing Return

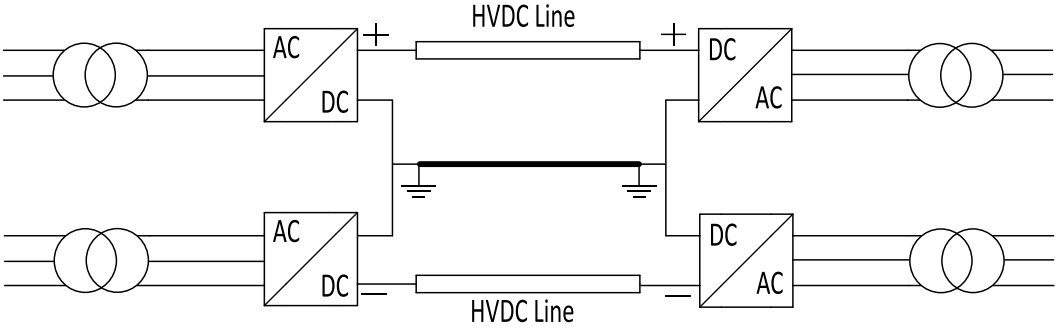

Figure 10 : The Bipolar Scheme with Metallic Earthing Return

Chapter 3

Power Electronics Converters in MV Applications

3.1. Voltage Source Converter and Current Source Converter

The potential interest in MVDC networks was explained in the previous chapter. In Figure 3, it was shown that the main element of the network to interface MVDC system is the AC-DC converter. It is needed to study the power converters used in the medium voltage level. There are mainly two types of converter used for AC to DC conversion: voltage source converters (VSCs) and Line Commutated Converters (LCCs). The main difference between these converters is the switch technology which is used to implement them. VSCs use self-commutating switches such as insulated gate bipolar transistors (IGBTs) which gives the possibility of high-frequency applications (over 1 kHz) with pulse width modulation (PWM) method while LCCs use thyristors which need a high synchronous voltage source to be triggered. The first generation of DC transmission systems used the LCCs because of the available switches at that time (thyristors and mercury valves) but by developing and improving IGBTs over decades and due to the advantages of VSCs [37], this type of converters are mostly preferred. However, some advantages of LCC HVDC schemes over VSC HVDC are [37]:

- Availability of thyristors in higher voltages (6-10 kV)
- Excellent over-current capability of thyristors
- Thyristors lower on-state voltage drop, cost, and less conduction losses comparing to IGBTs
- More mature systems
- Lower overall costs comparing to VSC HVDC
- Better response to DC faults

Despite these advantages, there are more promising advantages of VSCs in comparison to LCCs. Some of these advantages are as following [37]:

- VSCs have the capability of independent control of active and reactive power.
- Using PWM technique with the IGBTs allows to do the switching in higher frequencies. Considering this advantage, VSCs need much smaller sizes of filters in comparison to LCCs.
- Reversing of power flow is possible in a short time (50-100 ms) while in LCC, it has more constraints.
- Better response to AC faults
- In comparison to VSC, LCC injects significant low-order harmonics which requires large-scale passive filters installation which takes a lot of space.
- VSC needs smaller passive filters for reactive power compensation comparing to LCC.
- VSCs provide the possibility if multi-terminal systems due to easy control of the power transfer.

These important advantages of VSCs over LCCs have made VSCs more appealing since 1997 [37]. Moreover, LCCs more suitable for high voltage and high power DC applications while VSCs can be used in different voltage levels [37]. Moreover, with VSC, the power flow on the DC side can be

controlled without inverting the voltage polarity of the line [37]. All of These features make VSC a more promising converter type for medium voltage DC networks in comparison to LCCs.

3.2. Survey of Voltage Source Converter (VSC) Topologies

Voltage source converters can have different topologies. These topologies can be sorted in two general categories, two-level converter and multi-level converter. Depending on the desired number of output voltage levels, each topology needs a number of semiconductor devices and valves (a number of switches connected in series).

3.2.1. Two-Level Converter

The 2-L converter is probably the mostly-used topology in the industrial purposes [38]. This converter is made up of at least one leg and the most common 2-L VSC has three legs (phases). In each leg, there are two valves of switches. In low power applications, each leg needs one IGBT valve since a wide range of IGBTs in the range of 650 V – 6500 V is available [38]. While, in higher voltage applications, a series of IGBTs per valve is needed. The schematic of a 3-phase 2-L VSC is shown in Figure 11.

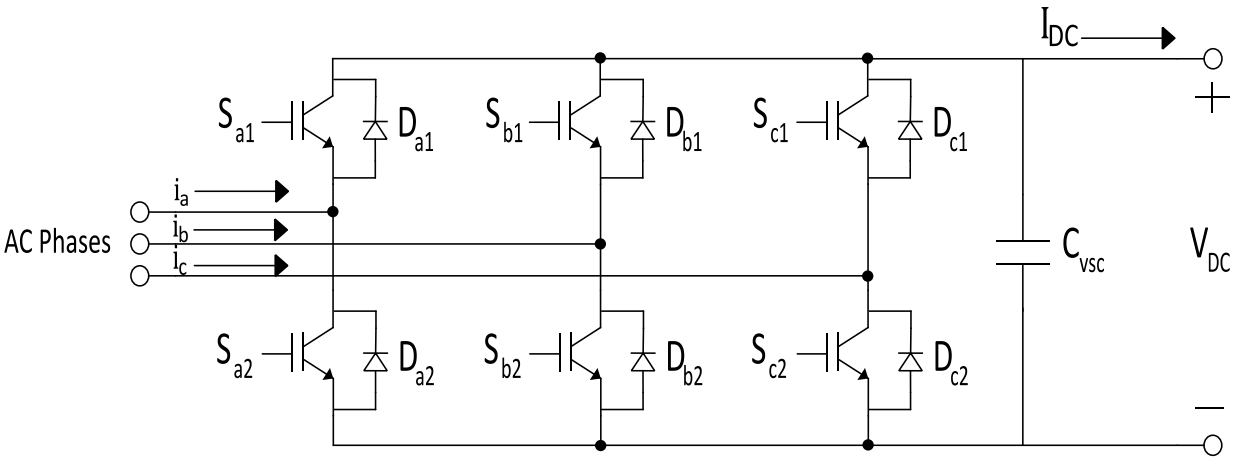

Figure 11 : The Schematic of the Active Two-Level Bridge Rectifier

This topology has some features such as following [37]:

- This topology is mostly applied for low voltage/power ratings (for example 1 kV, 1 MW)
- It requires a simple construction and consequently simple control technique.
- It uses the minimum number of switches in comparison to other topologies.
- Because of the high switching losses, the switching frequency is limited to around 1.5 kHz. This also imposes installing large AC filters.
- Poor DC fault ride-through
- Two-level converters have higher dv/dt stresses, electromagnetic interference, and lower efficiency [40].
- The insufficient blocking voltage of semiconductor switches makes this topology not very suitable for MV and HV applications. In this topology, the rated voltage of each switch must be greater than DC pole to pole and for example for having a 30 kV medium voltage DC grid,

this value will be minimum 30 kV while in the existing switches, a switch can withstand 6.5 kV as a maximum amount. This is one of the motivations to design multi-level topologies.

3.2.2. Neutral Point Clamped (NPC) Converter

In 1979, the first Pulse-Width Modulation (PWM) NPC converter was invented [39] [43]. This topology is now a popular topology for industrial applications in AC drives [43].In comparison, to 2-level topology, NPC the advantage of required lower blocking voltage for the IGBTs. Moreover, the harmonics generated by this topology is lower comparing to 2-level topology [38] [39]. Figure 12 shows the schematic of a 3-level 3-phase neutral point clamped converter.

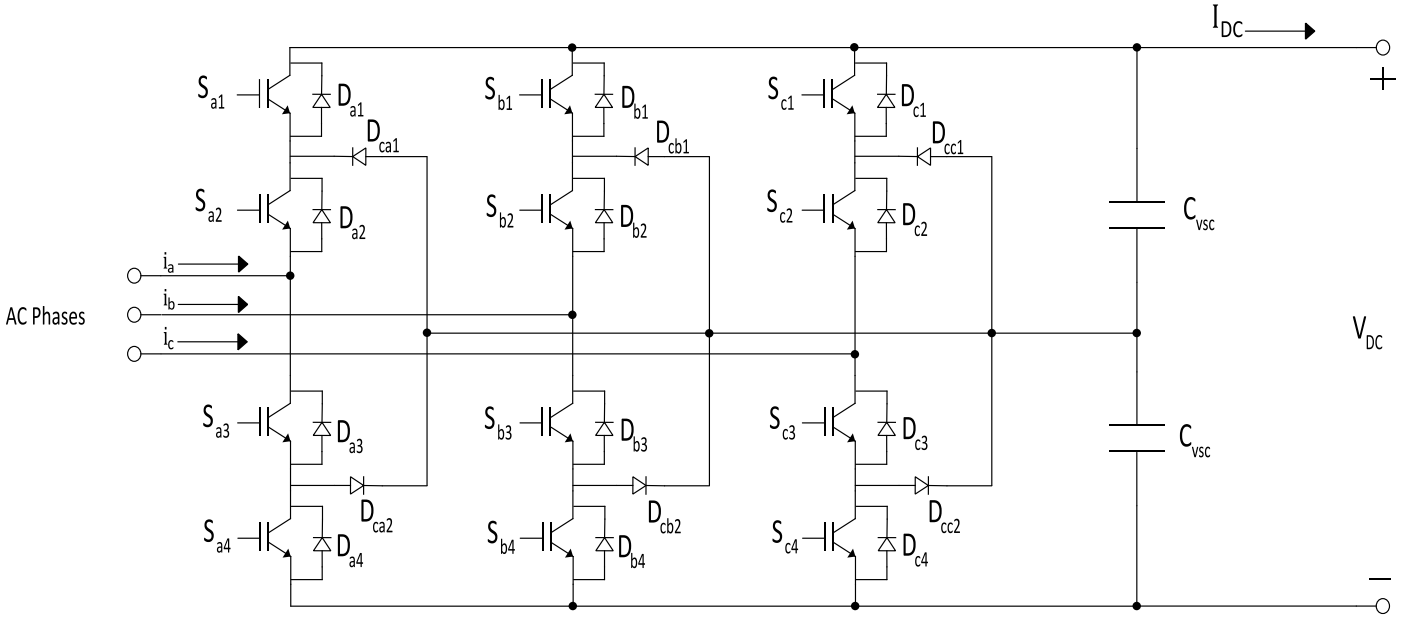

Figure 12 : The Schematic of a 3-Level Neutral Point Diode Clamped (NPC) Converter

An *n*-level NPC converter requires *n-1* DC capacitors, *2n-2* switches per phase, and *(n-1)(n-2)* clamping diodes *(n-1)* diodes per clamping point pairs) per phase and its output phase and line voltages have n and *2n-1* levels, respectively. For example, a 3-L NPC topology is composed of 4 IGBT valves per leg. This topology has some special features such as [41]:

- Multiple clamping points, voltage imbalance on the DC capacitors, implementation complexity of higher level NPC converters, and asymmetrical power loss distribution among semiconductor devices have restricted NPC topology to only 3 and 5-level configurations.
- As a comparison to have a pole to pole DC voltage of Vdc, with two-level converter, the voltage rating of each switch must be Vdc, while for 3-L NPC, each switch must withstand Vdc/2 in the nominal condition.

To enhance the voltage synthesis in an NPC converter (diode-clamped), clamping can be done by capacitors. This capacitors are called Flying Capacitors (FC) [42]. For the first time, ALSTOM used this topology in its ALSPA VDM6000 AC drive in 1990s [43].However, Flying Capacitors (FCs) might impose some practical constraints and additional costs [43]. Moreover, to overcome the disadvantage of uneven power loss distribution among semiconductors, clamping neutral points can be done by adding antiparallel switches such as IGBTs or IGCTs. This topology is called Active Neutral Point Clamped (ANPC) [43] [45]. The PCS 8000 AC drive manufactured by ABB uses this

topology [43] [46]. Due to the mentioned advantages of FC-based and ANPC converters, a combination of these two gives more robustness (from ANPC) and flexibility (from FC-based topology) [43]. As an example, ABB ACS2000 uses FC-based ANPC topology [43] [47].

3.2.3. Cascaded H-Bridge (CHB)

This topology is implemented by cascading some single phase modules [42]. Each of these bridge modules generates three voltage levels of *+Vdc*, 0, and *–Vdc*. This is made by connecting DC capacitors to the AC side via four semiconductor switches. Figure 13 shows a phase (leg) of this topology with *n* bridges.

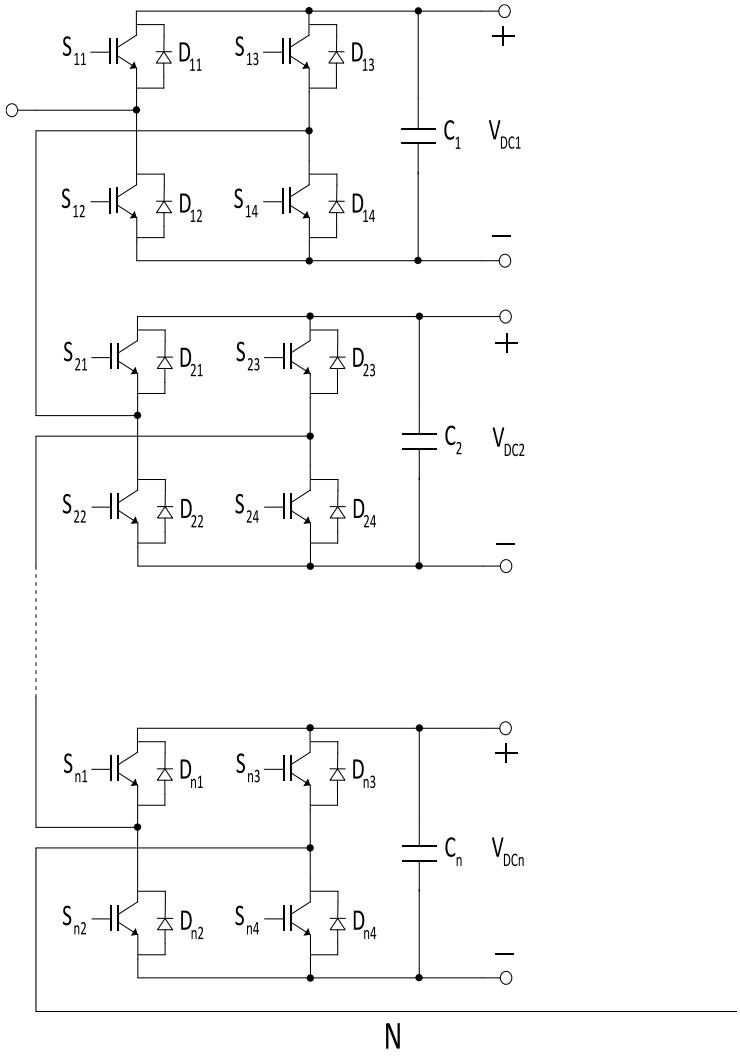

Figure 13 : The Schematic of a leg of the Cascaded H-Bridge Converter with n Bridges

Typically, for producing an *n*-level output waveform, *(n-1)/2* number of bridges are needed. Some of the features of this topology are [41]:

- It needs the minimum number of components comparing to other topologies for the same voltage level.
- It does not require any additional diodes or floating capacitors.
- The major drawback of this topology lies in the DC sources that for DC to AC conversion, it requires n separate DC sources per phase.

3.2.4. Modular Multilevel Converter (MMC)

MMC was proposed by Marquardt in 2003 [48]. Each leg of this converter consists of two arms and each arm includes a series connection of sub-modules (SMs) and an inductor (L_{arm}). Figure 14 shows the schematic of a 3-phase modular multilevel converter (MMC) with N number of sub-modules (SM). MMC is a promising alternative to conventional diode-clamped multi-level converters in medium/high voltage applications [37]. With the advantages of this topology such as flexibility of design, redundancy, lower harmonic contents and efficiency enhancement, it is expected that this topology is preferred in higher voltage applications [37] [49].

Depending on the requirements, each sub-module can have two configurations of half-bridge or full-bridge. The former is shown in Figure 16 and the latter in Figure 15.

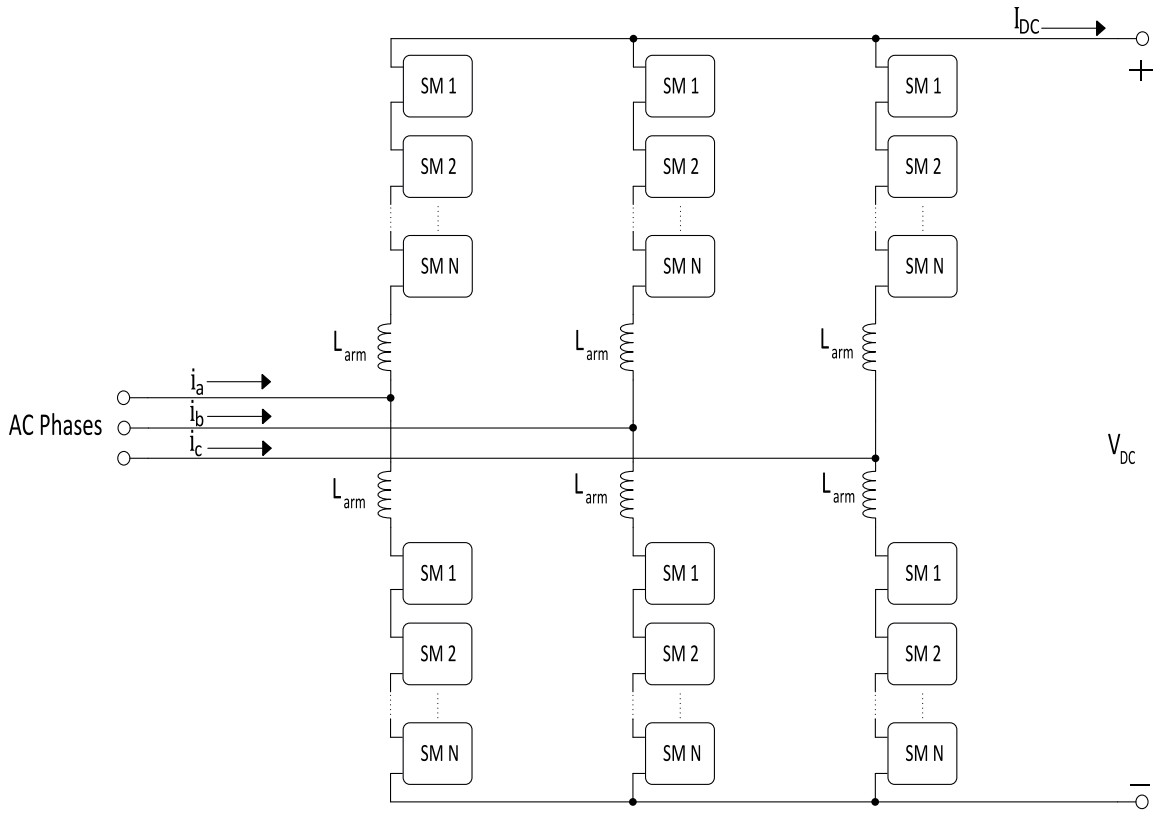

Figure 14 : The Schematic of a Modular Multilevel Converter (MMC)

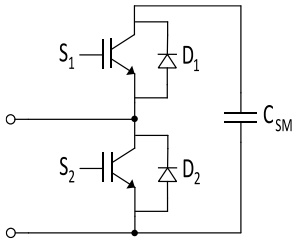

Figure 16 : Sub-module with Half-Bridge Configuration

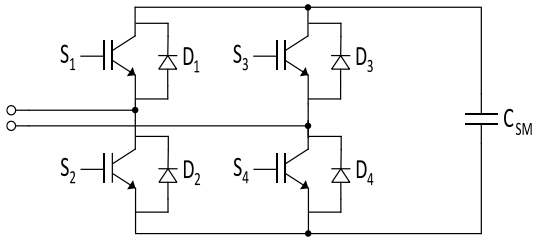

Figure 15 : Sub-module with Full-Bridge Configuration

In MMC with half-bridge sub-modules, each SM produces two voltage levels, *+Vdc* and 0. With full-bridge sub-modules, a third level, *-Vdc* can also be generated. This topology offers higher levels of voltage and theoretically, there is no limit for the number of cells and consequently number of levels. Moreover, with the increase in number of sub-modules, the requirement for filters will be waived as the harmonic contents become lower. This is a remarkable advantage over other topologies [37], [41]. There is also an important advantage of MMC with full-bridge sub-modules which improves the performance of converter during DC faults. However, using this configuration requires doubled number of semiconductor components and this increases semiconductor power losses and costs in comparison to the MMC with half-bridge sub-modules [50].

3.3. Existing AC-DC Converters in MV Applications

The AC to DC converters used today in medium voltage level can be found directly in the MVDC projects which have been implemented. Some of these projects which have been officially published can be found in the CIGRE technical brochure on medium voltage direct current (MVDC) grid feasibility study [51]. As an example, Angle DC project, under construction in the UK, is one of the most recent MVDC projects and it transforms power from 33 kV AC grid with conversion to a ±27 kVdc [53] [54].

The main problem to analyze the AC-DC converters used in the implemented MVDC projects is the lack of sufficient and reliable information related to them as the detail of most of these projects are not published. This shows that to find the converters used in MV applications, it is needed to look for MV converters in the equipment which have already equipped with the AC to DC conversion and operate in medium voltage. These equipment are:

- Medium Voltage AC Drives
- Static Synchronous Compensator (STATCOM)

To find the applied design in the mentioned equipment, several AC drives and STATCOMs from different manufacturers were analyzed. The results of this analysis will be explained from different points of view.

3.3.1. AC Drives

AC drive is an equipment used to control the speed of an AC motor by changing the frequency of the supplied voltage. So, as the frequency of electrical grid is constant, an AC drive converts AC voltage to DC and then finally, uses a DC to AC inverter to recreate AC voltage. As an example, the schematic of a typical AC drive is shown in Figure 17. We observe that in this conversion chain, the red part shown in this figure is a DC-AC inverter. If the motor is at medium voltage level, it can be proposed to adopt this DC-AC inverter to a grid application.

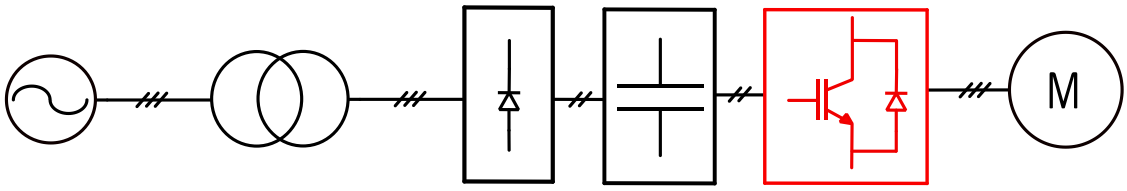

Figure 17 : The Single Line Diagram of a Typical AC Drive

Figure 18 shows a chart that summarizes the medium voltage AC drives designed by different manufacturers. The chart organizes the different converters by voltage and power ratings. Using this chart as a base, the main topologies used by the manufacturers can be presented as well as the switch technologies which are used on each case. These analyses are presented in Figure 19 and in Figure 20.

Figure 19 shows that the preferred topology to design an AC-DC converter in industry is dependent on the required voltage and power ratings. This analysis shows that the NPC topology is used up to 10 kV and 32 MW. This upper limit is achieved by General Electric (GE) MV7000 converter family [56]. Note that in this analysis, NPC refers to the '3-Level' NPC topology. For the MV7000 converter manufactured by GE, with 5-level NPC, it is possible to reach up to 13.8 kV and 48 MW [56]. Here, only 3-L NPC is considered.

For the case of CHB topologies, it has been found that it is used on MV converters with voltages between 6 kV and 11 kV and power up to 40 MW. This shows that as voltage increases, CHB is preferred in industry. The other topologies which are used in MV AC drives are the MMC and the Load Commutated Inverter (LCI) [57]. The MMC is proposed by Siemens for a voltage range around 14 kV [58].

It can also be observed that by increasing the voltage levels, the industrial solutions are cascaded-based topology converters (CHB or MMC). As it was mentioned in the previous parts implementation of MMC is expensive and has a lot of control complexities. This is the reason that this topology is used in HV converters and it can be seen that it is used only in the highest voltage MV AC drive.

Figure 20 shows the analysis of industrial AC drives from switch technology point of view. It was explained before that IGBTs are used in lower voltage applications of HVDC and it can be observed that in MV AC drives, this switch technology has been preferred due to the possibility of cascading converters. While, IGCT shows a significant merit in the high power converters without the need of cascading since IGCTs are capable of more current/power in comparison to IGBTs [59]. Due to the availability and benefits of thyristors in higher power/voltages, it has been used in one AC drive with the power rating of 85MW.

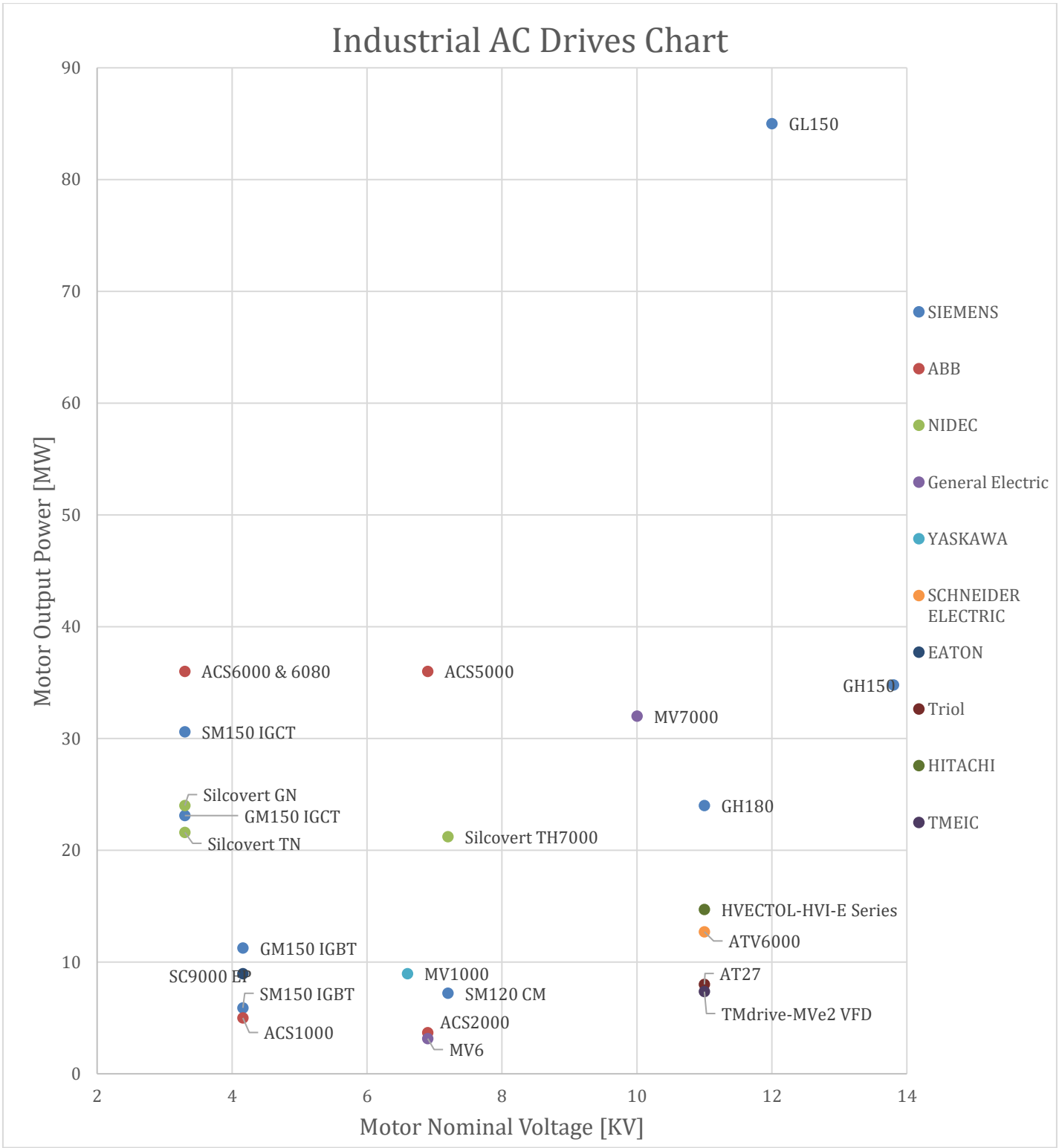

Figure 18 : The Medium Voltage AC Drives Used in Industry in Different Voltage and Power Ratings

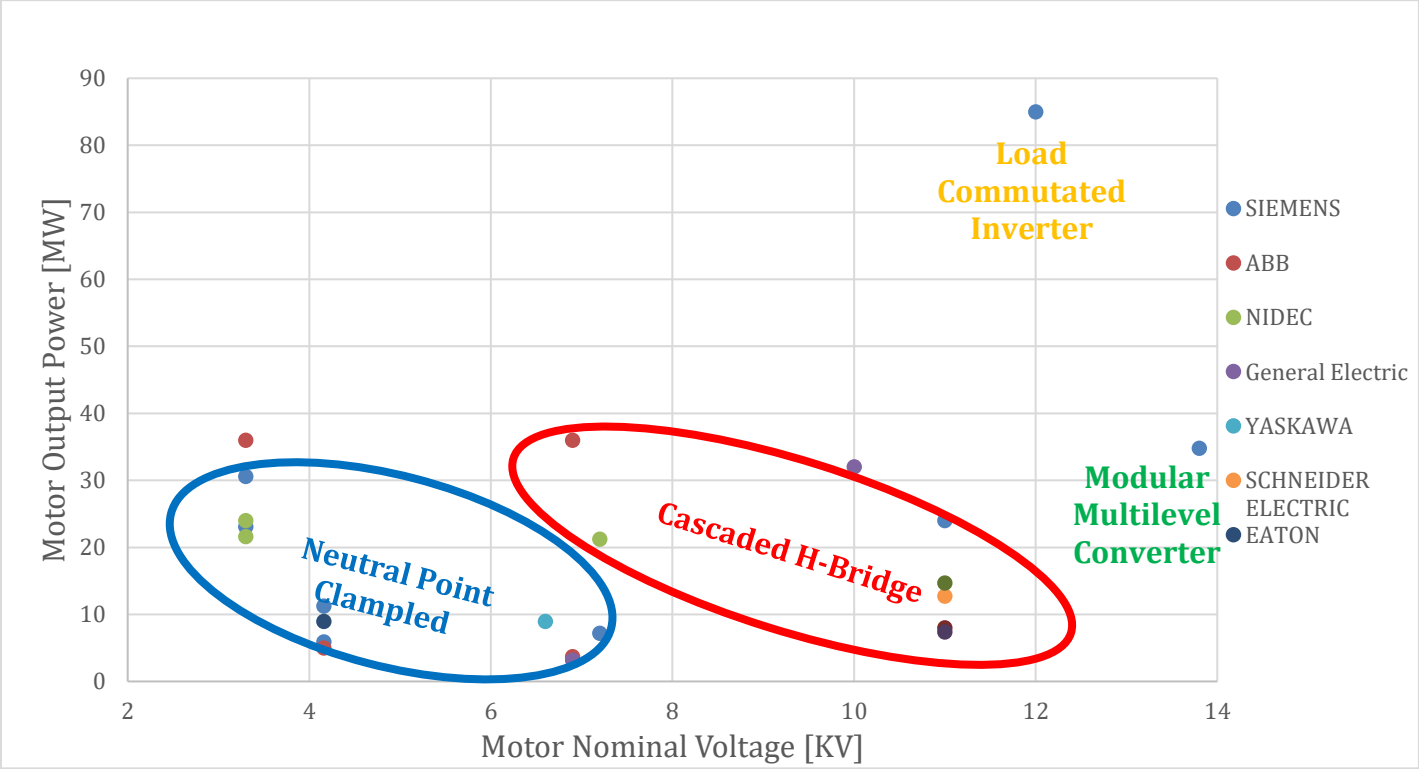

Figure 19 : The Industrial Medium Voltage AC Drives Addressing their Topologies in Different Voltage/Power Ratings

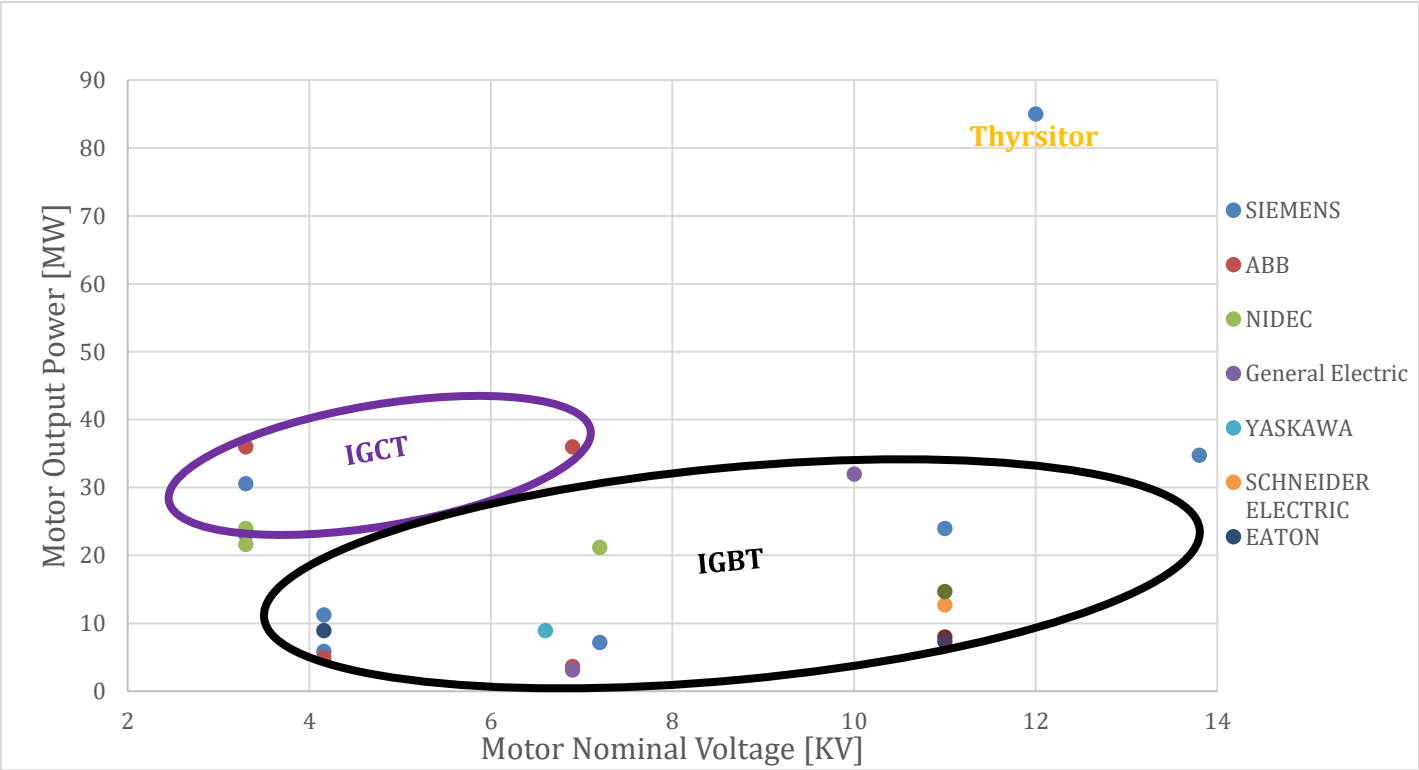

Figure 20 : The Industrial Medium Voltage AC Drives Addressing their Switch Technologies in Different Voltage/Power Ratings

3.3.2. STATCOM

The second equipment considered which includes an AC to DC conversion stage at medium voltage is Static synchronous compensator (STATCOM). STATCOM is a fast-acting element capable of providing or absorbing reactive current to regulate the voltage of AC grid at the point of connection [55]. STATCOM regulates voltage by exchanging power between a DC source and the AC grid in a very short time. This is done by an AC to DC converter. The typical schematic of a STATCOM is shown in Figure 21. Similar to the AC drive, the intended part to be studied is the converter inside the STATCOM.

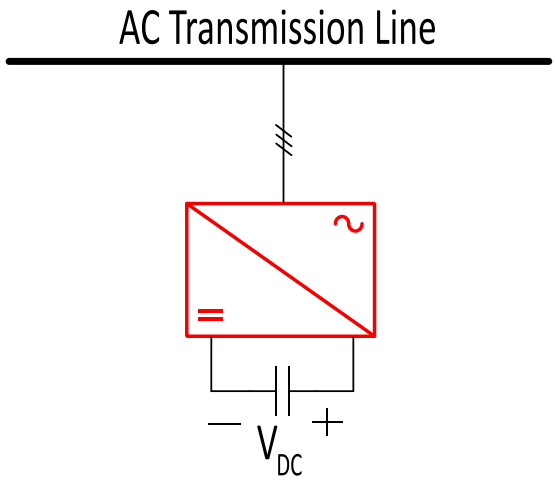

Figure 21 : The Single Line Diagram of a Typical STATCOM

There are few number of STATCOMs and the information related to their DC voltage has not been specified. Considering STATCOMs, Figure 22 illustrates a chart which in some of the available STATCOMs in industry according to their power rating and AC grid voltage rating is shown.

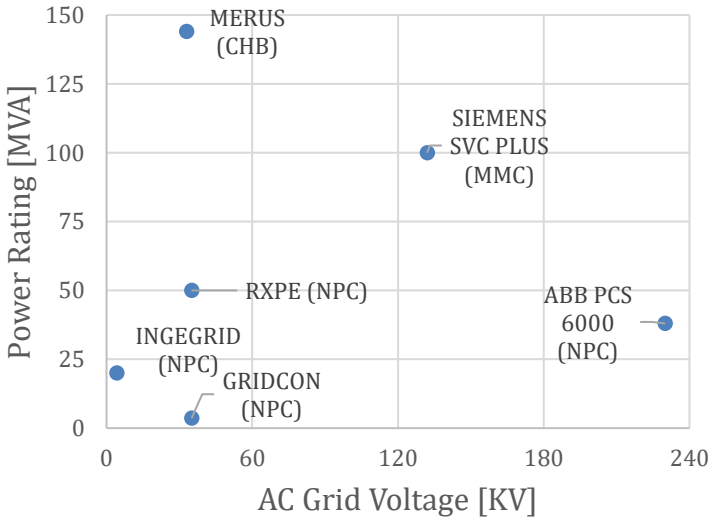

Figure 22 : The Manufactured STATCOMs Specifications Addressing Their Power Ratings, Topologes, and AC Grid Voltage Ratings

This chart shows that most of the STATCOMs with power rating up to 50 MW use 3-L NPC topology while for higher powers, MMC is preferred.

3.4. The Relationship between AC and DC Voltages of VSCs

After analysis of the MV converters in the AC drives and STATCOMs, since the DC voltage is desired and the mentioned voltages was AC voltage, the relationship between DC and AC voltages of these converters must be found. In VSCs, the AC and DC voltages are dependent on each other [37]. The relationship between the voltage on the AC and DC side of the VSC is dependent on the modulation technique which is applied to the IGBTs [37] [60]. To find their relationships, two Pulse-Width Modulation (PWM) techniques are focused. They are explained in following.

3.4.1. Sinusoidal PWM (PWM)

Normally, in a voltage source converter with SPWM (Sinusoidal Pulse-Width Modulation), the relationship between the DC and AC voltage of the AC-DC converter is defined as the following equation.

$$U_{DC} = 2\sqrt{\frac{2}{3}}\frac{U_{AC}}{m_a} \approx 1.6\frac{U_{AC}}{m_a} \qquad \textit{Eq. 1}$$

In this equation, U_{DC} is the pole to pole DC voltage, U_{AC} is the AC line to line RMS voltage, and m_a is the modulation index which must be less than 1 ($0 < m_a < 1$) to have a sinusoidal AC voltage. The ideal value for modulation index is 1. But due to the saturation of this index and loss of perfect sinusoidal waveform, this parameter is designed to be less than 1. Hence, it is normally less than 1 with a margin (for example 0.85 or 0.9).

Based on the Eq. 1 and the range of modulation index, we can conclude:

$$U_{DC} > 2\sqrt{\frac{2}{3}}U_{AC} \approx 1.6\,U_{AC} \qquad \textit{Eq. 2}$$

This equation means that a VSC with SPWM modulation and DC voltage of U_{DC} can generate maximum 0.625 U_{DC} AC line to line RMS voltage, however as it was mentioned, even this amount of AC voltage happens in an ideal condition with modulation index equal to 1 and practically, a slightly lower AC voltage is seen. This equation shows that in the achieved AC drives chart, the horizontal axis shows the AC side voltage of the converter and for the DC side, the voltage must be minimum 160% of this AC voltage. Therefore, the following equation for this chart is present:

$$U_{DC_{AC\ Drive\ Converter}} > 1.6\,U_{AC_{AC\ Drive\ Converter}} = U_{Motor}\ (Shown\ on\ the\ Horizontal\ Axis) \qquad \textit{Eq. 3}$$

3.4.2. Third Harmonic Injection PWM (THIPWM)

In [60], another PWM technique has been proposed that is called third harmonic injection pulse-width modulation (THIPWM). In this method, the reference waveform for modulation includes a sinusoidal waveform with the desired AC frequency (for example 50 Hz) and also another sinusoidal waveform with a three times AC frequency which refers to the third-order harmonic of the voltage on the AC side of the converter. The following equation shows the THIPWM modulation waveform:

$$THIPWM\ Signal: M = sin(\omega t) + Ksin(3\omega t) \qquad \textit{Eq. 4}$$

As the amplitude of modulation signal must be maintained less than 1, the optimized value for K can be found as 1/6. Finally, the commonly used THIPWM modulation signal to eliminate triple harmonics is as following:

$$THIPWM\ Signal: M = \frac{2}{\sqrt{3}}[sin(\omega t) + \frac{1}{6} sin(3\omega t)] \qquad Eq.\ 5$$

With this technique, all the triple harmonics will be significantly decreased (81%) while the first-harmonic which is desired is extended to 1.15 (the linear modulation region is extended) compared with 1 in conventional SPWM. Moreover, this analysis show the better performance of the converter in reduction of the THD. Overall, with THIPWM technique, the PWM gain is increased by 15% over the traditional PWM and the relationship between the DC and AC voltage of a VSC can be modified to the following equation:

$$U_{DC} = \frac{\sqrt{2}}{m_a} U_{AC} \approx \frac{1.4}{m_a}\ U_{AC} \qquad Eq.\ 6$$

In this equation U_{DC} is the DC pole to pole voltage and U_{AC} is the AC line to line RMS voltage and m_a is the modulation index ($0 < m_a < 1$). Therefore based on Eq. 6 and the range of modulation index to generate sinusoidal AC waveform, we can conclude:

$$U_{DC} > \sqrt{2} U_{AC} \approx 1.4\ U_{AC} \qquad Eq.\ 7$$

This equation shows that by injecting third-harmonic in the modulation signal, the current will be less than the converter with conventional PWM modulation and with the same DC voltage, the AC voltage will be 15% higher (the same amount of transferred power).

3.5. AC Drive Converters in MVDC Networks

Due to the few number of STATCOMs and the limited information, to finalize this analysis, only MV converters in AC drives will be focused. Considering, the AC drives, as the DC voltage is desired, it is needed to find the relationship between the DC and AC voltages of the AC drives. For the AC drives, AC voltage is the motor voltage. With considering the industrial AC drives in the MV level, and the conventional PWM technique to calculate the DC link voltage of analyzed AC drives from their AC voltage (See Eq. 2), the following table is proposed. This table presents the recommended voltage/power range to apply a topology based on the designs used in the industrial AC drives. This table only discusses the possible potential for each topology and in reality, based on the different requirements and future improvements, theses information may be updated. With THIPWM, the DC voltage ranges is a bit lower (See Eq. 7).

Topology	Minimum Recommended Converter DC Voltage Range (Pole to Pole)	Recommended Converter Power Range
3-L Neutral Point Clamped (NPC)	4.8 kV – 16 kV	3 MW - 32 MW
Cascaded H-Bridge (CHB)	9.6 kV – 17.6 kV	3 MW - 40 MW
Modular Multilevel Converter (MMC)	Greater than 22.4 kV	Greater than 23 MW
Load Commutate Inverter (LCI)	19.2 kV	85 MW

Table 1: The Recommended Voltage/Power Ranges considering the Industrial AC Drives

Moreover, in [54], the different topologies used in medium voltage application have been compared based on different criteria. It shows that with the same DC voltage rating 2-L VSC is more reliable than 3-L NPC but MMC is more reliable than both of these topologies. Moreover, the efficiency of MMC is more than 3-L NPC and both of them impose lower losses than 2-L VSC. Overall, from economical point of view, [54] proposes 3-L NPC topology for the converter with medium voltage up to 56 kV pole to pole DC voltage (±28 kVdc) and up to 23 MW while for the DC pole to pole voltage of 46 kV (±23 kVdc) and the power range of 23 MW and 33 MW, the most cost-effective topology is MMC. Moreover, it is strongly suggested that for the higher MVDC voltages and power ranges, MMC is more reliable and economical than other topologies due to the more availability of higher number of MMC sub-modules. Additionally, the other topology which is advantageous to use in higher MV voltages than 70 kV (±35 kVdc) is cascaded 3-L NPC which is deployed in Angle-DC project in the UK. In this project, 12 3-L NPC cells has been used with the bipolar line topology. Each cell has a power rating of 2.55 MVA (totally 30 MW) and 4.5 kV pole to pole DC voltage (totally 54 kV or ±27 kVdc) [54].

Chapter 4

Research Trends in MVDC Applications and Related Technologies

4.1. Introduction and Methodology

After a review on industrial works related to MVDC, a study of the research trends in the literature for this concept is essential. The goal of this review is finding the popular subjects related to MVDC which have been interesting in the researchers' views. There are a lot of publications can be found on different sources. It is interesting to analyze the interests related to this thesis work in the publications. Hence, we perform a review on the trends related to MVDC which can be found in literature.

The source which is used for this study is IEEE Xplore [64] and the method is looking for the number of articles by keywords related to MVDC, its related applications and technologies. For example, to find out which topology is more popular in the literature, the term 'MVDC' and the topologies like 'NPC' have been searched. Moreover, the time-interval to do this analysis is based on the current century and to see the trend of a topic related to MVDC (increasing or decreasing), the 21st century has been divided in four 5-years periods. So, the results have been analyzed in the following time-periods:

- 2001 – 2005
- 2006 – 2010
- 2011 – 2015
- 2016 - 2020

As an example, for the applied topologies in MVDC converters, considering number of articles in IEEE database for MVDC and its combination with these topologies of AC-DC conversion, Table 2 shows the results:

Keyword → / **Period ↓**	**MVDC**	**MVDC + Half Bridge**	**MVDC + Full Bridge**	**MVDC + NPC**	**MVDC + MMC**
2001 - 2005	247	5	9	13	0
2006 - 2010	438	10	20	23	4
2011 - 2015	1079	40	47	58	79
2016 - 2020	1999	106	146	75	280

Table 2: Number of Articles in IEEE Database with these Keywords Related to MVDC

4.2. Results and Conclusions

The results of this analysis have been ordered in different categories.

4.2.1. Trends of Topologies in MVDC

The result of topologies analysis used in the articles related to MVDC is shown in Figure 23. These results show that even if in industrial MV converters, 3-L NPC and CHB are very popular, in literature, MMC has been the most prominent topology for authors and researchers about MVDC. This shows that probably in the future with more development of MVDC networks, more industrial MV converters with MMC topology will be available given its significant potential to researchers' insight. Moreover, by more research and development of MMC, this topology has attracted a lot of interest in the recent decade of 21st century in comparison to the first decade.

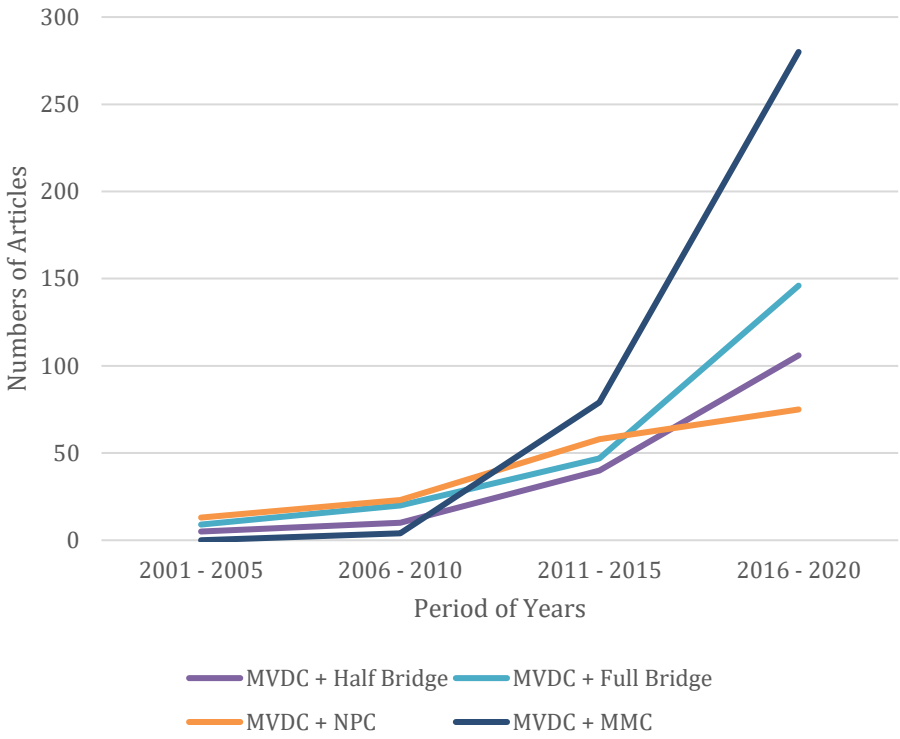

Figure 23 : Trends of Converter Topologies in articles related to MVDC Applications

4.2.2. Trends of Switch Technologies in MVDC

The result of switch technologies analysis used in the articles related to MVDC is shown in Figure 24. This analysis clearly confirms the industrial review and show that IGBT is the most common switch used in the design and research of the authors. After IGBT, they have been interested in thyristors while IGCT has not been appealing in the articles related to MVDC applications.

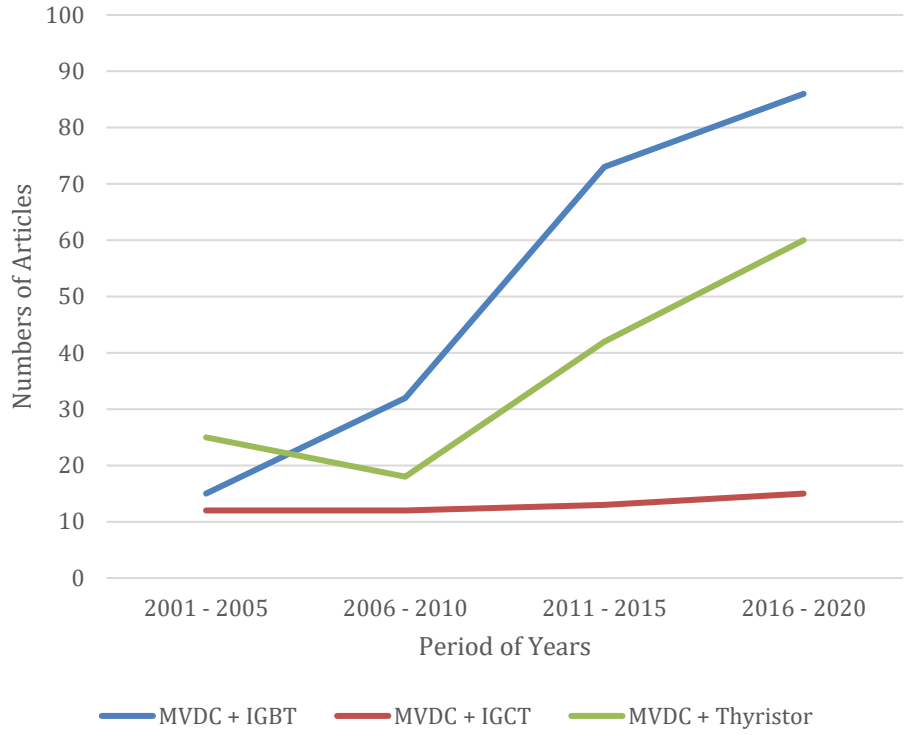

Figure 24 : Trends of Switch Technologies in articles related to MVDC Applications

4.2.3. Trends of renewable energy sources in MVDC

Figure 25 shows an overview of the trend of different renewable energy sources mentioned in the articles related to MVDC. These results show that potentially, wind and then PV are very compatible sources to be integrated in MVDC networks.

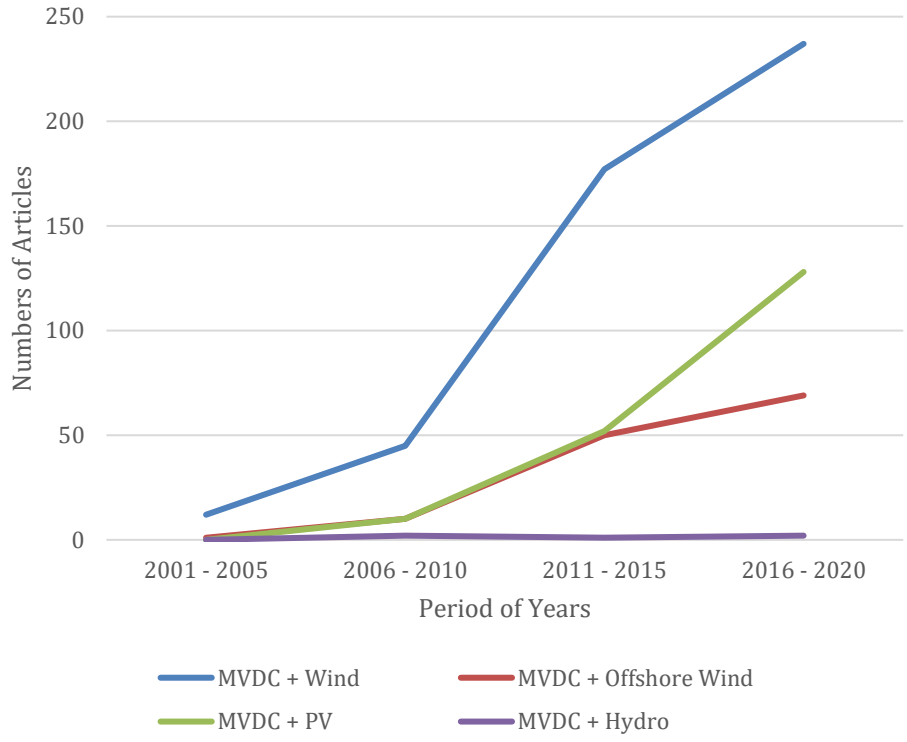

Figure 25 : Trends of Renewable Energy Sources in articles related to MVDC Applications

4.2.4. Trends of RES Locations in MVDC

The outcome of the potential locations for integration of renewable sources in the articles related to MVDC is shown in Figure 26. This analysis show a massive potential interest in the insight of researchers for integrating renewable energy sources into the MVDC networks on ships or in marine applications.

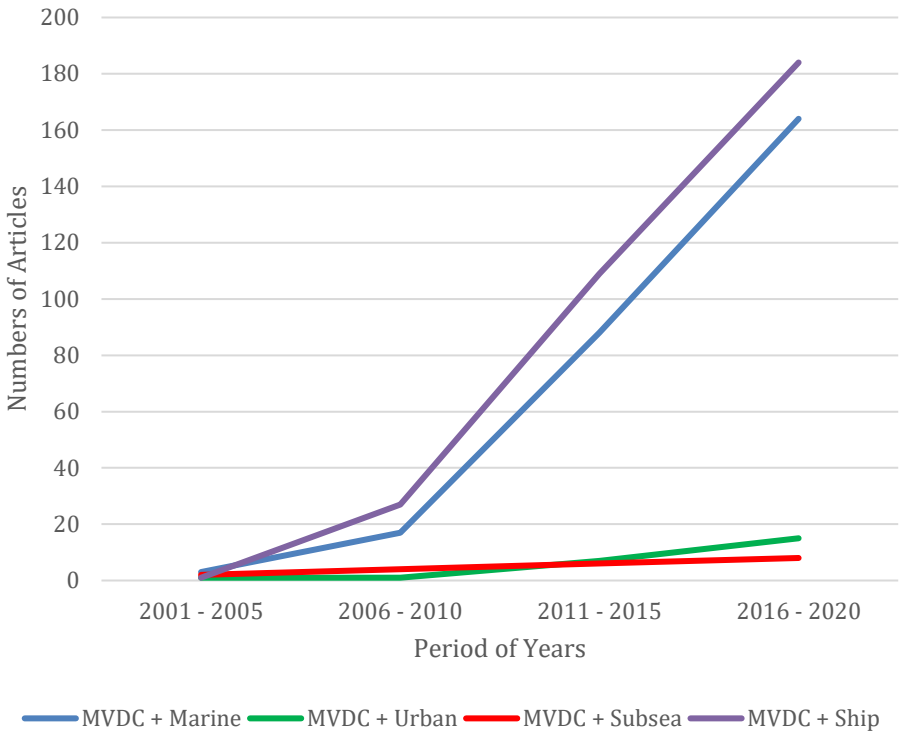

Figure 26 : Trends of Discussed Locations in articles related to MVDC Applications

4.2.5. Trends of the main equipment in the MVDC

This analysis demonstrates the interest of authors in medium-frequency transformers for MVDC networks and a fair amount of their interest in integrating storage system into the MVDC networks. The detailed results is shown in Figure 27.

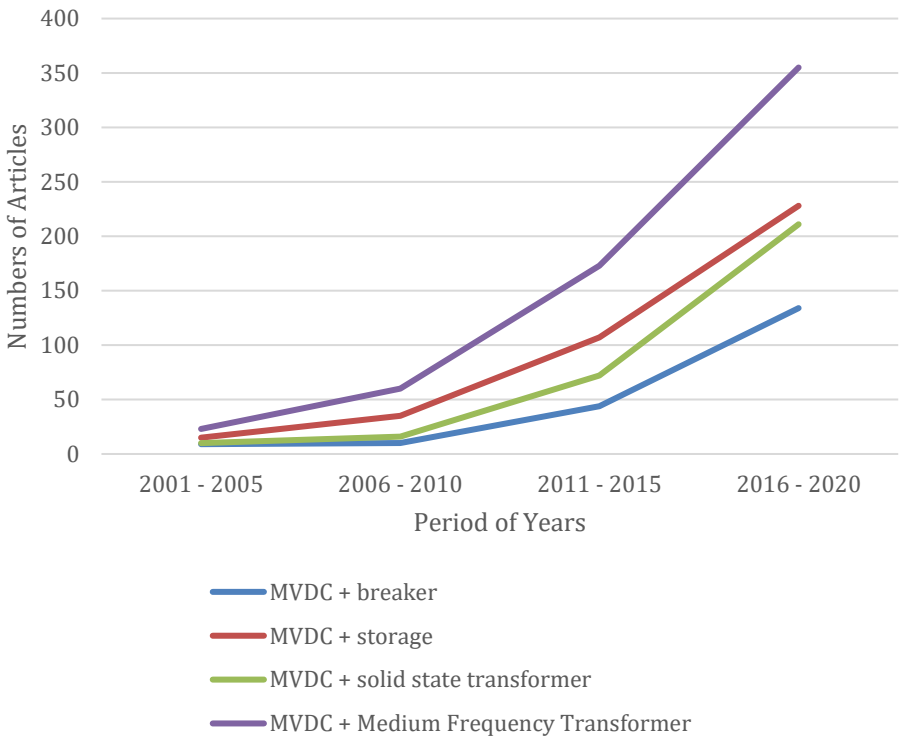

Figure 27 : Trends of Instruments in articles related to MVDC Applications

Chapter 5

Analysis of DC Faults on MV AC-DC Converters

5.1. Purpose

Reliability and safety is the goals of a power system. An electrical network must be designed in a way to transfer power to the customers reliably. Hence, there is an essential need for analyzing some events which may happen in an electrical network. Similarly, in the hybrid electrical networks, the reliability of AC-DC converters is very important during any condition. DC faults on AC-DC converters is a popular research topic in HVDC converters [65][66][67][68]. But due to the immaturity of MVDC networks and MV converters, it is needed to study this phenomenon in this voltage range. Faults can happen for different reasons, either internally inside a device or due to an external interference. In this chapter, DC faults in MVDC networks are studied addressing the technical limitations for the equipment in the AC-DC converters.

5.2. Study Case

The following figure shows the single line diagram of the network which will be considered to analyze the impacts of DC faults on MV AC-DC converters.

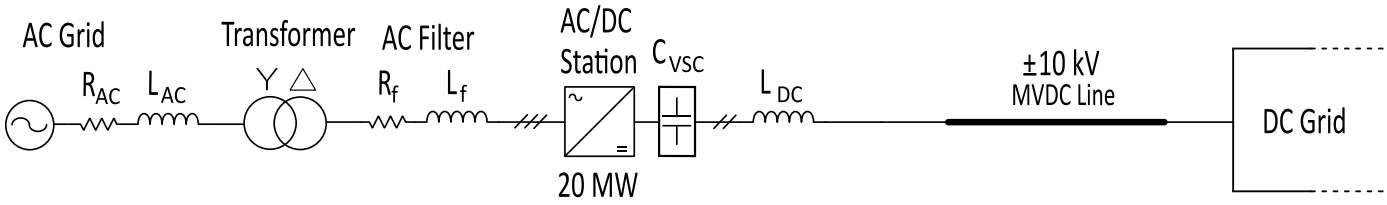

Figure 28 : Single Line Diagram of the Study Case Network

In the proposed network, we assume that the MVDC line is connected to the 225 kV AC grid via an AC-DC converter station. The considered nominal power for the station is 20 MW and the DC grid voltage is in the medium voltage range. A voltage of ±10 kV (20 kVdc pole to pole) is considered. These parameter are chosen based on the analysis done in [36].

5.2.1. Converter Design

The choice of the AC-DC converter for the case study is done considering the mentioned design requirements (20 MW, 20 kVdc pole to pole). Based on the analysis done in Chapter 3 on potential converter topologies for each voltage and power range, it is considered that 3-Level NPC is a good choice. Moreover, for the switch technology, IGBT is preferred.

NPC topology has been mostly used in AC drives. A DC fault inside an AC drive is unlikely, so the impact of this fault on AC-DC converters with NPC topology has not been analyzed yet. However in publications like [37], [69], [70], and [71], DC fault on AC-DC converter with 2-level topology has been studied. The identified advantages of NPC for MVDC networks make an in-depth analysis on DC fault on MV converters with this topology necessary.

As it was mentioned in Chapter 3, for a 3-L NPC, each switch in the topology must be rated with minimum half of the DC voltage (*Vdc/2*). Thus, for the retained study case, 10 kV, the topology will

need switches with rated voltage of 10 kV. Currently, in the market, the highest voltage switch which can be found is 6.5 kV IGBTs. However, a derating is generally is done for the use of IGBTs (for example it can be seen in the 6.5 kV IGBTs manufactured by ABB [61] or Infineon [62]), Thus a rated collector-emitter voltage of 3.6 kV in this study. Therefore, to implement the needed converter with 3-L NPC topology, there are two possible options:

- → One 3-L NPC with three 6.5 kV-IGBTs in series for each switch in the topology (totally 12 switches per phase and 36 switches for the converter): With this implementation, the size of converter will be smaller and as only one 3-L NPC converter will be used, less number of AC equipment (breakers, disconnectors, sensors, etc.) will be required. However, this implementation needs the balancing of the voltage on each IGBT, requiring snubber circuits [63]. This implementations is shown in and Figure 31.

- → Cascading n 3-L NPCs: With this method, the required power and voltage will be shared between all the converters, decreasing the individual constraints for each converter. This implementation is shown in Figure 30. Table 3 shows the required number of switches for different number of cascaded (series) converters considering 6.5 kV IGBT (rated at 3.6 kV). This method is similar to the applied design for the AC-DC station in the Angle DC project in the UK [54].

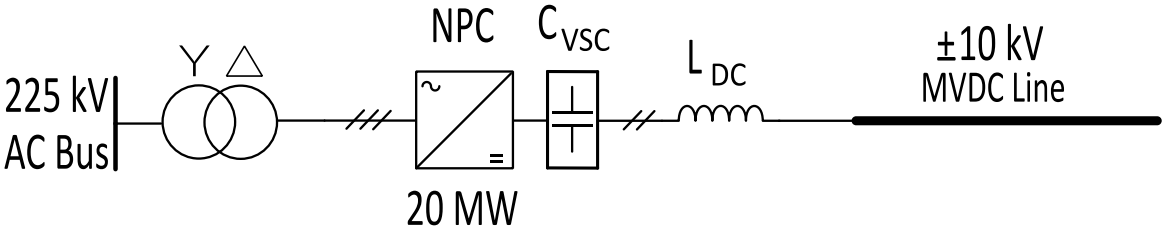

Figure 29 : The Schematic of Study Case Implementation with One NPC

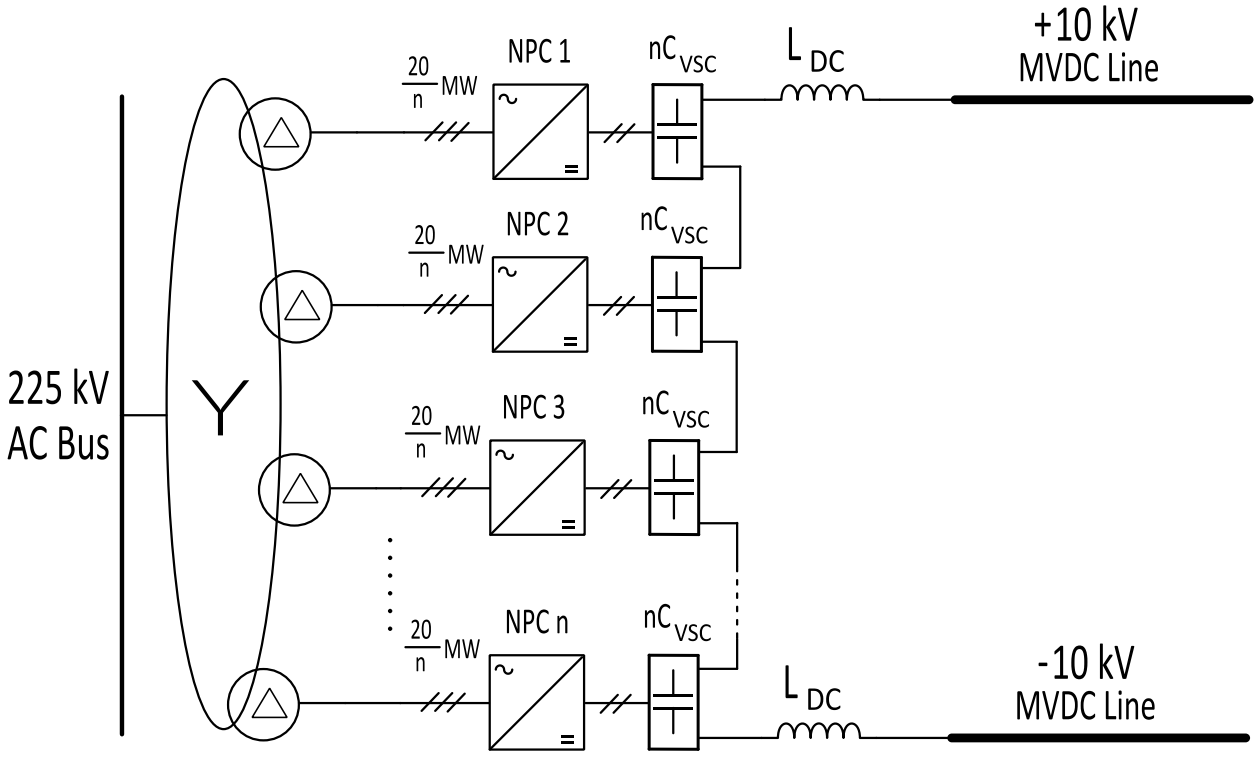

Figure 30 : The Schematic of Study Case Implementation with n NPCs

Number of Cascaded Converters with 3-L NPC Topology	Minimum Required Number of Switches
1	36
2	48
3	36
4	48

Table 3: The Number of 6.5kV IGBTs needed for Different Number of Cascaded NPCs

The first option is retained because of the mentioned advantages and also the simplicity of this model to analyze faults on AC-DC converter. However, this will not impact on the general conclusions. The schematic of the designed converter is shown in Figure 31.

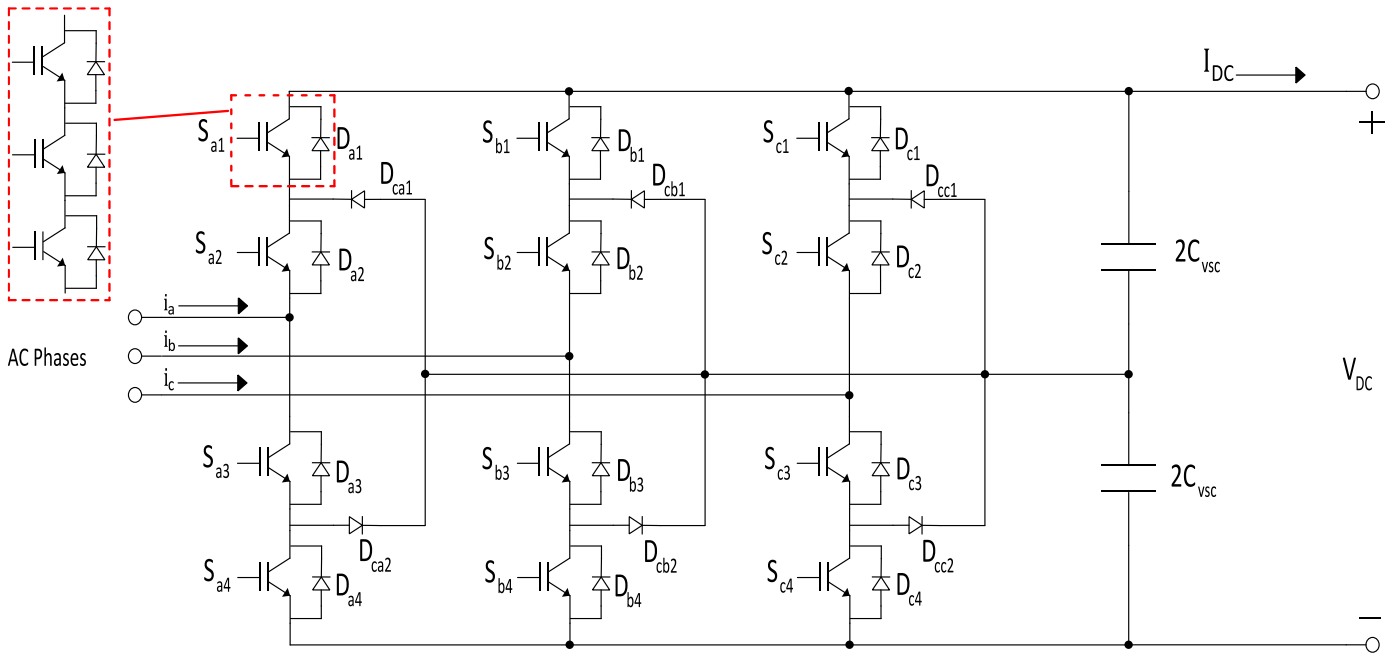

Figure 31 : The Schematic of the Designed Converter with 3-L NPC Topology

The current which is passing by a switch in a converter in the nominal condition and also the peak of this current are the other parameters to choose a proper switch for designing a converter. In other words, we can satisfy the voltage requirement by choosing a 6.5 kV switch but it is also required to fulfill the current constraints. This is explained in the sub-chapter related to switch selection.

5.2.2. Passive and Active Elements Specification

In this study case, the following elements are present:

AC grid short circuit resistance and inductance: These parameters are represented by R_{AC} and L_{AC} in the single line diagram of the network on Figure 28. Their values are specified according to the short circuit of the AC grid. A strong AC system is considered. Thus, the impedance related to the inductors of the network is much higher than the short circuit resistance (more than 7 times).

Transformer: A transformer with Y-Δ windings was considered. Considering the transformer with other vector groups are also possible but requires further studies. The nominal converter power is 20 MW, the transformer's apparent power is dimensioned a little higher at 24 MVA. For the voltage, a transformer is connected from one side to the 225 kV AC grid, its primary voltage will be matched with the voltage of AC grid and for the secondary side, the voltage will be related to the DC voltage of the converter. In chapter 3, it was explained that a VSC with THIPWM (Third harmonic Injection Pulse-Width Modulation) and DC voltage of U_{DC} can generate maximum 0.71 U_{DC} AC line to line RMS voltage (See Eq. 7).

In the retained study case, with 20 kVdc pole to pole voltage, the AC voltage of converter can be around 14.3 kV at the maximum modulation index ($m_a = 1$). Considering the practical value of modulation index which is around 0.85-0.9, the design of the secondary voltage of the transformer at 12 kV is selected.

Since the short-circuit impedance of transformer is very large, only short circuit impedance of the transformer can be considered. This figure shows the equivalent circuit of transformer seen by one side (primary or secondary). Moreover, due to the larger amount of transformer short circuit reactance in comparison to its resistance ($XRRatio = \frac{X_{tr}}{R_{tr}}, XRRatio \gg 15$), the resistance of transformer can be neglected and only its inductance can be considered. The short circuit inductance of the transformer can be calculated using the following formula:

$$L_{tr} = \frac{Z_{tr}}{2\pi f} . \left(\frac{V_{sec}}{V_{pri}}\right)^2 \qquad Eq.\ 8$$

In this formula:

L_{tr}: *The equivalent inductance of the transformer seen by the secondary side*

Z_{tr}: *The measured transformer impedance seen by primary side in short circuit test*

f: *AC grid Frequency*

V_{sec}: *The secondary voltage of the transformer* , V_{pri}: *The primary voltage of the transformer*

AC Filter: The resistance and inductance of this filter are shown with R_f and L_f in the single line diagram of the study case in Figure 28. This filter is needed to reduce the harmonics on the current generated by the converter. The main component of this filter in the study case is the filter inductance as its reactance is considered much larger than the resistance. Choosing a large value can reduce the total harmonics distortions (THD) significantly but this will increase the modulation index to violate 1 and enter the saturation area of the modulation because large AC filter imposes higher voltage drop and thus to regulate the AC voltage at a set-point, the modulation index will be forced to rise and violate the linear region ($0 < m_a < 1$). In the study case, it is assumed that the acceptable THD on the AC grid current is equal or less than 8% and the value of AC filter inductance is specified based on this limitation.

DC Link Capacitor (C_{VSC}): The DC capacitor is used to generate a DC voltage with low ripple from the rectified AC voltage coming from the converter. The value of DC link capacitor is designed in a way to have a ripple between 3-10 %. As a standard, the following equation is used to calculate a suitable amount for this capacitor [37]:

$$C_{VSC} = \frac{2S_{VSC}E_s}{V_{dc}^2} \qquad Eq.\ 9$$

In this equation:

C_{VSC}: $DC\ Link\ Capacitor\ for\ the\ DC\ side\ of\ VSC$, S_{VSC}: $The\ Power\ of\ the\ VSC$

E_s: $The\ Energy\ to\ Power\ Ratio$, V_{dc}: $The\ Pole\ to\ Pole\ DC\ Voltage\ of\ the\ VSC$

In practice, the value of E_s is in the range of 10 $kJMVA^{-1}$ and 50 $kJMVA^{-1}$ [37]. Assuming $E_s = 10\ kJMVA^{-1}$, the suggested value for the DC link capacitor is around 1 mF.

DC Inductor (L_{dc}): The DC inductor is used on the DC side of the converter for limiting the di/dt imposed by different phenomena such as faults to give enough time to the protection devices to detect and eliminate faults before damaging the equipment. The effect of DC inductor will be analyzed later during fault analysis.

MVDC Line: It consists of one cable per pole which current will be exchanged through that in ± 10 kVdc.

DC Grid: Some components can be present such as renewable energy sources (which will be explained in the next chapter) but for the proposed fault analysis, they are neglected since considering the contribution of these elements into the fault does not affect the AC-DC converter.

5.2.3. Semiconductor Switch Selection

As it was mentioned in the converter design, for AC-DC conversion, one converter with the topology of 3-L NPC with three series switches for each switch in the topology is supposed. The rated voltage of each of these switches must be at least 3.33 kV (assuming a correct voltage sharing). As it was mentioned, a 6.5 kV IGBT is a good choice however 4.5 kV IGBTs can also be used but higher number of switches is needed. Now, the nominal RMS current is also an important constraint and we have to check if this switch can carry the current of the converter in the nominal (steady-state) condition. Simulation (which will be explained in the next sub-chapter) of the study case shows that in this study case, the maximum RMS and the peak of current passing by each switch are 570 A and 1286 A, respectively. So, to choose a suitable IGBT for this application, the following conditions must be met:

- $Continous\ DC\ Forward\ Current : I_F > 570\ A$
- $Repetitive\ Peak\ Forward\ Current: I_{FRM} > 1286\ A$

For the 6.5 kV IGBTs mentioned in [61] and [62], the value of these parameters is as following:

- $I_F = 750\ A$
- $I_{FRM} = 1500\ A$

This shows that a 6.5 kV IGBT can fully fulfill the requirements. For this application, the 6.5 kV 750 A Infineon IGBT FZ750R65KE3 was chosen [62].

Overall, the most important parameters of the network are shown in Table 4:

Component of the Network	Specification
AC Grid RMS Line to Line Voltage	225 kV
Transformer	24 MVA, 225 kV/12 kV
Converter	3-L NPC VSC, 20 MW, 36 Infineon 6.5 kV 750 A IGBTs FZ750R65KE3
DC Link Capacitor	1 mF
DC Voltage	20 kV Pole to Pole (± 10 kVdc)

Table 4 : Specifications of some of the Elements in the Study Case Network

5.3. Theoretical Analysis of DC faults

In this section, DC faults on MV AC-DC converter are studied. There are two types of fault in the DC networks:

- Pole to Ground Fault
- Pole to Pole Fault

Both of these faults can cause some problems for the converter equipment in terms of high current and high di/dt which they impose on the converter equipment. The schematic of the network with pole to ground fault is shown in Figure 32. For a pole to ground fault, a simple way to limit the fault current is to add a resistor R_N in the ground connection of the 3-L NPC converter. As we can see, by installing this resistor, the impedance in the fault path is increased and therefore, the fault current is limited.

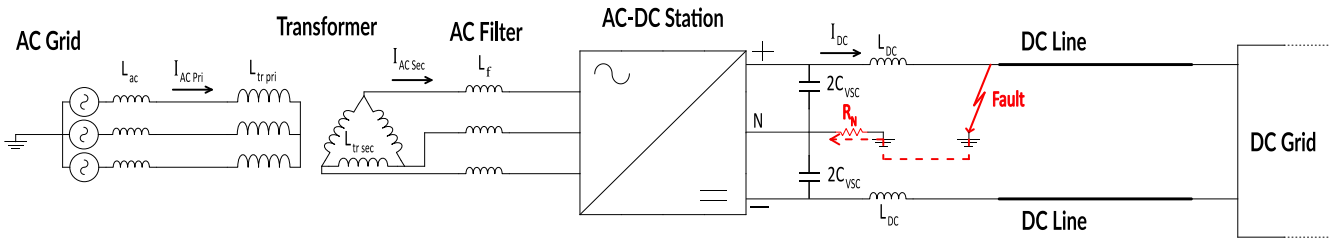

Figure 32 : Schematic of the Network with DC Pole to Ground Fault

For a pole to pole fault, it is not possible to install a resistor in the path of fault current because it imposes a voltage drop, increasing the losses in normal operation. Therefore, since the pole to

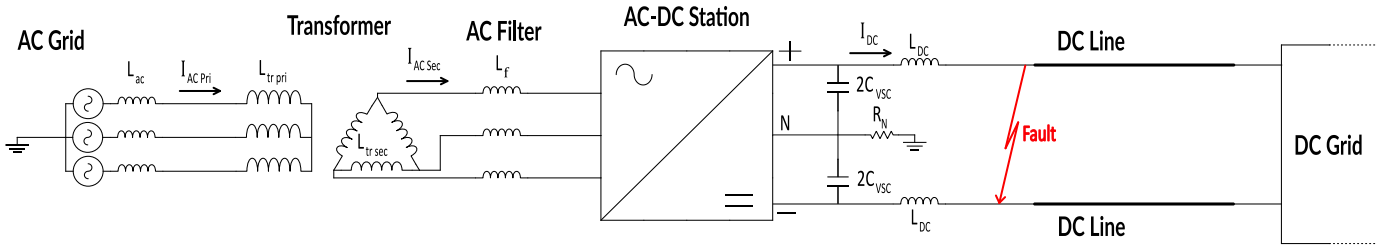

Figure 33 : Schematic of the Network with DC Pole to Pole Fault

ground fault currents can be limited by a resistor, the focus of the study will be done on pole to pole faults which pose more constraints to the converter. The schematic of the network with pole to pole DC fault is shown in Figure 33.

For now, it is assumed that the fault occurs on the terminals of the AC-DC station (right after DC inductors) as it is shown in the Figure 33. The detailed schematic of the converter with DC link capacitors and DC inductors during a DC pole to pole fault is shown in Figure 34 which is based on the schematic of the converter proposed in study case (See Figure 31).

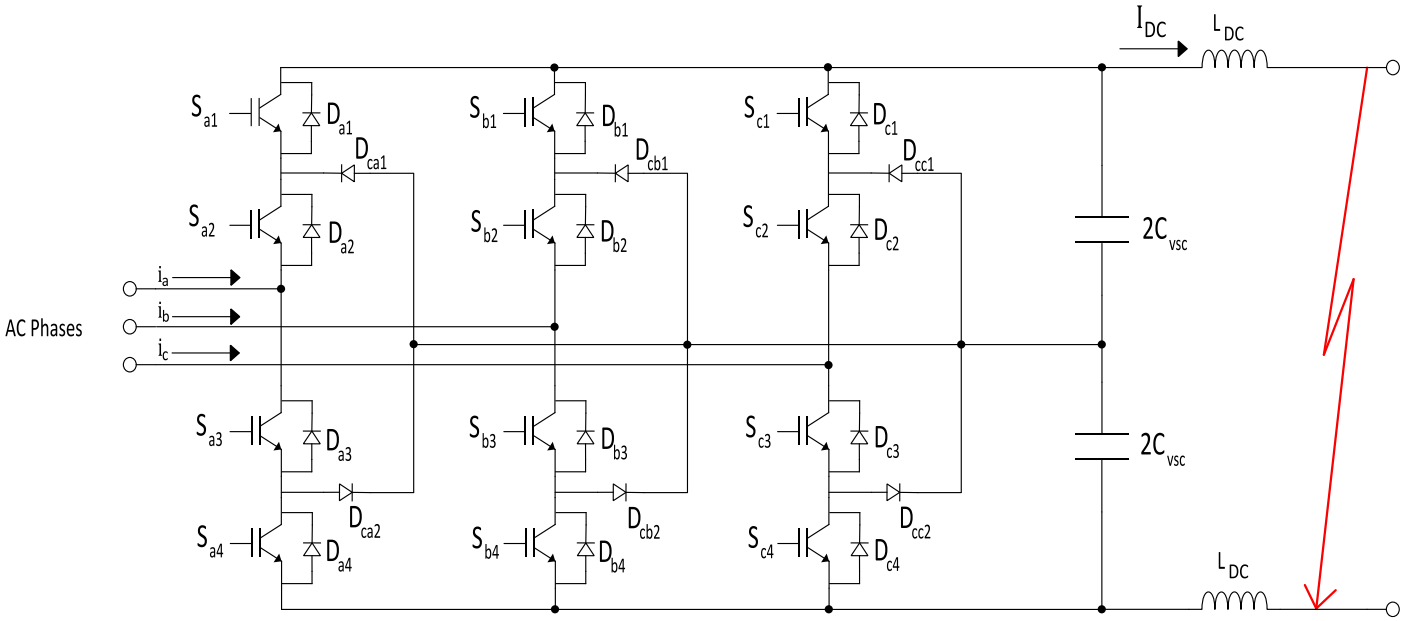

Figure 34 : Schematic of the Converter with a DC Pole to Pole Fault Close to the Converter

After happening this phenomenon, the current flowing through fault location (I_{DC} in Figure 34) experiences different steps. These steps are shown in Figure 35 and explained in the following. In Figure 35, t_{Fault} is the moment which fault occurs, t_{Peak} is the time which fault current reaches to its peak, and I_{Peak} is peak value of DC fault current.

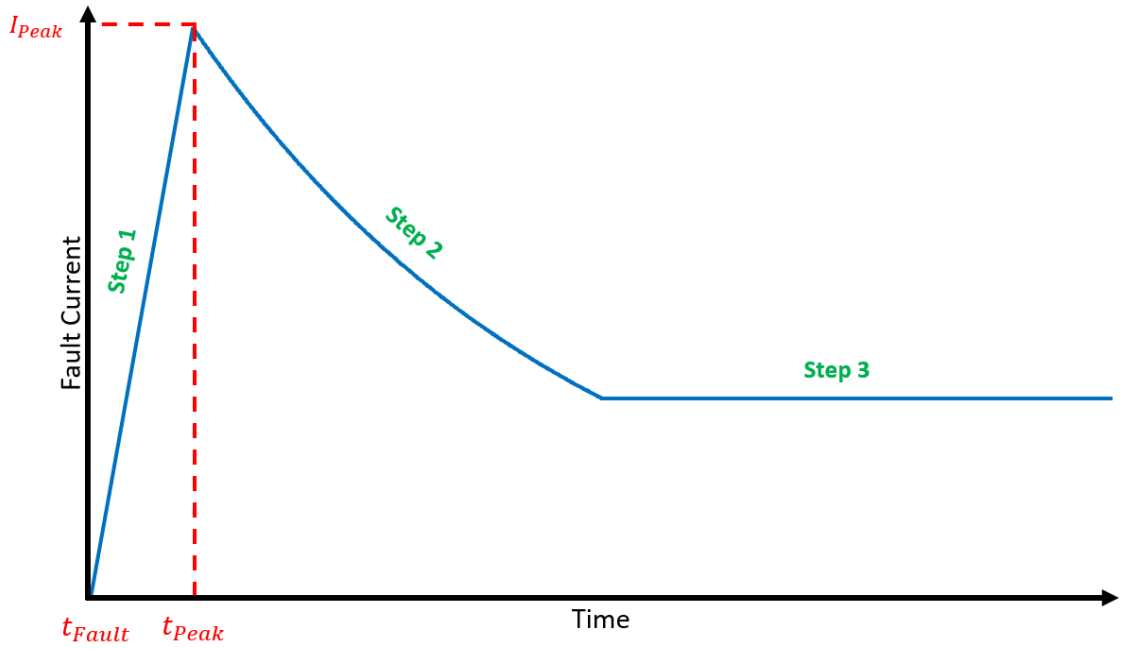

Figure 35 : Fault Current after DC Pole to Pole Fault

Step Zero: In this step, as the current of the switches start to rise, the protection of IGBTs will block all of them to prevent over-currents. Figure 36 shows the equivalent schematic of the converter after blocking IGBTs. Note that in this schematic, IGBTs are not shown since they are open due to blocking.

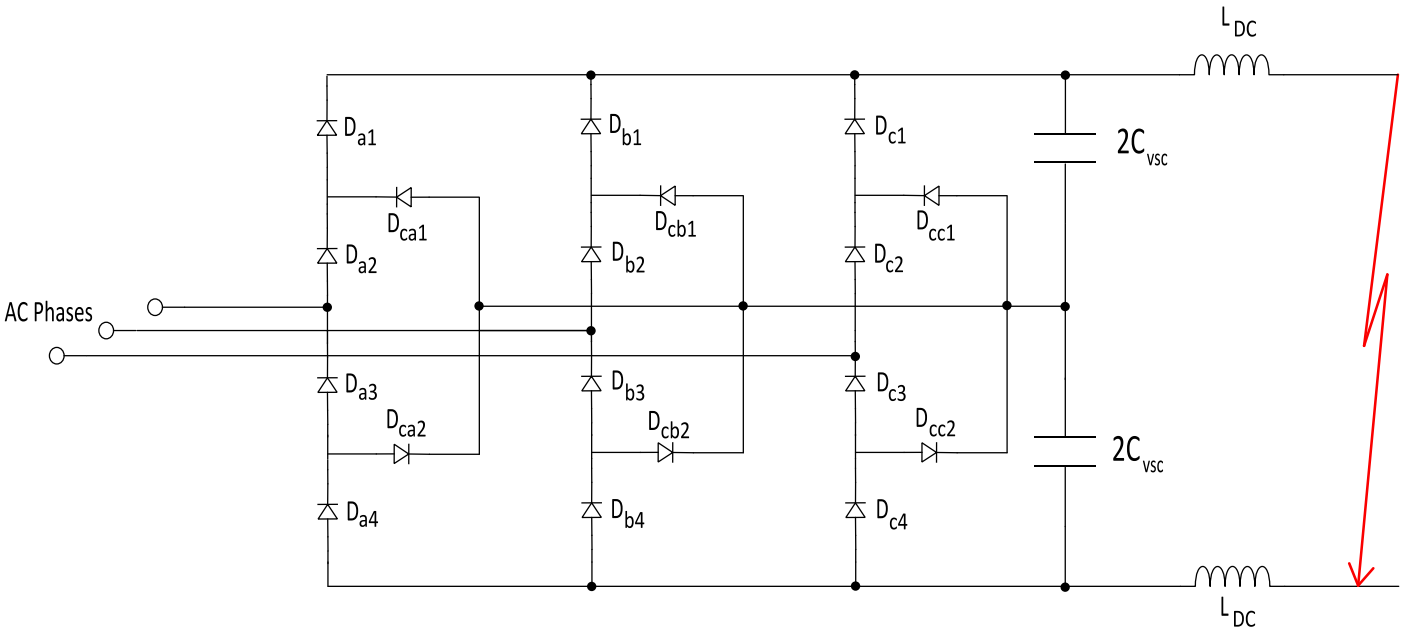

Figure 36 : Schematic of the Converter after Blocking IGBTs due to the DC Pole to Pole Fault

Step 1 (Discharge of the DC Link Capacitors into the Fault): By blocking the switches, the voltage of DC link capacitors which are fully charged drops to zero in a very short time (this time depends on the value of DC inductor, a larger L_{DC} results in longer time). Consequently, the DC current rises to a very high current and reaches a peak. In this period, the DC capacitors start discharging into

the fault path. The magnitude of the capacitor fault current is only limited by the impedance in the fault path (fault resistance). The DC inductors installed on the DC side limit the rise of the fault current. The equivalent circuit of the DC side in a short interval of time after fault will be an RLC circuit which is shown in Figure 37.

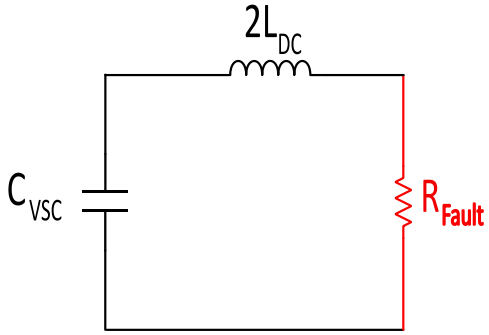

Figure 37 : Equivalent Circuit of the Fault Path by Discharge of DC Link Capacitor

In this circuit, $2L_{DC}$ is the pole to pole equivalent of DC inductors and R_{fault} is the fault resistance which it is assumed as a very small amount (0.01 Ω). Solving this circuit will give the peak of DC current and the rising time to reach this peak. By using Kirchhoff Voltage Law (KVL) law in the circuit shown in Figure 37, it can be written:

$$v_C + v_L + v_R = 0 \qquad \textit{Eq. 10}$$

By knowing the formula of the voltages of the capacitor, inductor, and resistor, we can write:

$$\frac{1}{C_{vsc}} \int i_{dc} dt + \frac{2L_{DC} di_{dc}}{dt} + R_{Fault} i_{dc} = 0 \qquad \textit{Eq. 11}$$

Solving this equation will give us the formula of DC current as following:

$$v_{Cvsc} = \frac{V_{dc0}\omega_{LC0}}{\omega_{LC}} e^{-\frac{t}{\tau}} sin(\omega_{LC} t + \beta) - \frac{I_{dc0}}{\omega_{LC} C_{vsc}} e^{-\frac{t}{\tau}} sin(\omega_{LC} t) \qquad \textit{Eq. 12}$$

$$i_{dc} = -\frac{I_{dc0}\omega_{LC0}}{\omega_{LC}} e^{-\frac{t}{\tau}} sin(\omega_{LC} t - \beta) + \frac{V_{dc0}}{\omega_{LC} 2L_{dc}} e^{-\frac{t}{\tau}} sin(\omega_{LC} t) \qquad \textit{Eq. 13}$$

where:

$$\omega_{LC} = \frac{1}{\sqrt{2L_{DC} C_{vsc}}} \quad , \quad \beta = \arctan\left(\frac{\omega_{LC} 2L_{DC}}{R_{Fault}}\right) \quad , \quad \tau = \frac{2L_{DC}}{R_{Fault}} \quad , \quad \omega_{LC0} = \sqrt{\omega_{LC}^2 + \frac{1}{\tau^2}}$$

I_{dc0} and V_{dc0} are the initial values at the faults instant. Peak of DC fault current (I_{Peak}) can be calculated by putting the derivative of DC current equal to zero ($\frac{di_{dc}}{dt} = 0$). Eq. 13 shows the impact of DC inductors (L_{DC}) on limiting the fault current as if there is no DC inductor ($L_{DC} = 0$), this current rises to infinity. Moreover, by solving this derivative equation for t, the peak time (t_{Peak}) can be calculated as following:

$$t_{peak} = \frac{2\pi\sqrt{2L_{dc}C}}{4} \qquad \textit{Eq. 14}$$

There is also another way for calculating the peak time. As we know, peak time is the time that the natural response of DC current reaches its maximum value. In other words, it is one quarter of the natural period of DC side in the LC circuit. Therefore we can write:

$$t_{peak} = \frac{Natural\ Response\ Period}{4} = \frac{T_{natural}}{4} = \frac{2\pi\sqrt{2L_{dc}C}}{4} \qquad Eq.\ 15$$

During this stage, there is no contribution to the fault current from the AC side of the VSC since converter equipment are not contributing to the fault and DC link capacitors are discharging in the fault via DC inductors.

Step 2 (Transient Period until Steady State): After the complete discharge of the capacitors, the DC inductors (which are now fully charged) start to discharge into the fault. Figure 38 shows the schematic of converter in this step.

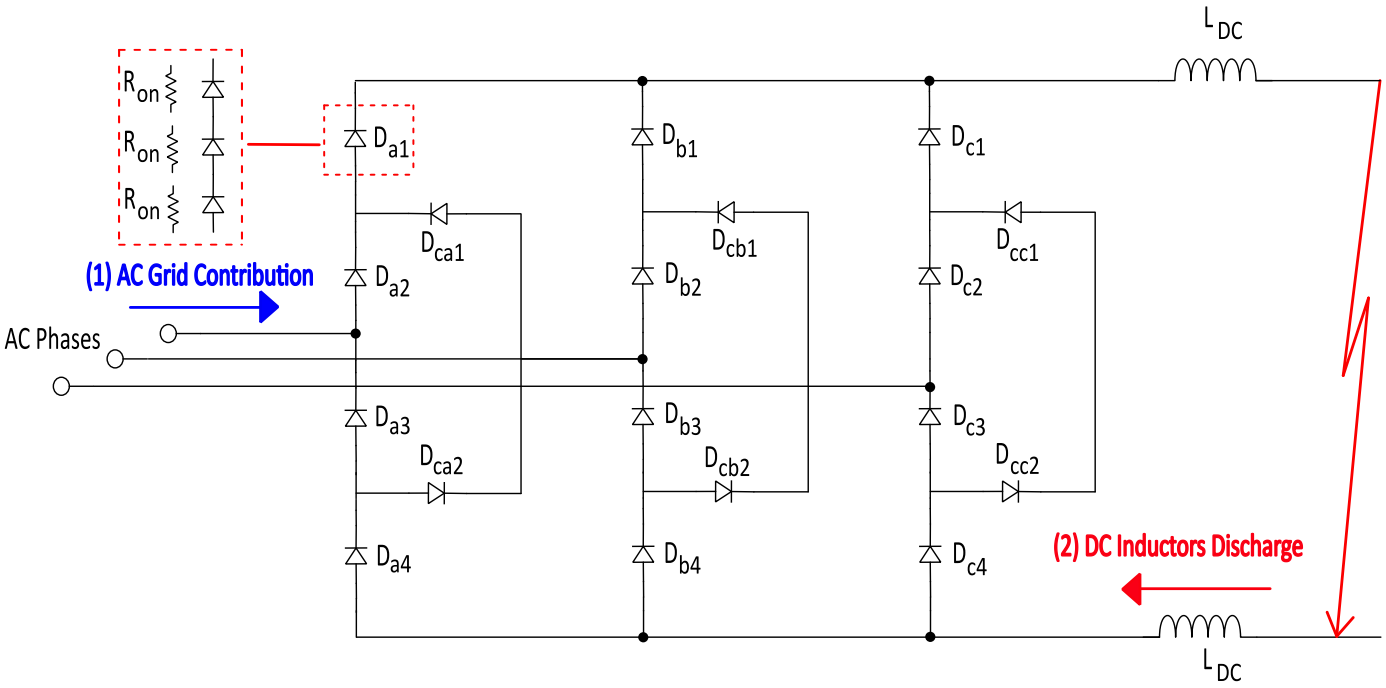

Figure 38 : Schematic of the Converter in the Transient Period

During this stage, DC inductors will be discharged into the fault and the fault current will freewheel by the converter diodes. From this step, AC side starts to contribute into the fault and high currents will be passed through diodes. It can be observed that DC pole to pole fault is seen as a three-phase short circuit from AC side. Hence, a rectified version of the current coming from AC grid will be flown through fault as this current passes through diodes. Therefore, during this period there are two contributions, one from AC grid and the other form the discharge of DC inductors and the diodes are experiencing two currents, one from AC side which is the rectified three-phase AC short circuit current and another current which is coming from DC side. The analysis on DC fault current shows a like-wise equation as following:

$$I_{DC} = Max\{I_{Rectified\ AC\ Three-Phase\ Short\ Circuit}, I_{dc_{IndDis}}\} \qquad Eq.\ 16$$

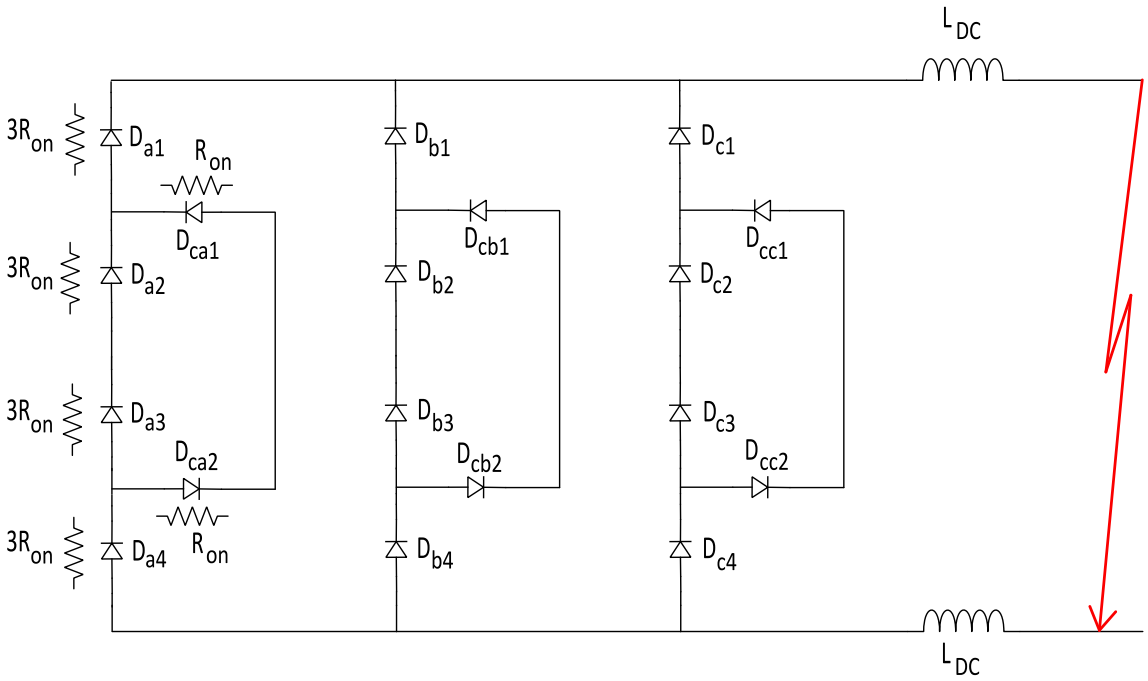

Figure 39 : Schematic of the Converter with Considering only the Discharge of DC Inductors Contribution

Presenting a super-position between these two currents, for the current coming from the discharge of DC inductors by neglecting the contribution of AC grid, the schematic of the converter shown in Figure 39 will be resulted.

Since each diode in the forward-biased condition acts as a resistor with the resistance of R_{on}, an equivalent circuit can be achieved by calculating the equivalent resistance of all the converter diodes. The schematic of this equivalent circuit is shown in Figure 40.

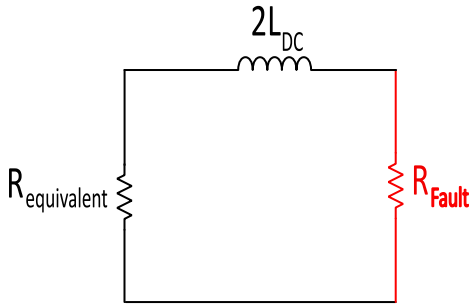

Figure 40 : Equivalent Circuit of the Converter Considering only DC Inductors Discharge

In this circuit, $R_{equivalent}$ represents the total equivalent resistance of all the diodes of the converter. We can find this parameter in the datasheet of the switch. As an example, for the retained IGBT, the following picture shows the forward current and voltage of the diode. With the shown linear approximation, the equivalent turn-on resistance of the freewheeling diode of this specific switch can be calculated as 2 mΩ.

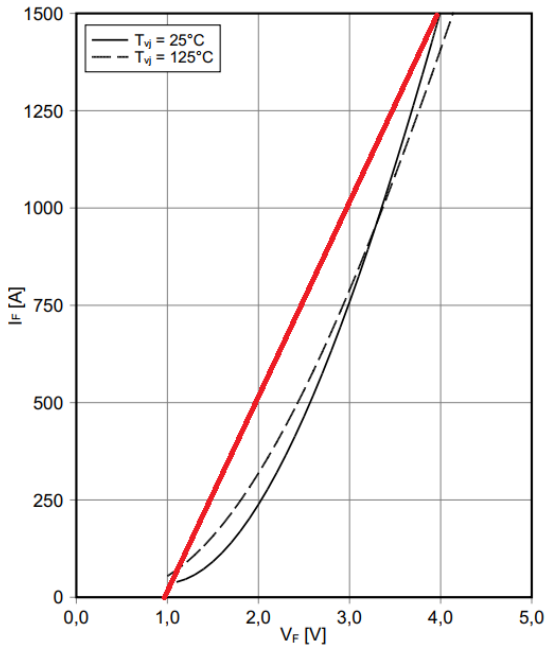

Figure 41 : The Graph of Current Passing by the Free Wheeling Diode of the Retained IGBT based on the Voltage [62]

Finally, the total equivalent resistance of the 3-L NPC can be calculated as following:

$$R_{equivalent} = R_{eq} = \frac{[3R_{on} + 3R_{on} + (6R_{on}||2R_{on})]}{3} = 2.5R_{on} \qquad Eq.\ 17$$

In this formula, R_{on} refers to the equivalent resistance of the freewheeling diode.

Considering the equivalent circuit (Figure 39), the DC current flowing in this circuit can be calculated as:

$$I_{dc_{IndDis}} = I_{Peak} e^{-\frac{(t-t_{Peak})}{\tau}} \qquad Eq.\ 18$$

In this equation, $I_{dc_{IndDis}}$ is the current coming from the discharge of DC inductors, I_{Peak} is the peak of DC fault current which was calculated in the previous step, and τ is time-constant of the current passing in this circuit ($\tau = \frac{2L_{DC}}{R_{Fault}+R_{eq}}$). Eq. 18 shows that the DC current coming from the super-position by only considering discharge of DC inductors will decrease exponentially as we are dealing with a RL circuit.

As it was mentioned, after pole to pole fault, AC side acts as three-phase short circuit; in steady state, a sinusoidal current will be present and in transient, there will be an additional decaying exponential current. The current on AC side can be calculated as:

$$i_{ac}(t) = I_{3PhShC_{Peakss}} \sin(\omega t + \alpha - \varphi) + \left[I_{ac} \sin(\alpha - \varphi_0) - I_{3PhShC_{Peakss}} \sin(\alpha - \varphi)\right] e^{-\frac{(t-t_{Peak})}{\tau}} \qquad Eq.\ 19$$

In this equation:

$I_{3PhShC_{Peakss}}$: *The peak of AC steady − state current after* 3 − *phase short circuit* (*or DC fault*)

$\omega = 2\pi f$ (100π) , α: *the phase reference of the three phases* $(0{,}120^{\circ}, 240^{\circ})$

I_{ac}: *The peak of AC current in nominal* (*normal*)*conditon* (*before fault*)

φ_0: *Phase of the desired AC phase at the fault moment*

$I_{3PhShC_{Peakss}}$ can be calculated like following:

$$I_{3PhShC_{Peakss}} = \frac{\sqrt{2}v_{AC}sin(\omega t + \varphi)}{\sqrt{R_T^2 + X_T^2}} \qquad Eq.\ 20$$

In this formula, v_{AC} is the line to line RMS voltage of AC grid on the secondary of transformer (for example in the retained study case, $v_{AC} = 12\ kv$) and $Z_T = R_T + jX_T = R_T + j\omega L_T$ is the total impedance seen by AC grid (transferred all to the secondary of transformer) which mainly includes transformer and AC filter inductances.

Moreover, φ and time constant of the decaying exponential term in the transient (τ) are:

$$\varphi = arctan\left(\frac{\omega L_T}{R_T}\right) \quad , \quad \tau = \frac{L_T}{R_T} \qquad Eq.\ 21$$

Based on Eq. 19, current of a phase on the AC side is shown in Figure 42.

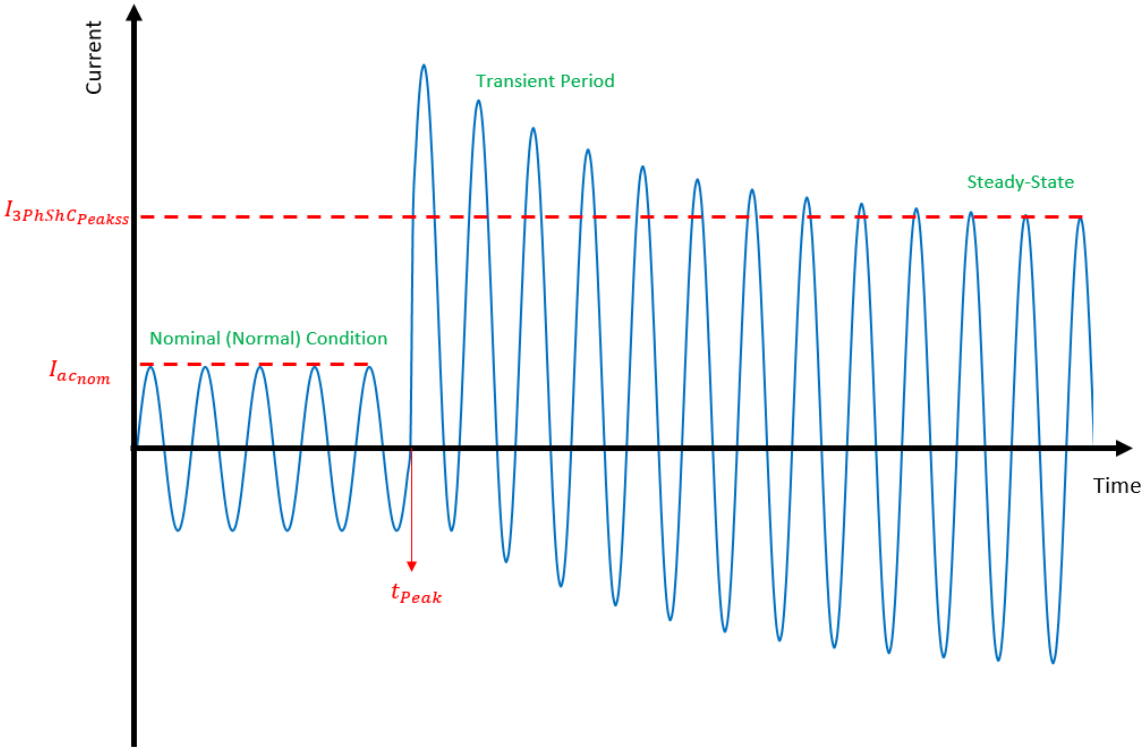

Figure 42 : Current of an AC Phase after DC Pole to Pole Fault on the Converter

During this stage, if the rectified current coming from the AC grid is more than the DC current coming from discharge of DC inductors, it will be dominant (based on Eq. 16) and if in opposite, the current coming from the DC inductors is higher, this current becomes dominant and the following equation is present:

$$i_{dc}(t) = I_{dc_{IndDis}} = i_{dc}(t_0)e^{-\frac{(t-t_0)}{\tau}} \qquad Eq.\ 22$$

In this equation, $t_0$is the instant which current coming from discharge of DC inductor becomes dominant on the rectified current of AC grid. Overall, DC fault current always follows one of these currents (mentioned in Eq. 16).

Step 3 (Steady State): In steady state, the transient effect of the DC current coming from the discharge of DC inductors will be fully disappeared and based on the Eq. 16, the DC current will be only given by the rectified AC three-phase short circuit current. In other words, the DC steady state current is peak of AC three phase short circuit current rectified by converter diodes and filtered by LC filter in the DC side. This value was given in Eq. 20.

5.4. Simulation Tool and Modelling

To analyze the fault in the proposed study case and study its impacts on the AC-DC converter, a model was developed and simulated in MATLAB Simulink SimPowerSystem based on the study case shown in Figure 28. The model is shown in Figure 43.

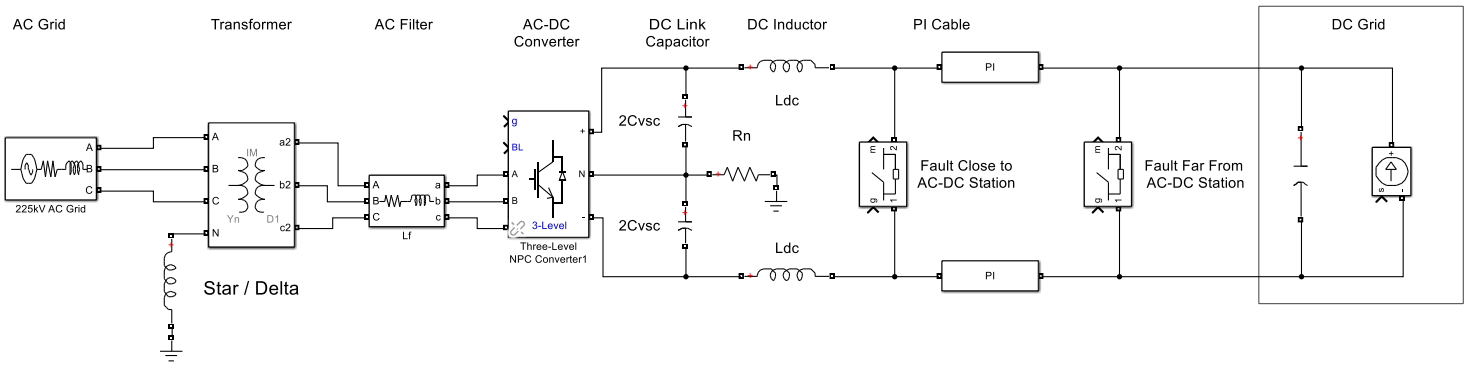

Figure 43 : The Schematic of the Simulated Model in MATLAB Simulink SimPowerSystem

Modelling MVDC Line: The MVDC line is modelled with an equivalent PI model per DC pole. The equivalent circuit of the MVDC line in two poles is shown in Figure 44 and the pole to pole equivalent circuit of the two MVDC lines is shown in Figure 45.

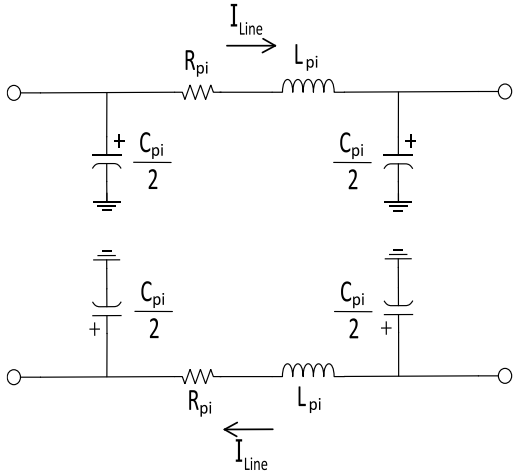

Figure 44 : The Equivalent Circuit of the MVDC Lines in Each DC Pole

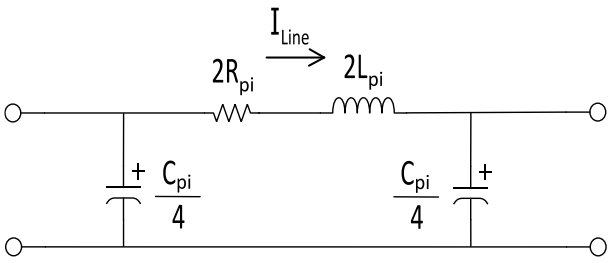

Figure 45 : The Total Pole to Pole Equivalent Circuit of the MVDC Line

5.5. Simulation Results

To simulate the network and verify the theoretical analysis done in pervious section, the model shown in Figure 43 is used. Figure 46 shows the DC current analyzed by theory, DC current obtained in simulation, and the current of phase A in AC side of the converter.

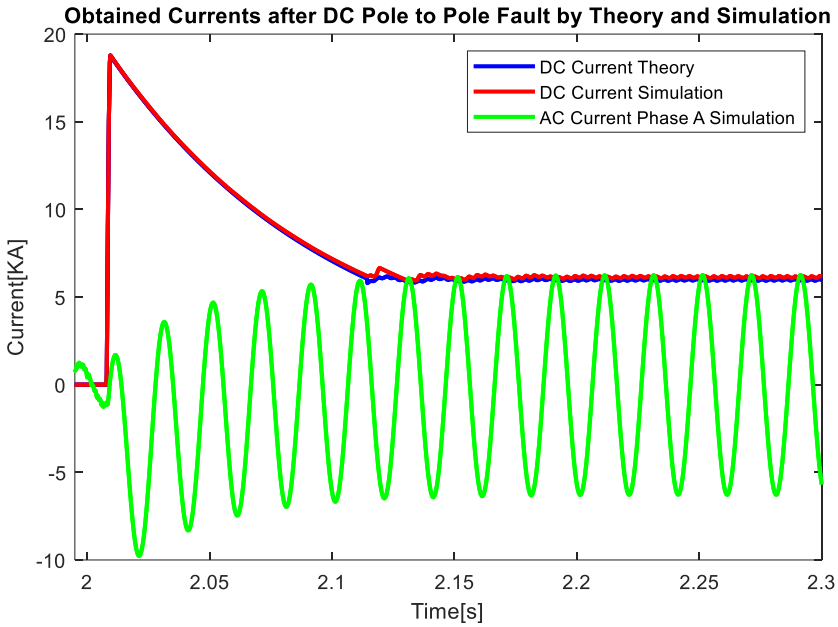

Figure 46 : The DC Current Achieved by Theory and Simulation Comparison and Phase A of AC Current

This figure confirms the assumptions of the previous analysis and the three steps of the network response are clear in this figure. Moreover, Figure 47 verifies that in all the process of fault in DC side, AC side acts like occurring a three-phase short circuit before the converter.

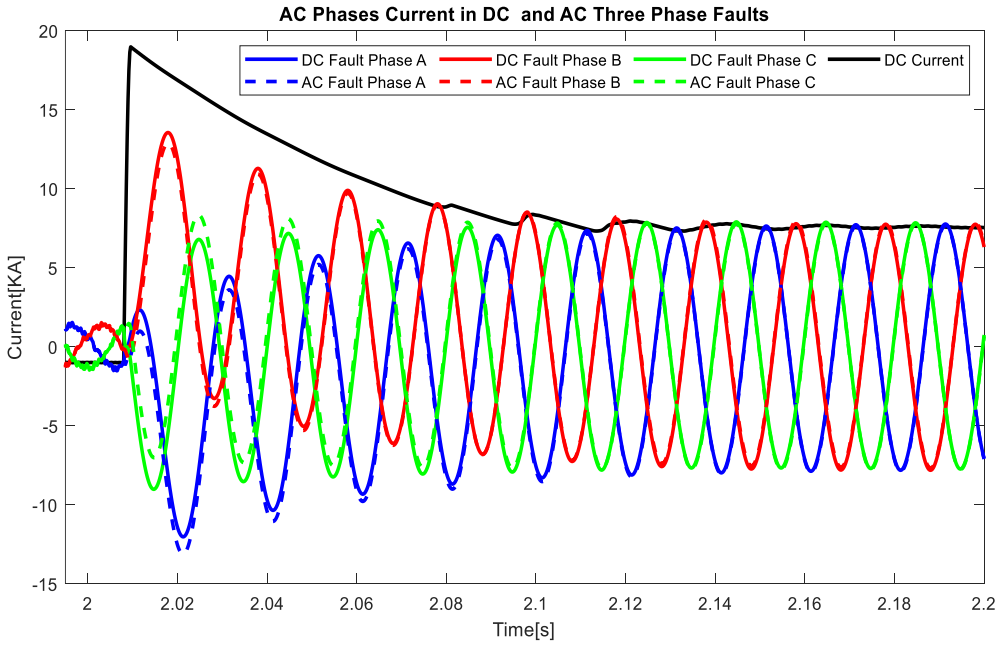

Figure 47 : The AC Phases Currents Comparison for a DC Pole to Pole Fault and AC 3-Ph Fault

5.6. Impact of DC Faults on AC-DC Converter

To analyze the impact of this fault on the AC-DC converter equipment, the current passing by each semiconductor is studied. Figure 48 shows the current passing by all diodes of one converter leg (phase).

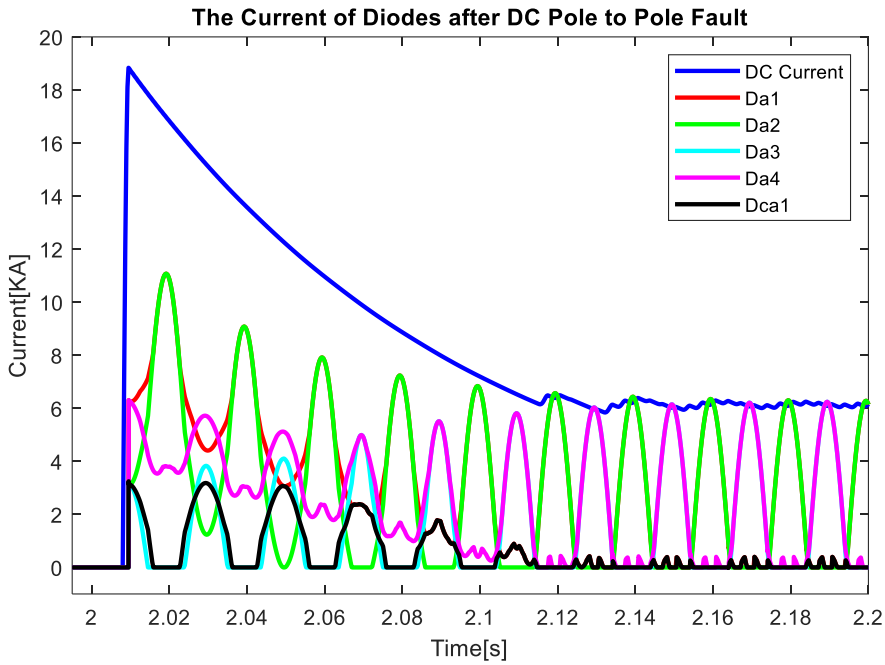

Figure 48 : Current Passing by Diodes of Converter in Phase A after DC Pole to Pole Fault

This figure shows that after DC pole to pole fault, the current of diodes in the converter can reach to a high amount, as an example, current of diode Da1 and Da2 has reached to approximately 12 kA. Considering the thermal limitation of diodes, the high level of currents could damage them. A parameter describes this limitation, is called 'Surge Current Integral' and it is expressed by I^2t. This parameter is limited for diodes. For any application, the value of I^2t must be always kept lower than the maximum allowed value. In the available IGBTs, this parameter is specified on a half-cycle basis. Assuming the amplitude I_{FSM} (the maximum allowable non- repetitive half-sine wave surge current) for the half-sine wave current, the surge current integral I^2t can be calculated based on Standard IEC 60747 as following:

$$\int_0^{t_p} I^2(t)dt = \frac{1}{2}.I_{FSM}^2.t_p \qquad \textit{Eq. 23}$$

In this formula, t_p is the time duration of half of sine-wave period. For example in the AC system with the frequency of 50 Hz, t_p is 10 ms.

This parameter can mostly be found on datasheet of semiconductors. In the retained IGBT for this study case, this parameter is 0.47 MA^2s. Figure 49 shows the variation of this parameter for diode Da1 (See Figure 34) after fault. In this figure, it is clear that approximately 20 ms after fault, the I^2t of this diode violates the maximum allowed value (0.47 MA^2s of I^2t is shown with a red Δ in Figure 49).

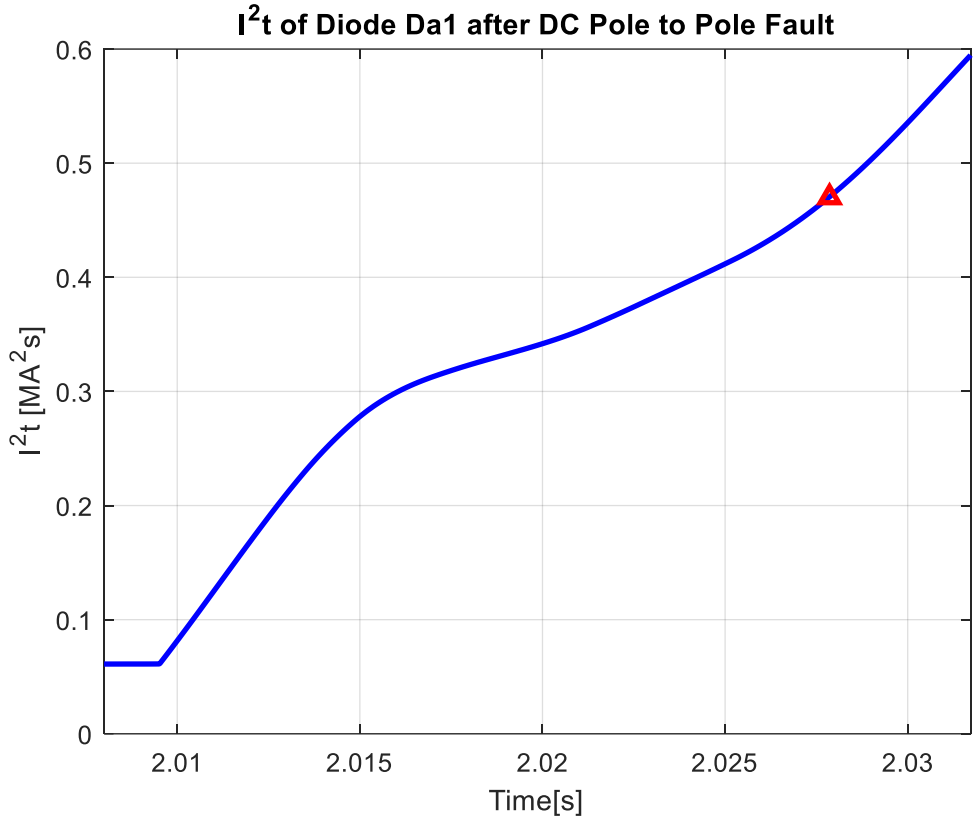

Figure 49 : I^2t of Diode Da1 after Fault

This violation could be a challenge and addresses the importance of proposing a solution to limit fault. But above that, it is important to analyze the impact of different parameters on current passing by diodes which potentially change this timing since it is needed to find the worst case which in the time to violate this constraint is minimum and protection must be fast enough to eliminate fault before that time.

5.6.1. Analysis of the impacts of different parameters

After identifying the problem, it is important to analyze the parameters which may affect on this issue. To find the worst case, i.e. the scenario which causes the maximum amount of current through diodes and so the maximum value of I^2t, different parameters and scenarios were analyzed which will be explained in the following.

Different Fault Moment Effect: In this scenario, the effect of having the fault at different moments of the AC cycle. To do this analysis, a fault at different moments (different AC cycle phase) was simulated and to compare the results, the DC currents obtained from simulation for all the different fault moments have been shifted to t=2s. Figure 50 shows results of this analysis.

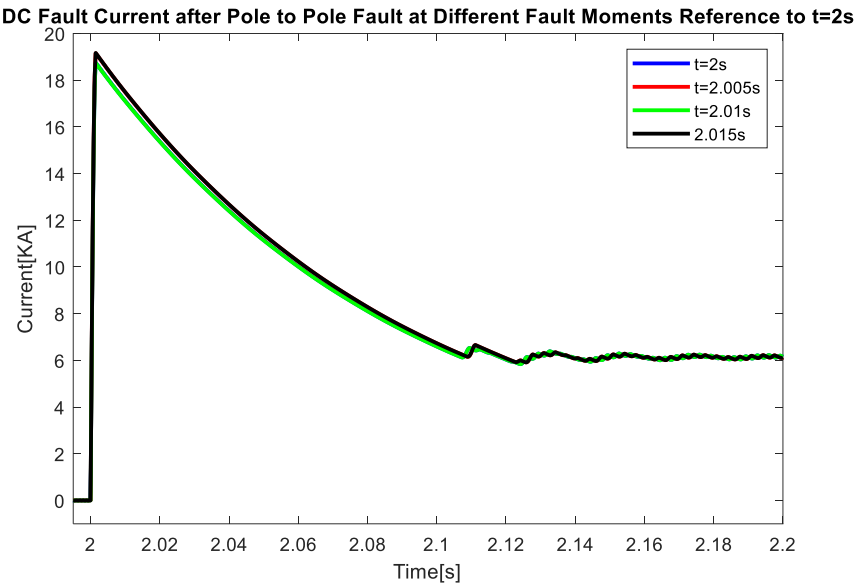

Figure 50 : DC Fault Current at Different Fault Moments in Reference to the Fault at t=2s

This figure shows that when the fault happens at different moments of the AC cycle, it has no impact on the DC fault current. This can be also verified by the theory which was mentioned previously. The reason is that in all the steps which were explained, the phase angle parameter did not exist in any equation and this confirms that the DC fault current is independent from fault moment.

Now, analyzing the impacts on the diodes, Figure 51 shows the I^2t of diode Da1 for the DC fault at different moments with reference to the fault at t=2s (i.e. all the I^2t obtained by different fault moments are shifted to t=2s). This figure represents the strong impact of fault moment on the current of the diode and as it can be seen, at 9.1 ms after fault, the I^2t of this diode has exceeded the maximum allowed (0.47 MA^2s). This shows that without a proper protection solution, in 9.1 ms after the DC pole to pole fault, some diodes of the converter will be damaged.

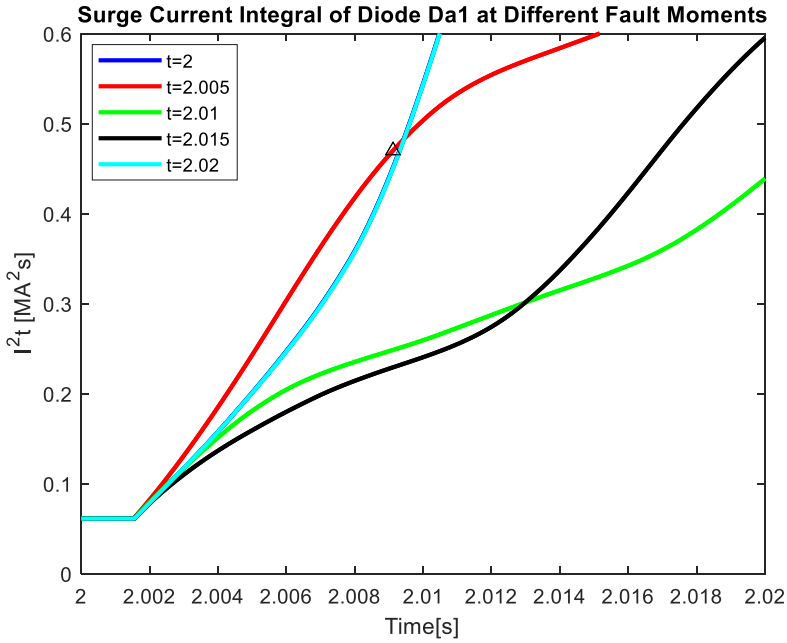

Figure 51 : I^2t of Diode Da1 after DC Pole to Pole Fault at Different Moments in Reference to the Fault at t=2s

DC Inductor Effect: As it was explained in Section 5.2.2 that the purpose of the DC inductor is to limit di/dt rate during faults. Figure 52 shows the effect of this parameter value on the DC fault current.

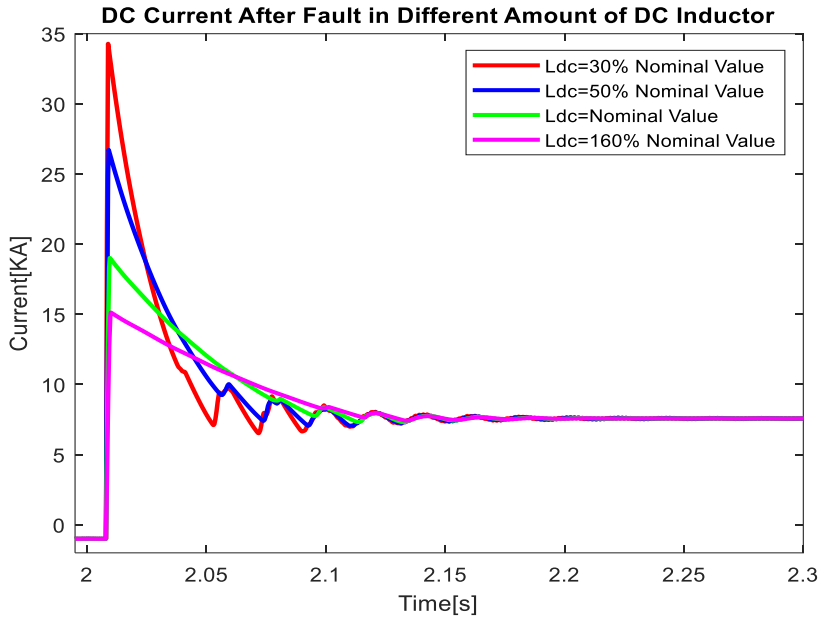

Figure 52 : The Impact of DC Inductor Value on the DC Fault Current

This analysis show the impact of DC inductor on the peak of DC fault current and during step 2 (explained in Section 0). Larger DC inductors can significantly limit the peak current while for lower DC inductors, the DC current peak value is higher. In addition with larger DC inductors, the needed time for protection action is longer while with lower DC inductors, protection system must act faster and this can be a serious constraint to design it. Regarding the protection of the AC-DC converter, a large value of DC inductor is preferable, however the cost of this inductor will be higher so a trade-off between cost and the di/dt limiting characteristic of this inductor must be performed.

AC Filter Inductance Effect: As it was explained in Section 5.2.2, AC filter is mainly used to decrease the THD of the current being injected by the converter in the AC system. According to the analysis done on Section 0, the value of this filter will change the steady-state current of AC three-phase short circuit (based on Eq. 20), it is expected that the steady-state value of DC fault current is dependent on the value of AC filter inductance. Figure 53 confirms these statements. The AC filter inductance has only one impact on the steady-state current and variation of this filter will not have any impact on the DC peak current.

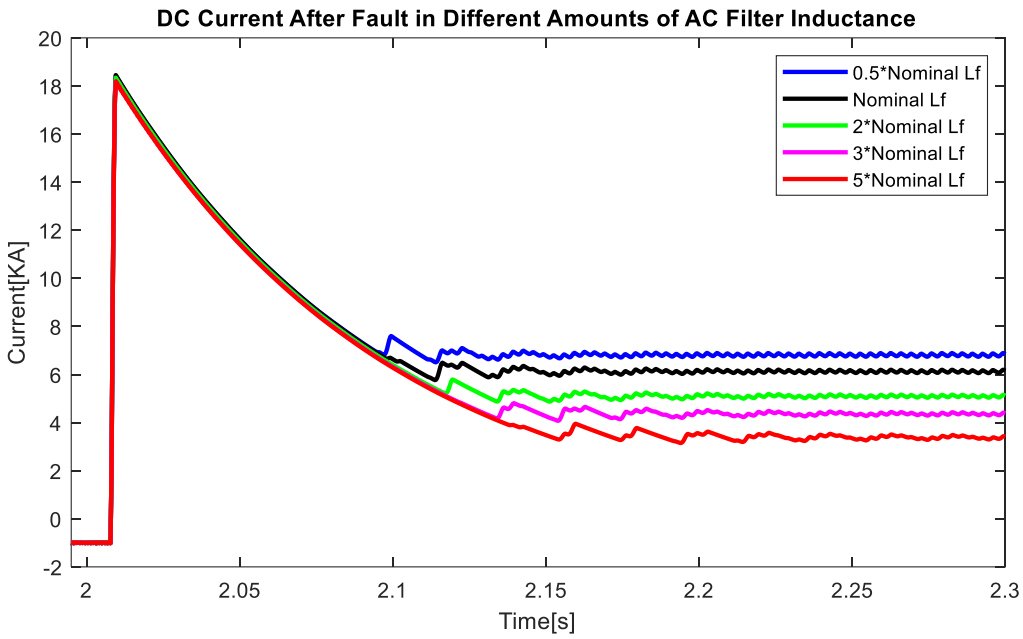

Figure 53 : Impact of AC Filter Inductance on the DC Fault Current

The Effect of Fault at Further Distances from AC-DC Station: In this part, the impacts of different fault distances from converter is analyzed. As it was explained, the MVDC line in each pole is modelled as a PI cable with series resistance-inductances and shunt capacitances. The pole to pole equivalent model of the MVDC lines in two poles was shown in Figure 45. Figure 54 presents the shape of DC fault current for fault at different distances from AC-DC station. In this figure, the reduction of peak of DC fault current by increasing the fault distance is clear and also it shows that the peak does not occur by discharge of DC link capacitors. The reason behind this is the interference of the impedances of MVDC line in the fault current. If we consider the equivalent circuit of the converter without considering AC side, as the impedance on the DC side has been increased, this will change the DC current coming from the equivalent circuit and also the rectified AC three-phase short circuit will be seen faster in the DC fault current (based on Eq. 16).

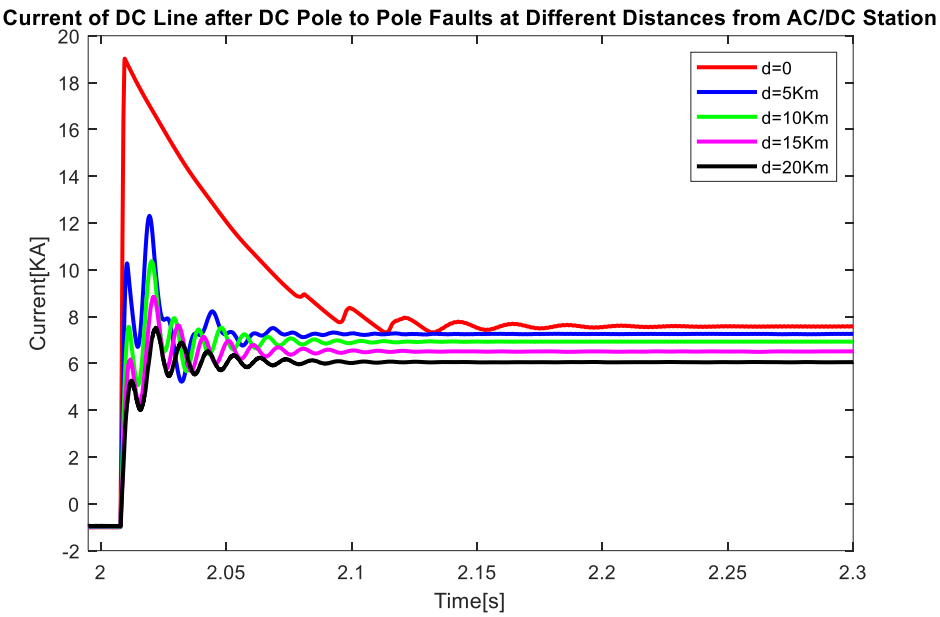

Figure 54 : The Effect of Fault at Different Distances from AC-DC Station on DC Fault Current Passing through DC Inductors

Overall, Figure 55 shows the impact of fault distance on the peak and steady state values of DC fault current. It can be seen that the peak of DC current will be reduced significantly by increasing fault distance.

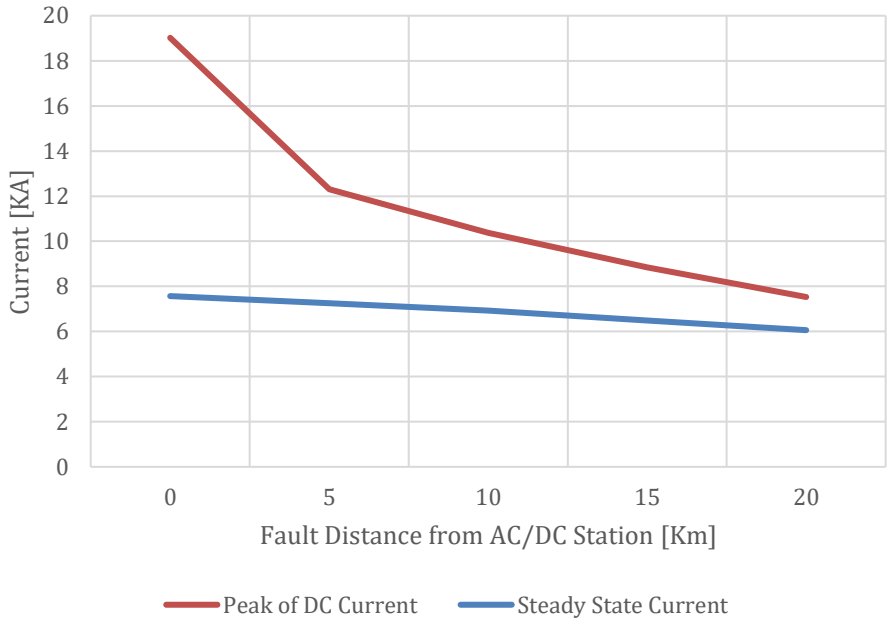

Figure 55 : The Effect of Fault Distance on Peak and Steady-State Values of DC Fault Current

Figure 56 and Figure 57 show the rising time to reach the peak and damping time of the DC fault current for fault at different distances from AC-DC station, respectively.

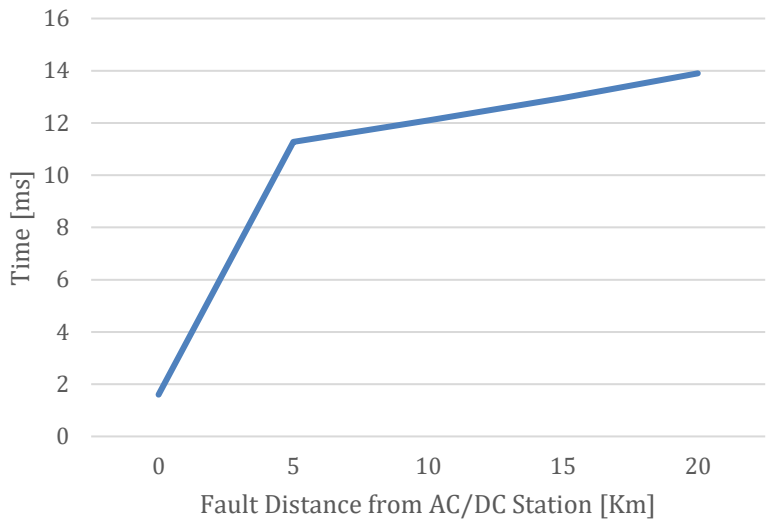

Figure 56 : The Effect of Fault Distance on the Rising Time to Reach the Peak of DC Fault Current

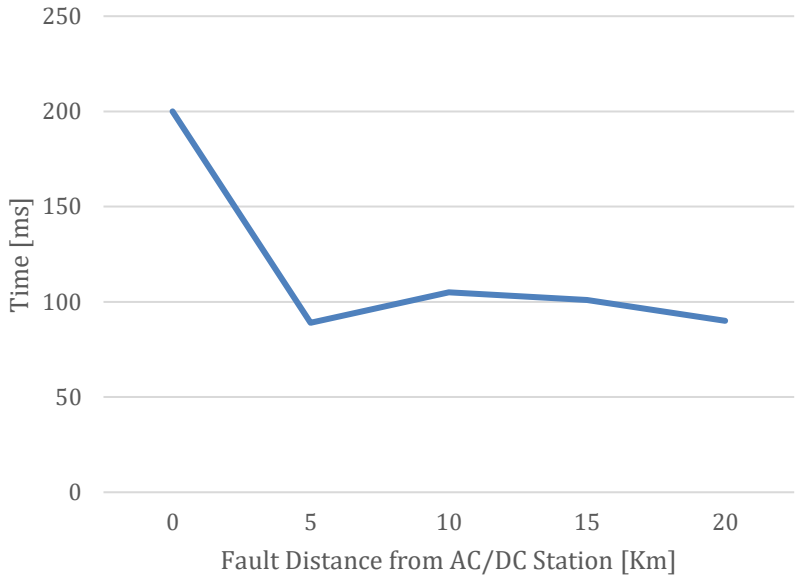

Figure 57 : The Effect of Fault Distance on the Damping Time of DC Fault Current

A reason for increasing the rising time may be the increase in the inductances on the DC which increases the time constant of the line. For faults at very far distances (> 25 km) from AC-DC station, the amount of DC impedance will be very large and no peak will be seen as the fault current will be fully damped by these impedances. So, the maximum fault currents for these cases is equal to the steady-state current.

Effect of Fault at Different Moments and Distances from AC-DC Station: Even if fault happens at a further distance from AC-DC station, there will be no impact by different fault moments on the DC fault current. This means that in further distances which AC rectified current will be dominant on the current coming from discharge of DC inductors (Step 2 of the fault explained in section 0), this current will be the same at different fault moments and overall, the DC fault current will not change. Figure 58 shows the DC fault current after a pole to pole fault at 20 km from AC-DC converter addressing different fault moments with a reference to fault at t=2s.

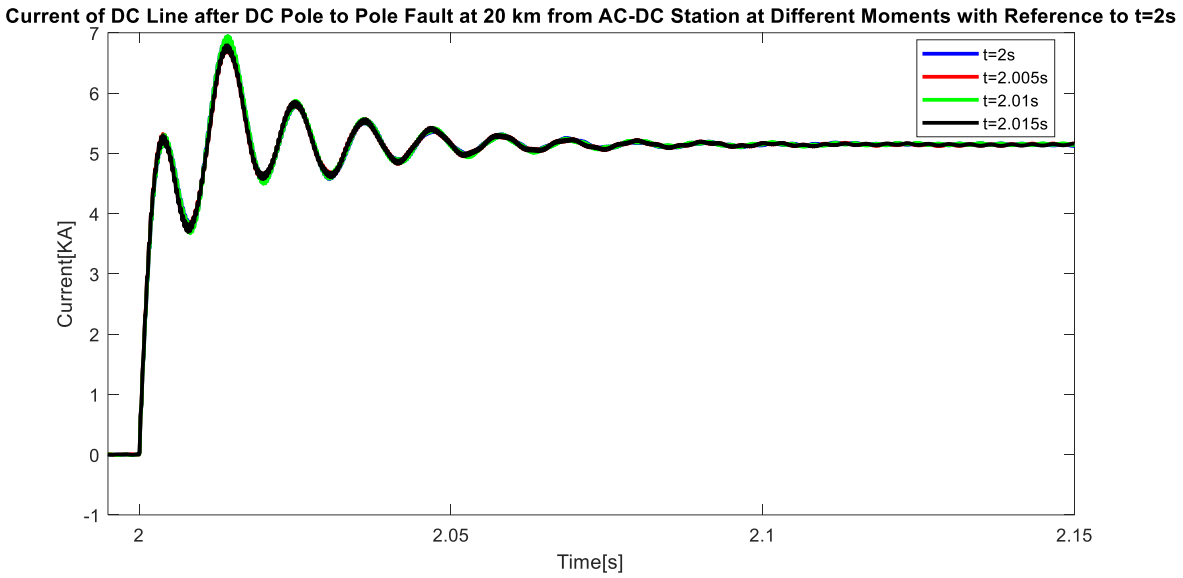

Figure 58 : DC Fault Current after Pole to Pole Fault at 20 km from AC-DC Converter at Different Fault Moments in Reference to the fault at t=2s (Shifted all the Waveforms to this moment)

All these analysis show that the worst case is when the DC inductor (L_{DC}) is low and fault happens at t=2 or t=2.005 (90˚ or 270˚) (for diode Da1).

5.7. Comparison between Impacts of DC Fault on NPC and Two-Level Converters

In Section 5.2.1, it was explained that DC faults was analyzed on two-level converters in some publications. The analysis of differences between responses of the AC-DC converters with 2-level and NPC topologies can be interesting. The only main difference between these topologies is the existence of clamping diodes in the NPC converter (See diodes Dca1 and Dca2 in the phase A of the converter in Figure 31). Assuming that main number of diodes in these topologies is the same (in 2-level, we have two switches per switch in the topology), Figure 59 shows the results with two-level and NPC topologies (Figure 11 shows the schematic of 2-level topology).

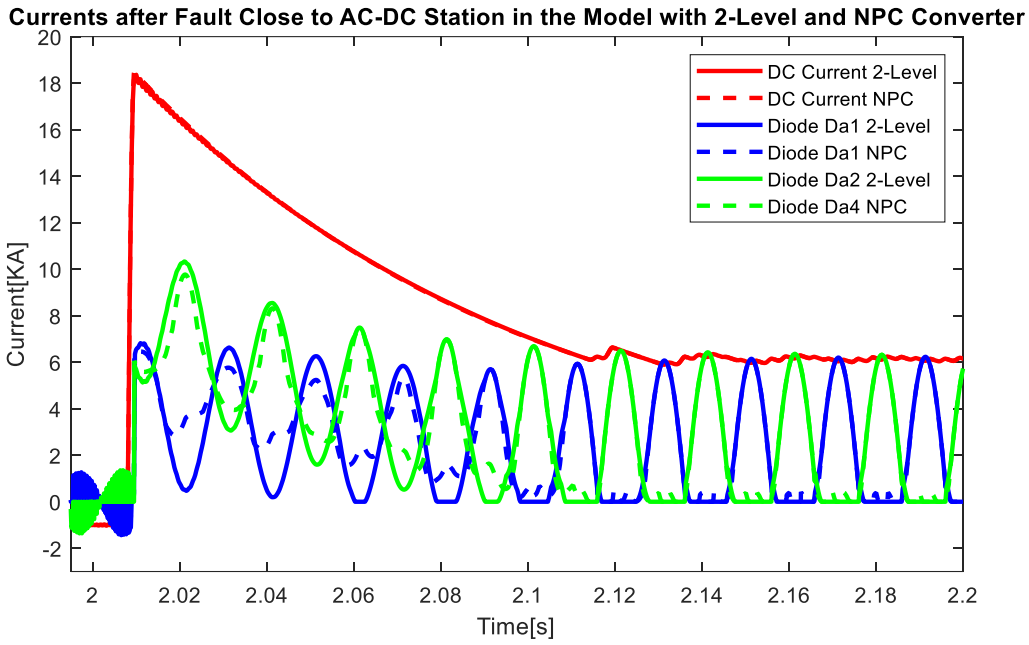

Figure 59 : The Comparison of Current after DC Pole to Pole Fault in Different Topologies of AC-DC Converter

This figure has two important results:

- The DC fault current in both topologies is the same. This is verifying the three steps which were proposed to theoretically analyze DC pole to pole fault on AC-DC converter.
- This figure also shows that peak of current passing by the diodes in these topologies is approximately the same, however there is a little difference which is due to the clamping diodes. Since the peak of current in both topologies is approximately the same, this analysis which was done foe NPC topology is also valid for 2-L converter.

As a perspective, the current passing by clamping diodes after DC fault on NPC topology can be studied. This might be necessary for dimensioning diodes with the appropriate I^2t.

Chapter 6

Study of Over-voltage in the MVDC Networks

6.1. Purpose

The motivations behind MVDC networks were explained in Section 2.3. These networks have the potential of hosting renewable energy sources in for example railway applications [76]. Moreover, there has been an interest in implementing these networks with integrated power sources for example on ships [20] [77]. Hence, there may be some issues related to the interaction between DC network elements and AC-DC converter. In this chapter, the focus is on the over-voltage phenomenon which happens in MVDC networks. No publication about this problem in HVDC applications was found however it might be present. The reason behind this over-voltage problem is explained in detail and the possible solution to prevent or limit it is proposed.

6.2. Study Case

The study case used for studying this problem is the previous one which was explained in the fault chapter. The only difference is the participation of renewable sources in the MVDC grid which are connected to the MVDC lines via a voltage source converters. The single line diagram of the study case is shown in Figure 60.

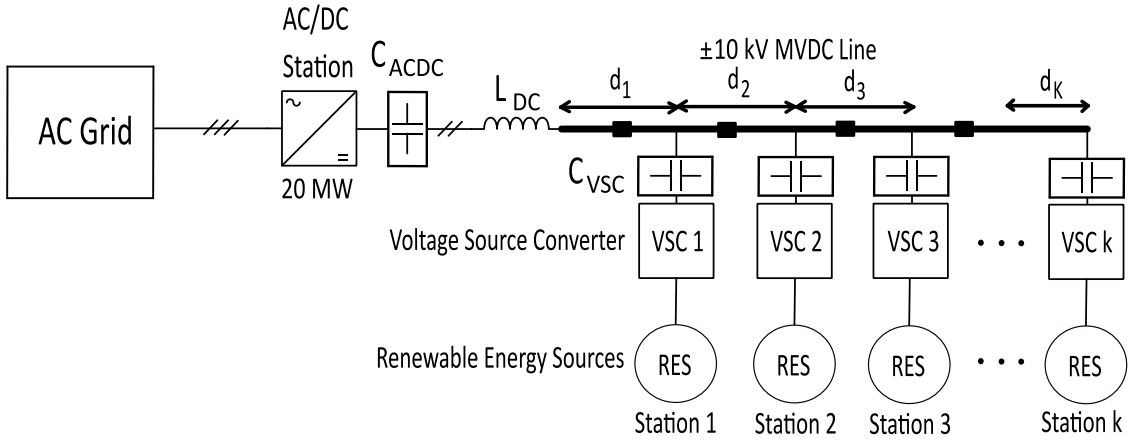

Figure 60 : Single Line Diagram of the Study Case Network

In this study case, K number of RES stations are connected to the MVDC. The distance between these stations are shown with d_1, d_2, d_3,..., and d_K. This distance will change the parameters of cables (PI Model) between these stations. Table 5 shows some parameters of this study case.

Network Component/Parameter	Component Specification
Number of RES Stations	K
MVDC Line Length	d_{total}
Distance Between Stations	$d_1 = d_2 = d_3 = \cdots = d_K = \frac{d_{total}}{K}$
RES Station Injected Power and Current	$Each\ RES: P_{RES} = \frac{20\ MW}{K}, I_{RES} = \frac{P_{RES}}{20\ kV}\ (Totally\ 1\ kA)$
VSCs Capacitance (C_{VSC})	$C_{VSC} \ll C_{ACDC}$ (Since Power of AC-DC converter is several time higher than the power of each VSC)

Table 5 : The Scpecification of some of the Elements of the Study Case Network

It is also assumed that there is no communication between RES stations and the AC-DC station.

6.3. Theoretical Analysis

In a normal condition (steady state) of this network, 20 MW power is injected by renewable sources to the AC grid in a 20 kVdc pole to pole bus. The AC-DC station controls the DC voltage.

If for any reason due to an internal fault or an intentional reason, the AC-DC converter is blocked (all IGBTs are open), the VSCs connected to the renewable sources do not necessarily detect this blocking. As a consequent, they will maintain injecting power into the MVDC line, which will make the DC voltage to vary from the nominal value. The controllers of VSCs are designed in a way to block them if their DC voltage goes out of a pre-defined margin of 1.1 p.u. (22 kV).

Figure 61 shows the detailed schematic of the network after blocking AC-DC converter and it can be seen that after blocking, AC-DC converter is isolated from DC network. Here, it is assumed that however by blocking AC-DC station and opening all IGBTs, AC and DC sides are still connected via converter diodes, as long as the voltage on DC side does not go below the AC grid rectified value, diodes do not conduct and they can be ignored.

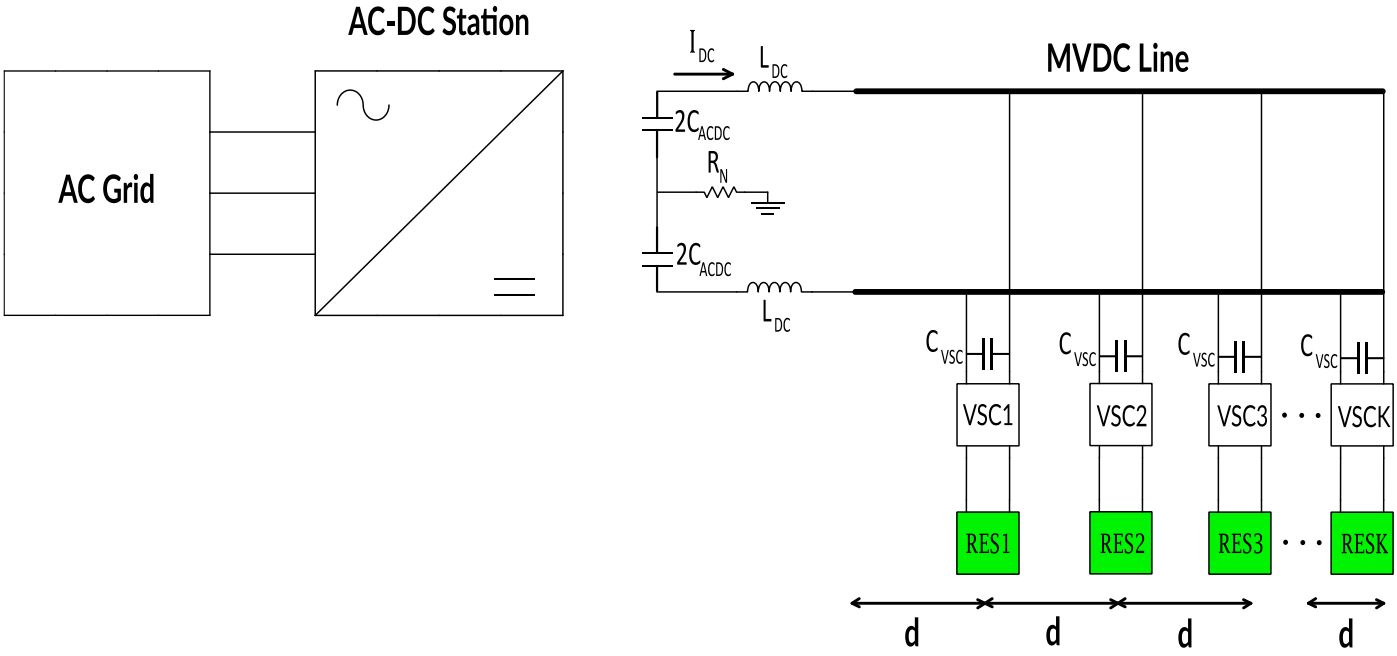

Figure 61 : The Schematic of the Network after Blocking the AC-DC Converter

By blocking the AC-DC station, the VSCs keep injecting power into the DC grid. Since the DC side is no longer controlled by AC-DC station, the voltage of MVDC grid will increase. Soon after by hitting the upper-limit of 1.1 p.u. (22 kV), the controllers of VSCs block all of them. The schematic of this step after blocking all the VSCs connected to RES station has been shown in Figure 62 (the assumption in previous part for blocking AC-DC station is present in this condition as well and diodes are VSCs are ignored).

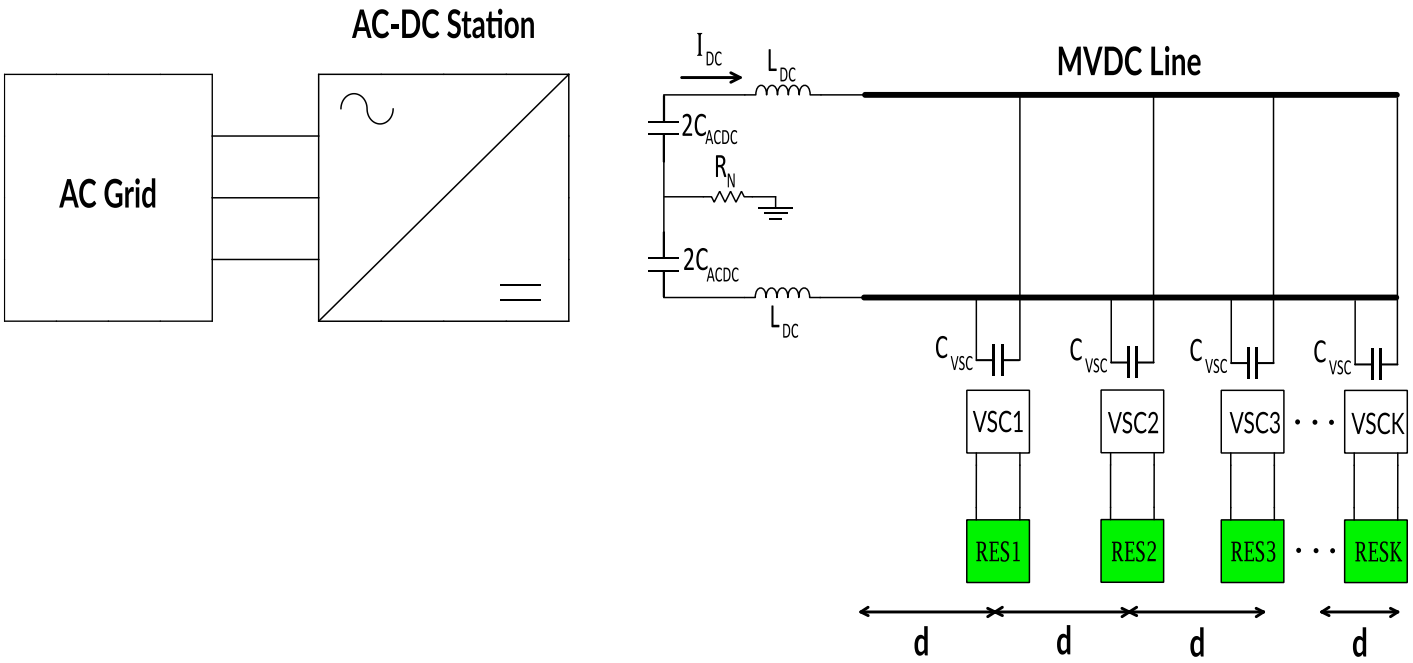

Figure 62 : Schematic of the Network after Blocking AC-DC Converter and the VSCs connected to RES Stations

At this moment, the passive elements of the network such as AC-DC capacitor and VSC capacitors, and the cable have been fully charged, they will start to discharge into the other elements of the network. A resonance phenomena occurs.

The equivalent circuit of the DC grid after blocking AC-DC converter and VSCs connected to the RES stations is shown in Figure 63.

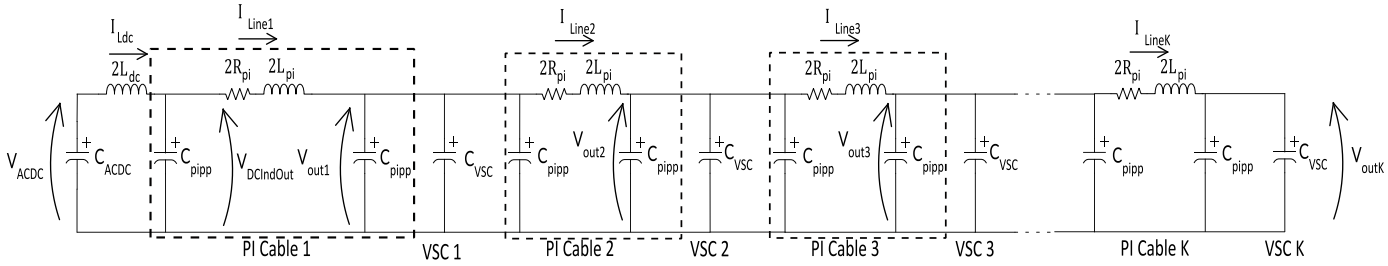

Figure 63 : The Equivalent Circuit of DC Grid after Blocking AC-DC Converter and the VSCs connected

In this circuit, C_{pipp} is pole to pole equivalent capacitance of the PI cable which is equal to $\frac{C_{pi}}{4}$ (See Figure 45). It is considered that all the capacitances are charged at 20 kV and the inductors are energized at the nominal current which was injected by the RES stations; for example, DC inductors see the maximum injected current which is equal to the total current injected by all the RES stations and it is 1 kA.

6.4. Equivalent Circuit Model

To simulate this phenomena and monitor the results, MATLAB Simulink SimPowerSystem is used.

At this point, only 4 RES stations are considered. Following table shows some of the specification of the network and the assumption which are made.

Network Component/Parameter	Component Specification
Number of RES Stations	K = 4
MVDC Line Length	20 km
Distance Between Stations	$d_1 = d_2 = d_3 = d_4 = d = \frac{Total\ MVDC\ Line\ Length}{K} = 5\ km$
RES Station Injected Power	$Each\ RES: \frac{20\ MW}{K} = 5\ MW, \frac{5\ MW}{20\ kV} = 250\ A\ (Totally\ 1\ kA)$
VSCs Capacitance (C_{VSC})	$C^*_{VSC} = 5\ C_{VSC} \ll C_{ACDC}$

Table 6: The Specification of some of the Elements of the Study case Network

Therefore, it is assumed that there are 4 main RES stations which each includes 5 renewable energy sources and the DC link capacitor for each VSC connected to these main stations include 5 VSC capacitors which was explained before.

The single line diagram of this network and SimPowerSystem model which was used to analyze this phenomenon are shown in Figure 64 and Figure 65, respectively.

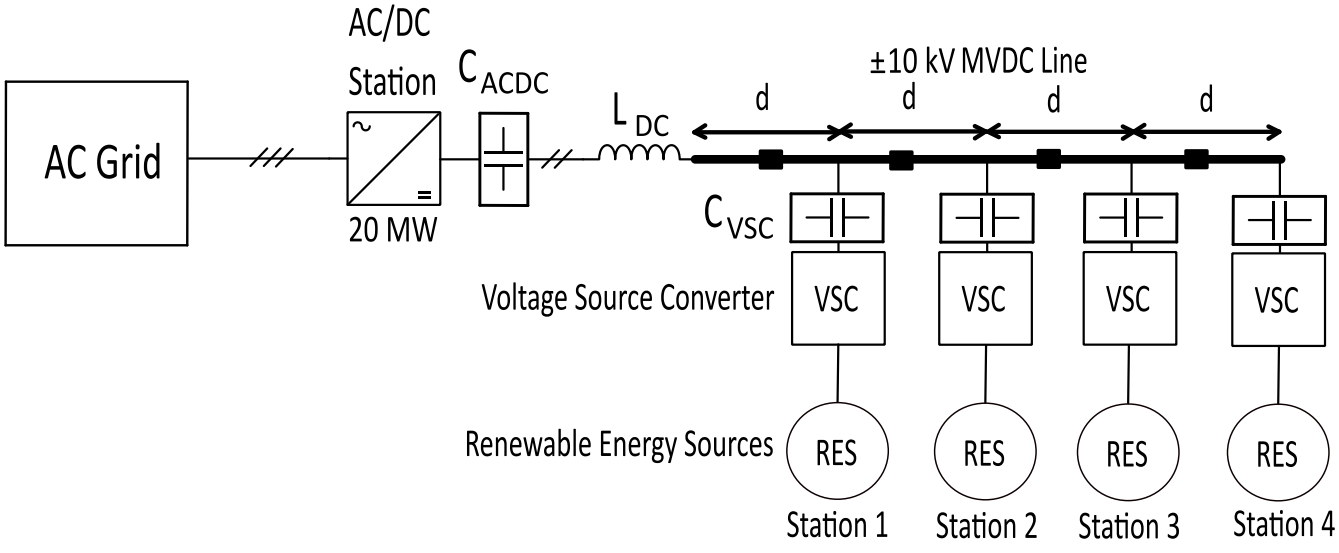

Figure 64 : Single Line Diagram of the Network with 4 Main RES Stations

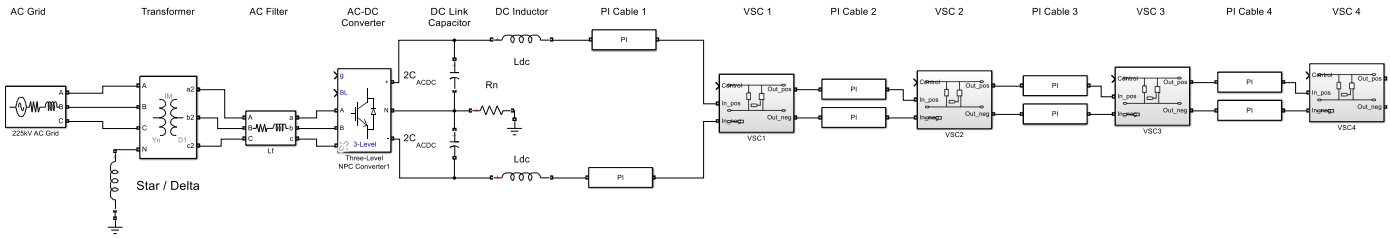

Figure 65 : The Simulation Model in MATLAB SimPowerSystem

In this model, the VSCs are modelled with a controlled-current source and a parallel capacitor which is C_{vsc}. The VSC model is shown in Figure 66.

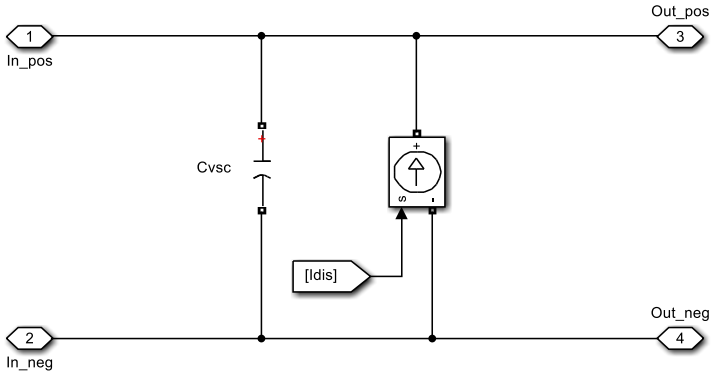

Figure 66 : Voltage Source Converter Model

6.5. Equivalent Circuit Simulation Results

Finally, by modelling the study case in the MATLAB SimPowerSystem, we can observe that an over-voltage appears caused by the resonance of the passive elements of the grid. This is shown in Figure 67. In the simulation, we assume that the AC-DC converter is blocked at t=2s.

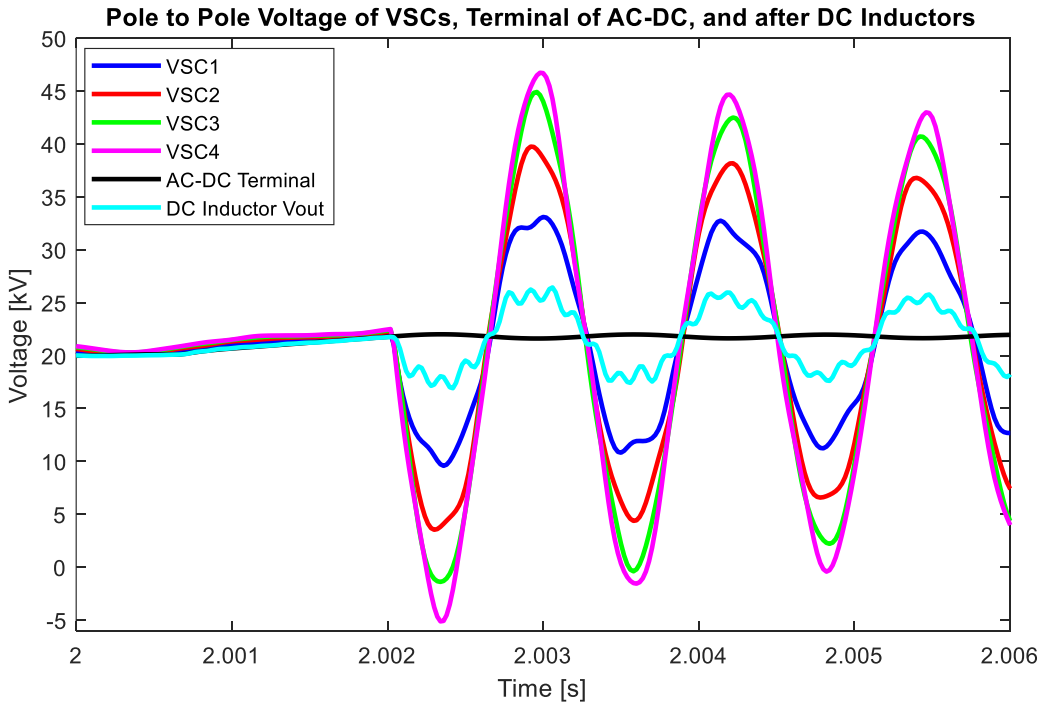

Figure 67 : The Voltages of DC Grid after Blocking AC-DC Station

This figure clearly shows that after blocking AC-DC converter, the RES stations have injected power to the DC grid and this has increase the voltage to 1.1 p.u. (22 kV) which has caused blocking VSCs as well. After that, due to the resonance loop, the voltage of VSCs have been increased. The following table shows the over-voltage amount seen at different nodes of the DC grid.

DC Grid Location	Pole to Pole Over-voltage
AC-DC Terminal	2 kV (0.1 p.u.)
Output of DC Inductor	6 kV (0.3 p.u.)
VSC 1	13 kV (0.65 p.u.)
VSC 2	20 kV (1 p.u.)
VSC 3	25 kV (1.25 p.u.)
VSC 4	26 kV (1.3 p.u.)

Table 7 : The Amount of Over-voltage at Different Locations of the DC Networks

It can be seen that:

- Voltage on the terminal of AC-DC converter is almost not affected by this phenomenon and it has remained in the acceptable range.
- Voltage of all VSCs and the output of DC inductors have been significantly affected in this phenomenon and it is visible that the distance from AC-DC station has a direct relationship with the amount of over-voltage; further locations from AC-DC station will have more over-voltage and therefore, the further VSC which is VSC 4 has the maximum over-voltage.

6.6. State-Space Model

In previous section, the over-voltage issue within a model with few number of stations was analyzed and some assumptions were considered. But a more appropriate method to analyze the real system with higher number of RES stations (K=40 for example) is needed. This can be done mathematically by a state-space modelling of the DC grid including the AC-DC converter. Power, voltage of the network remain constant and other specification can be calculated using the table in Section 6.2.

In this model, AC-DC converter is modelled as a controlled-current source (with current I_{in}) and a parallel capacitor which is C_{ACDC}. The control signal of this current source comes from a controller which changes the input current injected by converter following the change in the output DC pole to pole voltage. The control scheme is shown in Figure 68.

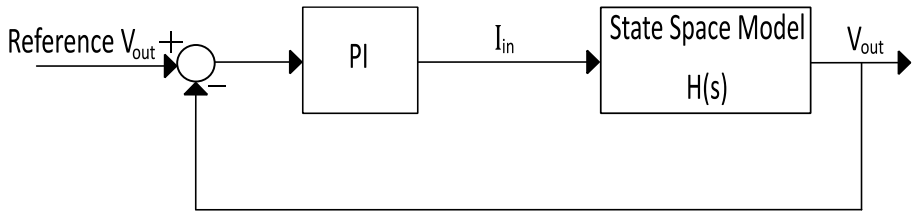

Figure 68 : Control Scheme Applied in the State-Space Model

In this scheme, the reference output voltage is the desired voltage set-point which is 20 kV and the V_{out} is the voltage measured on the capacitor C_{ACDC}.

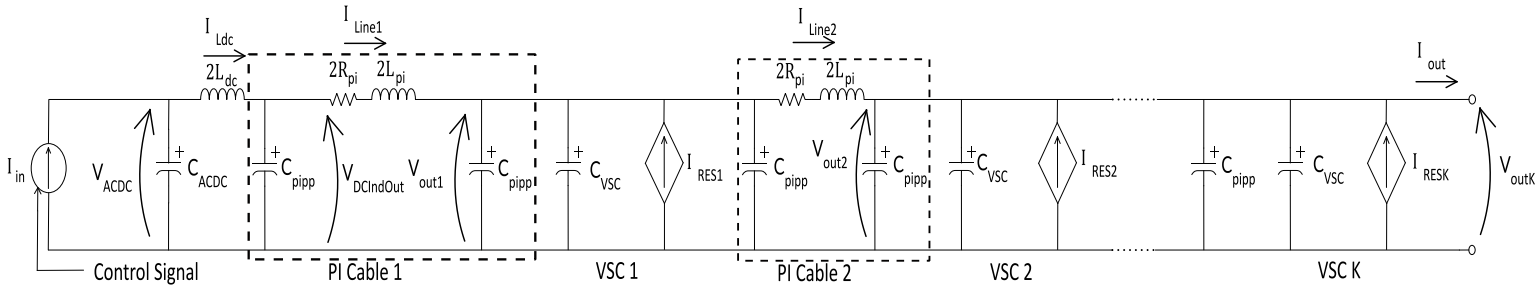

Figure 69 : Equivalent Circuit of the DC Grid Including AC-DC Converter

The equivalent circuit of the DC grid considering the AC-DC converter is shown in Figure 69.

In this circuit, I_{RES_i} is the current injected by RES station (i) and it is assumed that all the stations inject the same power and current. Totally 1 kA is injected to the AC grid by RES stations.

The state space model is described by Eq. 24, where state space variables (X) are the current of the inductors and voltage of the capacitor. U is the matrix of the system inputs, i.e. the currents I_{RES_i}

being injected by RES stations and the current on the AC-DC station, I_{in}. Matrix U has been given by Eq. 25.

$$\begin{cases}\dot{X} = A.X + B.U \\ Y = C.X + D.U\end{cases} \qquad \textit{Eq. 24}$$

In these equations, X is the state-space vector and U is the vector input of the system (I_L: I_{line}).

$$X = \begin{bmatrix} V_{out1} \\ I_{L1} \\ V_{out2} \\ I_{L2} \\ \vdots \\ V_{outK} \\ I_{LK} \\ V_{DCIndOut} \\ I_{Ldc} \\ V_{ACDC} \end{bmatrix}, U = \begin{bmatrix} I_{in} \\ I_{RES1} \\ I_{RES2} \\ \vdots \\ I_{RESK} \\ I_{out} \end{bmatrix} \qquad \textit{Eq. 25}$$

Now, to find the relationships between state-space parameters and the system inputs based on the Eq. 24., the KVL and Kirchhoff Current Law (KCL) rules have been applied:

$$\begin{cases} C_t = 2C_{pipp} + C_{VSC} \\ I_{C_t} = I_{Line1} + I_{RES1} - I_{Line2} \\ I_{C_t} = C_t.\dfrac{dV_{out1}}{dt} = C_t.\dot{V}_{out1} \end{cases} \Rightarrow \dot{V}_{out} = \frac{I_{Line1}}{C_t} + \frac{I_{RES1}}{C_t} - \frac{I_{Line2}}{C_t} \qquad \textit{Eq. 26}$$

$$\begin{cases} V_{L_{pi}} + V_{R_{pi}} = V_{DCIndOut} - V_{out1} \\ V_{L_{pi}} = 2L_{pi}.\dfrac{dI_{Line1}}{dt} = 2L_{pi}.\dot{I}_{Line1} \end{cases} \Longrightarrow \dot{I}_{Line} = -\frac{1}{2L_{pi}}V_{out1} - \frac{R_{pi}}{L_{pi}}I_{Line1} + \frac{1}{2L_{pi}}V_{DCIndOut} \qquad \textit{Eq. 27}$$

$$\begin{cases} I_{C_{pipp}} = I_{in} - I_{Line1} \\ I_{C_{pipp}} = C_{pipp}.\dfrac{dV_{DCIndOut}}{dt} = C_{pipp}.\dot{V}_{DCIndOut} \end{cases} \Rightarrow \dot{V}_{DCIndOut} = -\frac{I_{Line1}}{C_{pipp}} + \frac{I_{Ldc}}{C_{pipp}} \qquad \textit{Eq. 28}$$

The other equations can be found similarly as repetitive blocks can be considered for any number of RES stations like following:

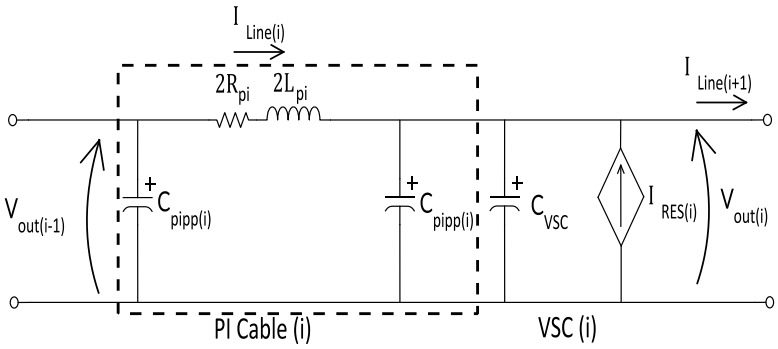

Figure 70 : Repetitive Blocks in the Circuit of State-Space Model

Figure 70 shows a block which is presenting each RES station and the cable before it (K blocks totally). Using this block and the KVL and KCL rules inside it, the equations for all the RES station can be found.

Finally, by finding all the equations, based on the Eq. 24, the matrices of A, B, C, and D for the retained study case can be found as following matrices:

$$A=\begin{bmatrix}
0 & \frac{1}{C_t} & 0 & \frac{-1}{C_t} & \cdots & 0 & 0 & 0 & 0 & 0 & 0 & \cdots & 0 & 0 & 0 & 0 & 0\\
\frac{-1}{2L_{pi}} & \frac{-R_{pi}}{L_{pi}} & 0 & 0 & \cdots & 0 & 0 & 0 & 0 & 0 & 0 & \cdots & 0 & 0 & \frac{1}{2L_{pi}} & 0 & 0\\
0 & 0 & 0 & \frac{1}{C_t} & \cdots & 0 & 0 & 0 & 0 & 0 & 0 & \cdots & 0 & 0 & 0 & 0 & 0\\
\frac{1}{2L_{pi}} & 0 & \frac{-1}{2L_{pi}} & \frac{-R_{pi}}{L_{pi}} & \cdots & 0 & 0 & 0 & 0 & 0 & 0 & \cdots & 0 & 0 & 0 & 0 & 0\\
\vdots & \vdots & \vdots & \vdots & \ddots & \vdots & \vdots & \vdots & \vdots & \vdots & \vdots & \ddots & \vdots & \vdots & \vdots & \vdots & \vdots\\
0 & 0 & 0 & 0 & \cdots & 0 & \frac{1}{C_t} & 0 & \frac{-1}{C_t} & 0 & 0 & \cdots & 0 & 0 & 0 & 0 & 0\\
0 & 0 & 0 & 0 & \cdots & \frac{-1}{2L_{pi}} & \frac{-R_{pi}}{L_{pi}} & 0 & 0 & 0 & 0 & \cdots & 0 & 0 & 0 & 0 & 0\\
0 & 0 & 0 & 0 & \cdots & 0 & 0 & 0 & \frac{1}{C_t} & 0 & \frac{-1}{C_t} & \cdots & 0 & 0 & 0 & 0 & 0\\
0 & 0 & 0 & 0 & \cdots & \frac{1}{2L_{pi}} & 0 & \frac{-1}{2L_{pi}} & \frac{-R_{pi}}{L_{pi}} & 0 & 0 & \cdots & 0 & 0 & 0 & 0 & 0\\
0 & 0 & 0 & 0 & \cdots & 0 & 0 & 0 & 0 & 0 & \frac{1}{C_t} & \cdots & 0 & 0 & 0 & 0 & 0\\
0 & 0 & 0 & 0 & \cdots & 0 & 0 & \frac{1}{2L_{pi}} & 0 & \frac{-1}{2L_{pi}} & \frac{-R_{pi}}{L_{pi}} & \cdots & 0 & 0 & 0 & 0 & 0\\
\vdots & \vdots & \vdots & \vdots & \ddots & \vdots & \vdots & \vdots & \vdots & \vdots & \vdots & \ddots & \vdots & \vdots & \vdots & \vdots & \vdots\\
0 & 0 & 0 & 0 & \cdots & 0 & 0 & 0 & 0 & 0 & 0 & \cdots & 0 & \frac{1}{C_t} & 0 & 0 & 0\\
0 & 0 & 0 & 0 & \cdots & 0 & 0 & 0 & 0 & 0 & 0 & \cdots & \frac{-1}{2L_{pi}} & \frac{-R_{pi}}{L_{pi}} & 0 & 0 & 0\\
0 & \frac{-1}{C_{pipp}} & 0 & 0 & \cdots & 0 & 0 & 0 & 0 & 0 & 0 & \cdots & 0 & 0 & 0 & \frac{1}{C_{pipp}} & 0\\
0 & 0 & 0 & 0 & \cdots & 0 & 0 & 0 & 0 & 0 & 0 & \cdots & 0 & 0 & \frac{-1}{2L_{DC}} & 0 & \frac{1}{2L_{DC}}\\
0 & 0 & 0 & 0 & \cdots & 0 & 0 & 0 & 0 & 0 & 0 & \cdots & 0 & 0 & 0 & \frac{-1}{C_{ACDC}} & 0
\end{bmatrix}$$

Eq. 29

$$B=\begin{bmatrix}
0 & \frac{1}{C_t} & 0 & \cdots & 0 & 0 & 0 & \cdots & 0 & 0\\
0 & 0 & 0 & \cdots & 0 & 0 & 0 & \cdots & 0 & 0\\
0 & 0 & \frac{1}{C_t} & \cdots & 0 & 0 & 0 & \cdots & 0 & 0\\
0 & 0 & 0 & \cdots & 0 & 0 & 0 & \cdots & 0 & 0\\
\vdots & \vdots & \vdots & \ddots & \vdots & \vdots & \vdots & \ddots & \vdots & \vdots\\
0 & 0 & 0 & \cdots & \frac{1}{C_t} & 0 & 0 & \cdots & 0 & 0\\
0 & 0 & 0 & \cdots & 0 & 0 & 0 & \cdots & 0 & 0\\
0 & 0 & 0 & \cdots & 0 & \frac{1}{C_t} & 0 & \cdots & 0 & 0\\
0 & 0 & 0 & \cdots & 0 & 0 & 0 & \cdots & 0 & 0\\
0 & 0 & 0 & \cdots & 0 & 0 & \frac{1}{C_t} & \cdots & 0 & 0\\
\vdots & \vdots & \vdots & \ddots & \vdots & \vdots & \vdots & \ddots & \vdots & \vdots\\
0 & 0 & 0 & \cdots & 0 & 0 & 0 & \cdots & \frac{1}{C_t} & \frac{-1}{C_t}\\
0 & 0 & 0 & \cdots & 0 & 0 & 0 & \cdots & 0 & 0\\
0 & 0 & 0 & \cdots & 0 & 0 & 0 & \cdots & 0 & 0\\
0 & 0 & 0 & \cdots & 0 & 0 & 0 & \cdots & 0 & 0\\
\frac{1}{C_{ACDC}} & 0 & 0 & \cdots & 0 & 0 & 0 & \cdots & 0 & 0
\end{bmatrix}$$

Eq. 30

6.7. State-Space Model Results

To validate the model, the state-space model is simulated for K=4 for the same configuration took into account in the simulation done on the previous section. Both results are compared on Figure 71. This figure shows the voltage waveforms achieved from the state-space model (dashed lines) and the real model with SimPowerSystem (solid lines) after blocking AC-DC converter.

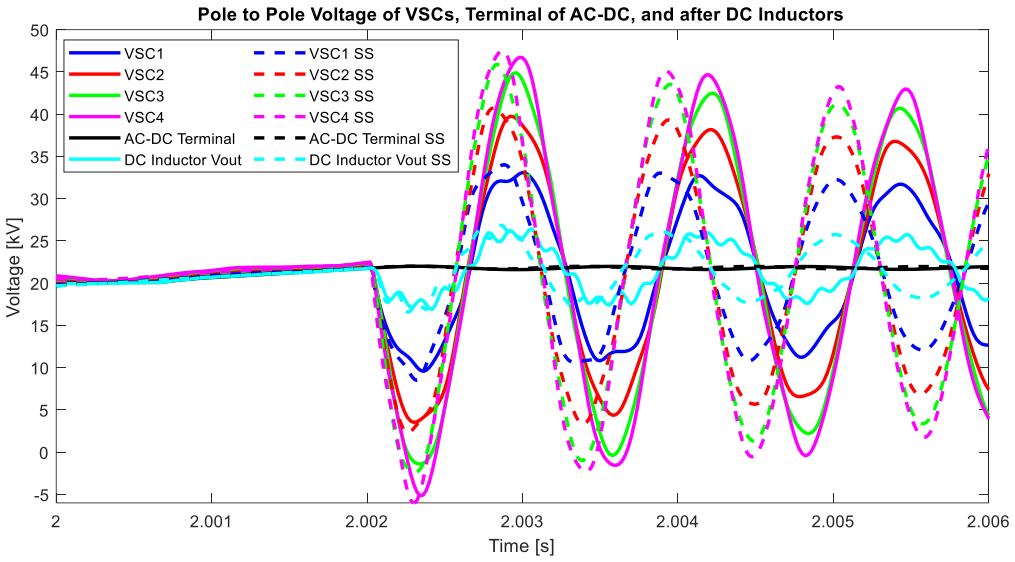

Figure 71 : The Comparison of Voltages Waveforms Achieved from State-Space and SimPowerSystem Models

The results show a high accuracy of state-space model for calculating the amount of over-voltage. The timing difference between waveforms is due to the different solving method of the two models. The SimPowerSystem model runs on discrete-time solving method while state-space model gives the result by continuous solver. A solution to improve this difference is to use the same (or close) solving method for both of the models. For example, if the time-step of the SimPowerSystem model decreases and becomes closer to continuous solving, this phase differences will be less.

With state-space modelling of the DC grid including AC-DC converter, we are able to simulate a network with any number of renewable energy sources and also the distances between RES stations can be chosen arbitrarily. For the study case, 40 RES stations were considered and its single line diagram was shown in Figure 60, the voltages waveforms of the VSCs after blocking AC-DC converter are shown in Figure 72 (Each color represents DC pole to pole voltage waveform in the output of a VSC connected to a RES station and also the DC pole to pole voltages in the output of DC inductors and on the terminal of AC-DC converter). This model verifies that after blocking AC-DC converter, the over-voltage on further VSC is (which is VSC 40) is the highest between all the VSCs and it is approximately 25 kV (1.25 p.u.).

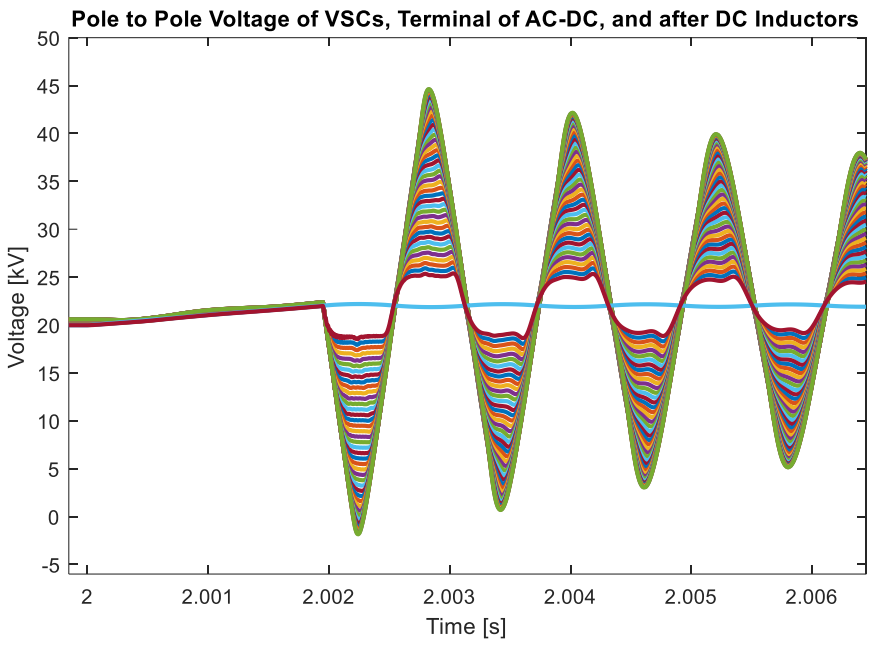

Figure 72 : The Voltages Waveforms of 40 VSCs after Blocking AC-DC Converter (Each Color: One VSC connected to a RES Station)

The amount of over-voltage was also analyzed for configuration of the network with different nominal voltages in the medium voltage range. For this analysis, two different assumptions were considered. In one analysis, the injected power be DC network was assumed constant ($P_{Total_{DC}} = 20\ MW$). In the other scenario, it was assumed that the current injected by DC network is constant for the networks with different DC pole to pole voltages ($I_{Total_{DC}} = 1\ kA$). The results are shown in Figure 73.

This figure shows that for higher line voltages, this problem is present but the over-voltage amount relative to the nominal DC pole to pole voltage (per unit) is significantly reduced and in some point, it is negligible while for the lower ranges of line voltage, the caused over-voltage is significant. Moreover, this analysis shows that when injected current is the same, the relative over-voltage (Per Unit) in higher voltages is a bit more than the scenario with same injected power by DC network. In this figure the maximum over-voltage which can be seen by the furthest VSC has been considered.

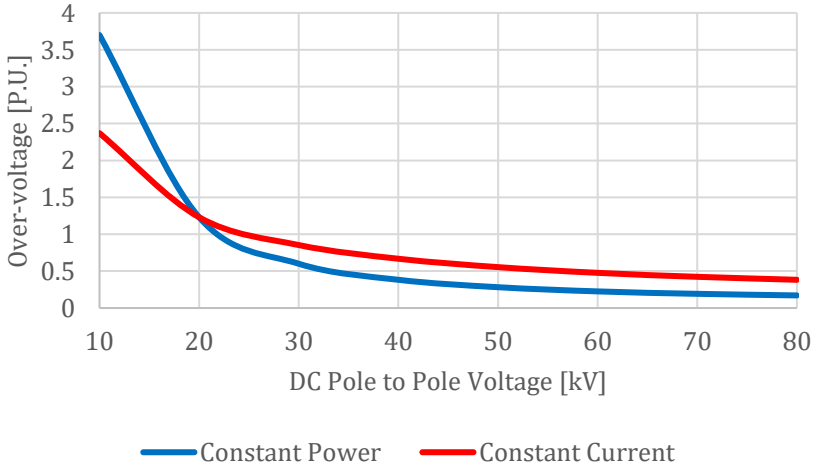

Figure 73 : The Effect of DC Pole to Pole Voltage on the Maximum Over-voltage in the Networks with Same Injected Power/Current by DC Network

6.8. Possible Solution

The (C_{VSC}) was assumed small in comparison to the DC link capacitor on the terminal of AC-DC converter (C_{ACDC}). This significant difference will impact on the energy exchange between these capacitors. During resonance, there is s transfer of energy between these capacitors. For the same amount of energy (charge or discharge), the variation of voltage is different for VSCs and AC-DC converter. The following equation shows the relationship between change of energy for a capacitor and change in its voltage:

$$\Delta E_{capacitor} = \frac{1}{2} C \Delta V_{capacitor}^2 \qquad \textit{Eq. 31}$$

In this equation, $\Delta E_{capacitor}$is the change in energy of a capacitor with capacitance of C depending the change on its voltage ($\Delta V_{capacitor}$). From this equation, it can be calculated that:

$$\Delta V_{capacitor} = \sqrt{\frac{2\Delta E_{capacitor}}{C}} \qquad \textit{Eq. 32}$$

Hence, for the same amount of energy exchange, a smaller capacitor has a higher voltage change. Therefore, the over-voltage amount on the output of VSCs connected to RES station is significantly higher than the AC-DC station terminal.

A solution to limit the transient over-voltage can be increasing the value of VSCs (connected to renewable sources) DC link capacitor to partially compensate the mentioned difference. The developed state-space model allows to apply this change in the capacitors value. Figure 74 shows the effect of increasing C_{VSC} on the over-voltage.

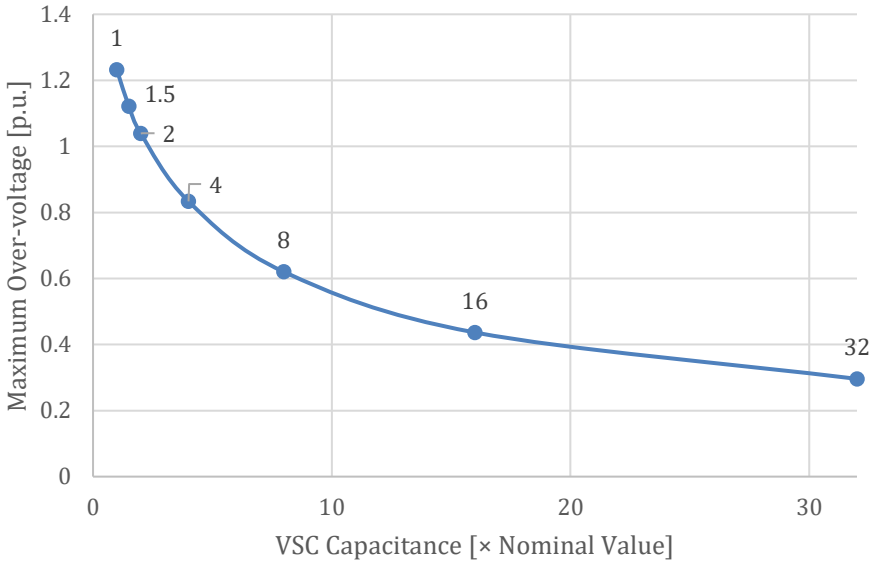

Figure 74 : The Effect of Increasing the Capacitance of DC Link Capacitor of VSCs Connected to Renewable Sources

It is visible that increasing the capacitance of DC link capacitor of the VSCs connected to RES stations, can reduce the over-voltage remarkably. However, this implies adding additional capacitors which will impact the VSC size and cost.

Chapter 7

Conclusions and Perspectives

The negative impacts of the increase in the temperature of the world have motivated all the sectors to move towards sustainability and energy transition. As a consequence, reduction of using fossil fuels and Increasing use of natural resources to generate electricity is essential. Hence, in the future, the consumption and generation of electricity is expected to be higher. Due to the limited capacity of existing Alternating Current (AC) networks, an extension in the capacity of the electrical networks is required. The advantages of DC transmission allow to increase the capacity of electrical networks and accelerate energy transition more efficiently and economically. In the high voltage ranges, HVDC networks have been implemented but in medium voltage ranges, it has been mostly handled by AC. With increase in the DC loads such as electric vehicles and interest in integrating renewable sources in MV level, MVDC networks could be an interesting choice.

To enable future MVDC systems, AC to DC conversion is needed to interface the AC and DC networks. In this work, a state-of-the-art review on the industrial MV AC-DC converters was done. With this review, the recommended topologies for different voltage and power ranges were proposed. Then, the trends related to MVDC networks in literature were studied. This showed the potential applications and interests related to MVDC in the researchers' insights.

DC faults on MV AC-DC converter were studied. To analyze this phenomenon, a study case of an MV converter with power rating of 20 MW and DC voltage of ±10 kV was considered. The chosen topology for AC-DC converter was a 3-L NPC. This was based on the results of state-of-the-art review. It was observed that is not significant research on DC faults on 3-L NPC topology, and thus this work can contribute to this area. First, the problem was analyzed theoretically and then it was verified using MATLAB SimPowerSystem. It was seen that s DC pole to pole fault is a serious problem for the converter diodes. So the effect of different parameters on DC faults was deeply analyzed. It was shown that for a DC fault on MV converter with 3-L NPC topology, the worst case is when DC inductor is very small and for each freewheeling diode depends on the fault moment. Moreover, the comparison of DC fault on 3-L NPC and 2-L converters showed that the constraints are similar in terms or the sizing of diodes. However, some works are still needed to be done to analyze the behavior of clamping diodes in order to properly size them against faults.

In the final chapter, transient overvoltages in MVDC networks was analyzed. It was dound out thatThis transient happens as a consequence of blocking AC-DC converters in an MVDC network with integrated renewable energy sources. This phenomenon is an over-voltage that happens as a consequence of blocking AC-DC converters in an MVDC network with integrated renewable energy sources. It was noticed that this problem also exists in HV levels but in medium voltage ranges, it is relatively higher. A state-space model was proposed to analyze this problem in the networks with any number of renewable energy sources with less computational effort. It was identified that this phenomenon happens mainly due to smaller capacitance of distributed VSCs around the line comparing with the main capacitor of AC-DC converter. Finally, this fact was a motivation to increase the capacitance of these VSCs and reduce the over-voltage. Hence, over-sizing some elements is needed so a deeper research seems essential.

This work identified many perspectives related to the MVDC networks. In this work, only DC fault and over-voltage were focused. With developing higher number of MVDC projects, there may be some other issues which need to be studied. Moreover, there may be an interest for MMC topology. This implies studiyng likely issues related to this converter in medium voltage level. Basically, it

needs a more in-depth analysis to find the recommended topologies in the MV level. For example, in the higher voltages of MV level (20 kV – 80 kV), it is needed to identify the preferred topologies. Additionally, with the development of switches in higher voltage/power ratings, the potentials of applying 3-L NPC in higher DC voltages should be analyzed. It is also an interesting perspective to design 3-L NPC converters with swithces using Wide Band-Gap (WBG) semiconductors such as Silicon Carbide (SiC). Moreover, the importance of DC networks in distribution level was analyzed. Hence, an intersting perspective is development of DC-DC converters for interfacing HVDC, MVDC, and LVDC networks in the future.

Chapter 8

Appendices

8.1. Possible Solutions for Converter Protection from DC Faults

It was explained in Section 3.3 that MV converters have been mostly used in some equipment which include AC to DC conversion such as AC drives. The probability of occurring a DC fault inside an AC drive is very low. Hence, a comprehensive research on the protection of MV converter from DC faults has not been done yet. In following, the potential solutions for MV converter protection from DC faults are explained. First solution is a solution which can be concluded from previous analysis. Considering converters in HVDC applications, the protection solutions used in the converters in these voltage levels could be helpful for MV converters protection as well. Thus, the other solutions are proposed based on the protection schemes in HV converters.

8.1.1. Over-dimensioning Converter Diodes

In the previous sections, it was pointed out that the main problem of DC faults is the risk of damaging converter diodes. It was noticed that due to the limited value of diodes I^2t, in a short time (in the retained study case, 9.1 ms) after fault, this parameter will be exceeded. Hence, there are two solutions:

- If the diodes with higher I^2t are used, this problem might be solved depending on the fault duration. This can be done by installing diodes with higher capability of withstanding fault current (higher I^2t). The availability of such a diode is a limiting constraint. Moreover, after fault, I^2t of the diode increases to a very high amount in a very short time. So, installing diodes with higher I^2t only makes the time of damage a little longer (a few milliseconds). For a very short faults (milliseconds), this solution might be useful.
- The other solution is installing some diodes in parallel to share fault current and thermal constraints. This solution is shown in Figure 75. With this solution, the I^2t of one diode in the previous case, will be shared between all the diodes and the time to exceed the maximum allowed I^2t increases. A constraint to apply this solution is increase in size and costs of the converter. Moreover, comparing to previous solution, this solution is suitable for longer duration faults. But still after a critical time, if fault remains, diodes will be damaged.

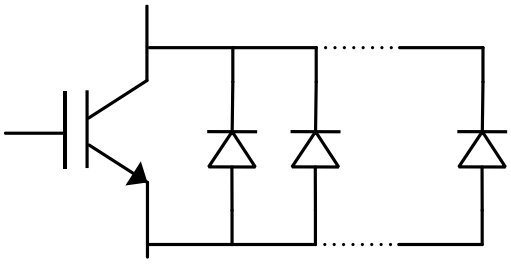

Figure 75 : Installing some Diodes in Parallel to Share Fault Current

8.1.2. Full-Bridge Sub-modules (Specialized for MV Converters with MMC topology)

In Section 3.3.1 was mentioned that in the higher voltages of medium voltage range (20 kV – 80 kV), MMC can be a promising topology. Moreover, it was explained in Section 3.2.4 that due to the advantages of MMC, this topology is preferred in HVDC applications. Hence, the DC fault protection solutions for MMC topology could be potential solutions for MV converters. To protect MMC converter from DC faults, using full-bridge sub-modules is a prominent solution however it increases cost and size of converter significantly [37] [72]. A full-bridge sub-module is shown in Figure 15.

8.1.3. Protective Thyristor Switch

Using full-bridge sub-modules implies increase in size and cost. To protect MMC converter with half-bridge sub-modules, a protective thyristor switch can be installed on each sub-module [73][74][75]. This protection scheme is shown in Figure 76.

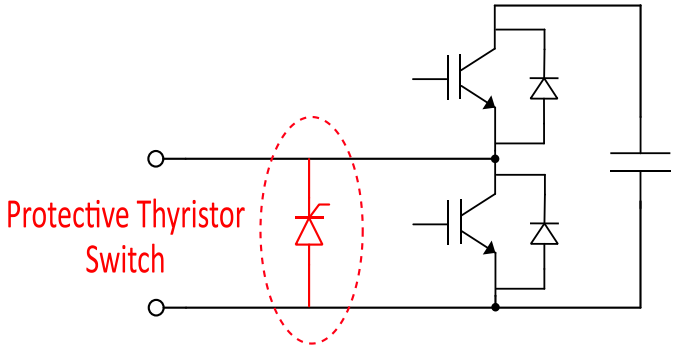

Figure 76 : Protective Thyristor Switch for Half-Bridge MMC Converter Protection from DC Faults

In the normal condition, thyristor switch is off while in the fault condition, it will be triggered and fault current will be passed through it. So, no current passes through freewheeling diodes and they will remain undamaged. This solution can be used for the medium voltage MMC converters with half-bridge sub-modules. It also can be useful for protecting 3-L NPC converter but this is a perspective. Hence, implementing this protection solution in 3-L NPC converter should be analyzed deeply in the future.

Bibliography

[1] International Energy Agency (IEA), “World energy outlook 2018,” Tech. Rep., IEA, 2018; www.iea.org/weo2018.

[2] REN21, “Renewables 2019 Global Status Report,” REN21 Secretariat,, Paris, June 2019. [Online]. Available: http://www.ren21.net/gsr-2019/

[3] UCSUA, “Benefits of renewable energy use,” [Online]. Available https://www.ucsusa.org/resources/benefits-renewable-energy-use

[4] Power-technology, “The world’s most used renewable power sources,” [Online]. Available https://www.power-technology.com/features/featurethe-worlds-most-used-renewable-power-sources-4160168/

[5] Lazard, “Levelized cost of energy 2018,” [Online]. Available https://www.lazard.com/perspective/levelized-cost-of-energy-andlevelized-cost-of-storage-2018/

[6] EIA (U.S. Energy Information Administration), “Renewable energy incentives,” [Online]. Available https://www.eia.gov/energyexplained/renewable-sources/incentives.php

[7] EPA (U.S. Environmental Protection Agency), “Local Renewable Energy Benefits and Resources,” [Online]. Avalable https://www.epa.gov/statelocalenergy/local-renewable-energy-benefits-and-resources

[8] Forbes, “Five Market Trends Drivign Energy Transition,” [Online]. Available https://www.forbes.com/sites/feliciajackson/2021/01/25/five-market-trends-driving-energy-transition/?sh=5a5ac4dd5077

[9] H. Holttinen et al., "System impact studies for near 100% renewable energy systems dominated by inverter based variable generation," in IEEE Transactions on Power Systems, doi: 10.1109/TPWRS.2020.3034924.

[10] Our World, “The Future is Electric,” [Online]. Available https://ourworld.unu.edu/en/the-future-is-electric

[11] GlobeNewswire, “Electric Vehicle Market to Register Growth 40.7% by 2027,” [Online]. Available https://www.globenewswire.com/news-release/2021/01/09/2155831/0/en/Electric-Vehicle-Market-to-Register-Growth-40-7-by-2027.html

[12] Scherba, A., et al., Modeling impacts of roof reflectivity, integrated photovoltaic panels and green roof systems on sensible heat flux into the urban environment. Building and Environment, 2011. 46(12): p. 2542-2551.

[13] NS Energy, “Why global investments in renewable energy capacity increased in 2019,” [Online]. Available https://www.nsenergybusiness.com/features/renewable-energy-investment/

[14] X. Chen, J. Lv, M. B. McElroy, X. Han, C. P. Nielsen and J. Wen, "Power System Capacity Expansion Under Higher Penetration of Renewables Considering Flexibility Constraints

and Low Carbon Policies," in IEEE Transactions on Power Systems, vol. 33, no. 6, pp. 6240-6253, Nov. 2018, doi: 10.1109/TPWRS.2018.2827003.

[15] Stokman, H. (n.d.). OUR VISION: THE SECOND GRID. Retrieved March 11, 2021, from https://www.dc.systems/vision/the-second-grid

[16] H. Krishnamoorthy, M. Daniel, J. Ramos-Ruiz, P. Enjeti, L. Liu and E. Aeloiza, "Isolated AC–DC Converter Using Medium Frequency Transformer for Off-Shore Wind Turbine DC Collection Grid," in IEEE Transactions on Industrial Electronics, vol. 64, no. 11, pp. 8939-8947, Nov. 2017, doi: 10.1109/TIE.2017.2652405.

[17] H. M. M. Maruf, B. Mitra, P. K. Sahu, M. Manjrekar and B. H. Chowdhury, "Hybrid High Voltage AC/DC system for interfacing off-shore power generations with on-shore grid," SoutheastCon 2016, Norfolk, VA, USA, 2016, pp. 1-2, doi: 10.1109/SECON.2016.7506707.

[18] M. Abbasi and J. Lam, "A new three-phase soft-switched bridgeless AC/DC step-up converter with current fed voltage doubler modules for DC grid in wind systems," 2018 IEEE Applied Power Electronics Conference and Exposition (APEC), San Antonio, TX, USA, 2018, pp. 44-51, doi: 10.1109/APEC.2018.8340987.

[19] S. S. Gjerde, P. K. Olsen and T. M. Undeland, "A transformerless generator-converter concept making feasible a 100 kV low weight offshore wind turbine Part II - The converter," 2012 IEEE Energy Conversion Congress and Exposition (ECCE), Raleigh, NC, USA, 2012, pp. 253-260, doi: 10.1109/ECCE.2012.6342815.

[20] T. V. Vu, D. Gonsoulin, D. Perkins, B. Papari, H. Vahedi and C. S. Edrington, "Distributed control implementation for zonal MVDC ship power systems," 2017 IEEE Electric Ship Technologies Symposium (ESTS), Arlington, VA, USA, 2017, pp. 539-543, doi: 10.1109/ESTS.2017.8069334.

[21] E. Kimbark, Direct Current Transmission. New York: Wiley Interscience, 1971

[22] L. de Andrade and T. P. de Leão, "A brief history of direct current in electrical power systems," 2012 Third IEEE HISTory of ELectro-technology CONference (HISTELCON), Pavia, Italy, 2012, pp. 1-6, doi: 10.1109/HISTELCON.2012.6487566.

[23] ENERGY.GOV, “The War of the Currents: AC vs. DC Power,” [Online]. Available https://www.energy.gov/articles/war-currents-ac-vs-dc-power

[24] ALL ABOUT CIRCUITS, “What Is the Skin Effect?,” [Online]. Available https://www.allaboutcircuits.com/textbook/alternating-current/chpt-3/more-on-the-skin-effect/

[25] ELECTRICAL TALKS, “What is Skin Effect? How to reduce and minimize it? Its Pros and Cons?,” [Online]. Available https://electricaltalks.com/what-is-skin-effect-how-to-reduce-and-minimize-its-pros-and-cons/

[26] CIRCUIT GLOBE, “Proximity Effect,” [Online]. Available https://circuitglobe.com/proximity-effect.html

[27] M. H. Okba, M. H. Saied, M. Z. Mostafa and T. M. Abdel- Moneim, "High voltage direct current transmission - A review, part I," 2012 IEEE Energytech, Cleveland, OH, USA, 2012, pp. 1-7, doi: 10.1109/EnergyTech.2012.6304650.

[28] Pérez-Molina, María José, D. Marene Larruskain, Pablo Eguía López, and Garikoitz Buigues. "Challenges for protection of future HVDC grids." Frontiers in Energy Research 8 (2020): 33.

[29] M. P. Bahrman, "OVERVIEW OF HVDC TRANSMISSION", IEEEIPES T&D, Power Systems Conference and Exposition, PSCE '06, 2006.DOI: 10.1109/PSCE.2006.296221.

[30] CARBON TRUST, “Investigation into DC arraysas a means of connecting offshore wind farms,” [Online]. Available https://www.carbontrust.com/resources/investigation-into-dc-arrays-as-a-means-of-connecting-offshore-wind-farms.

[31] Electrical Easy, “HVDC Vs. HVAC Transmission,” [Online]. Available https://www.electricaleasy.com/2016/02/hvdc-vs-hvac.html

[32] 1. P Bowles, V. Burtnyk, C. C. Diemond, M. A. Lebow, E. G. Neudrof, D. Povh, E. C. Starr, C. W. Taylor, and R. A. Walling, edited by C. T. WU "AC-DC economics and alternatives- 1987 panel session report," IEEE trans. on power delivery, vol. 5, pp. 1241-1248, Nov. 1990.

[33] Zavattoni, L. (2014). Conduction phenomena through gas and insulating solids in HVDC Gas Insulated Substations, and consequences on electric field distribution. Villeurbanne: Universit´ede Grenoble.

[34] Juan Paez Alvarez. DC-DC converter for the interconnection of HVDC networks. Electric power. Université Grenoble Alpes, 2019. English. ffNNT : 2019GREAT075ff. fftel-03132552

[35] W. Leterme, P. Tielens, S. De Boeck and D. Van Hertem, "Overview of Grounding and Configuration Options for Meshed HVDC Networks," in IEEE Transactions on Power Delivery, vol. 29, no. 6, pp. 2467-2475, Dec. 2014, doi: 10.1109/TPWRD.2014.2331106.

[36] P. Le Métayer, J. Paez, P. Dworakowski, S. Touré, C. Buttay, D. Dujic, E. Lamard, “Break-even distance for MVDC electricity networks according to power loss criteria”, accepted for publication at EPE 2021

[37] Jovcic, D. , “High Voltage Direct Current Transmission, Converters, Systems, and DC Networks”, 2nd Edition, John Wiley & Sons, 2015

[38] Dworakowski, Piotr, (2020), “Modelling and analysis of medium frequency transformers for power converters,” 1-120.

[39] A. Nabae, I. Takahashi, and H. Akagi, “A New Neutral-Point-Clamped PWM Inverter,” IEEE Transactions on Industry Applications, vol. IA-17, no. 5, pp. 518–523, Sep. 1981

[40] A. Marzoughi, R. Burgos, D. Boroyevich and Y. Xue, "Design and comparison of cascaded H-bridge, modular multilevel converter and 5-L active neutral point clamped topologies for drive application," 2015 IEEE Energy Conversion Congress and Exposition (ECCE), Montreal, QC, Canada, 2015, pp. 4033-4039, doi: 10.1109/ECCE.2015.7310229.

[41] Bonilla, Carlos Castillo, and Sweta Merilyn Tigga. "Design and performance comparison of Two-level and Multilevel Converters for HVDC Applications." (2011).

[42] J. Rodriguez, Jih-Sheng Lai and Fang Zheng Peng, "Multilevel inverters: a survey of topologies, controls, and applications," in IEEE Transactions on Industrial Electronics, vol. 49, no. 4, pp. 724-738, Aug. 2002, doi: 10.1109/TIE.2002.801052.

[43] V. Dargahi et al., "Fundamental Circuit Topology of Duo-Active-Neutral-Point-Clamped, Duo-Neutral-Point-Clamped, and Duo-Neutral-Point-Piloted Multilevel Converters," in IEEE Journal of Emerging and Selected Topics in Power Electronics, vol. 7, no. 2, pp. 1224-1242, June 2019, doi: 10.1109/JESTPE.2018.2859313.

[44] T. A. Meynard and H. Foch, “Multi-level choppers for high voltage applications,” EPE J., vol. 2, no. 1, pp. 45–50, 1992.

[45] T. Bruckner and S. Bernet, “Loss balancing in three-level voltage source inverters applying active NPC switches,” in Proc. IEEE 32nd Annu. Power Electron. Spec. Conf., vol. 2, Jun. 2001, pp. 1135–1140.

[46] ABB, “PCS 8000 variable-speed converter,” [Online]. Available https://new.abb.com/power-converters-inverters/energy-storage-grid-stabilization/converters-for-pumped-storage-plants/pcs-8000-variable-speed-converter

[47] ABB Medium Voltage Drive ACS2000, https://new.abb.com/drives/medium-voltage-ac-drives/acs2000

[48] A. Lesnicar and R. Marquardt, “An innovative modular multilevel converter topology suitable for a wide power range,” in 2003 IEEE Bologna Power Tech Conference Proceedings, 2003, vol. 3, pp. 6 pp. Vol.3-.

[49] Wang, Yang, Ahmet Aksoz, Thomas Geury, Salih Baris Ozturk, Omer Cihan Kivanc, and Omar Hegazy. "A Review of Modular Multilevel Converters for Stationary Applications." Applied Sciences 10, no. 21 (2020): 7719.

[50] P. S. Jones and C. C. Davidson, "Calculation of power losses for MMC-based VSC HVDC stations," 2013 15th European Conference on Power Electronics and Applications (EPE), Lille, France, 2013, pp. 1-10, doi: 10.1109/EPE.2013.6631955.

[51] CIGRE WG C6.31, ‘Medium voltage direct current (MVDC) grid feasibility study’, e-cigre, 27-Feb-2020. [Online]. Available: https://e-cigre.org/publication/793-medium-voltage-direct-current-mvdc-gridfeasibility-study.

[52] F. Mura and R. W. De Doncker, "Design aspects of a medium-voltage direct current (MVDC) grid for a university campus," 8th International Conference on Power Electronics - ECCE Asia, Jeju, Korea (South), 2011, pp. 2359-2366, doi: 10.1109/ICPE.2011.5944508.

[53] J. Yu, K. Smith, M. Urizarbarrena, N. MacLeod, R. Bryans and A. Moon, "Initial designs for the ANGLE DC project; converting existing AC cable and overhead line into DC operation," 13th IET International Conference on AC and DC Power Transmission (ACDC 2017), Manchester, UK, 2017, pp. 1-6, doi: 10.1049/cp.2017.0002.

[54] G. Abeynayake, G. Li, T. Joseph, J. Liang and W. Ming, "Reliability and Cost-oriented Analysis, Comparison and Selection of Multi-level MVdc Converters," in IEEE Transactions on Power Delivery, doi: 10.1109/TPWRD.2021.3051531.

[55] B. Singh, R. Saha, A. Chandra and K. Al-Haddad, "Static synchronous compensators (STATCOM): a review," in IET Power Electronics, vol. 2, no. 4, pp. 297-324, July 2009.

[56] General Electric, “MV7000 Converter Press Pack (PP),” [Online]. Available https://www.gepowerconversion.com/sites/default/files/GEA30737C%20MV7000%20Press%20Pack.pdf

[57] TMEIC, “Variable Frequency Drives – a Comparison of VSI versus LCI Systems,” [Online]. Abailable

tmeic.com/Repository/Media/Comparison%20of%20VSI%20versus%20LCI%20Systems%20FINAL.pdf

[58] Siemens, “SNAMICS PERFECT HARMONY GH150,” [Online]. Available https://assets.new.siemens.com/siemens/assets/public.1564669468.18aa6fa6-7bfa-450a-8328-2cfe787e8844.gh150acbrochurejune2019.pdf

[59] ABB, “IGCT Technology – A Quantom Leap for High-power Converters,” [Online]. Available https://library.e.abb.com/public/d627aeaa2f9f8b24c1256f4100480fa0/PT_IGCT.pdf

[60] Ibrahim, Zulkifilie & Hossain, M.L. & Bugis, Ismadi & Mahadi, Nik & Abu hasim, Ahmad shukri. (2014). Simulation investigation of SPWM, THIPWM and SVPWM techniques for three phase voltage source inverter. International Journal of Power Electronics and Drive Systems. 4. 10.11591/ijpeds.v4i2.5833.

[61] ABB HiPak 6.5 kV 750 A IGBT 5SNA 0750G650300, Datasheet: http://search.abb.com/library/Download.aspx?DocumentID=5SYA%201600-03&LanguageCode=en&DocumentPartId=&Action=Launch

[62] Infinoen 6.5 kV, 750 A IGBT FZ750R65KE3, Datasheet: https://www.infineon.com/dgdl/Infineon-FZ750R65KE3-DataSheet-v03_04-EN.pdf?fileId=db3a304325afd6e00126461fd3936974

[63] K. Sasagawa, Y. Abe and K. Matsuse, "Voltage-balancing method for IGBTs connected in series," in IEEE Transactions on Industry Applications, vol. 40, no. 4, pp. 1025-1030, July-Aug. 2004, doi: 10.1109/TIA.2004.830794.

[64] Institue of Electrical and Electronics Engineers (IEEE), Available https://ieeexplore.ieee.org/Xplore/home.jsp

[65] Judge, P.D., Chaffey, G., Wang, M., Zerihun Dejene, F., Beerten, J., Green, T.C., Van Hertem, D. and Leterme, W. (2019), “Power-system level classification of voltage-source HVDC converter stations based upon DC fault handling capabilities,” IET Renewable Power Generation, 13: 2899-2912. https://doi.org/10.1049/iet-rpg.2019.0462

[66] M. A. Abdel-Moamen, S. A. Shaaban and F. Jurado, "France-Spain HVDC transmission system with hybrid modular multilevel converter and alternate-arm converter," 2017 Innovations in Power and Advanced Computing Technologies (i-PACT), Vellore, India, 2017, pp. 1-6, doi: 10.1109/IPACT.2017.8245001.

[67] Xu, Zheng, et al. "DC fault analysis and clearance solutions of MMC-HVDC systems." *Energies* 11.4 (2018): 941.

[68] Xu, Zheng; Xiao, Huangqing; Xiao, Liang; Zhang, Zheren. 2018. "DC Fault Analysis and Clearance Solutions of MMC-HVDC Systems" Energies 11, no. 4: 941. https://doi.org/10.3390/en11040941

[69] Hadeed Ahmed Sher, Khaled E. Addoweesh, Yasin Khan, Effect of short circuited DC link capacitor of an AC–DC–AC inverter on the performance of induction motor, Journal of King Saud University - Engineering Sciences, Volume 28, Issue 2, 2016, Pages 199-206, ISSN 1018-3639, https://doi.org/10.1016/j.jksues.2014.03.003.

[70] Gao, Yuqun; Han, Yongxia; Zhang, Jinghan; Xiao, Fanglei; Zhao, Yuming; Li, Licheng. 2019. "Study on Fault Current Characteristics and Current Limiting Method of Plug-In Devices in VSC-DC Distribution System" Energies 12, no. 16: 3159. https://doi.org/10.3390/en12163159

[71] Khelif, Amine & Azeddine, Bendiabdellah & Eddine, Cherif. (2020). Short-circuit fault diagnosis of the DC-Link capacitor and its impact on an electrical drive system.

International Journal of Electrical and Computer Engineering (IJECE). 10. 2807-2814. 10.11591/ijece.v10i3.pp2807-2814.

[72] Falahi, Ghazal. "Design, Modeling and Control of Modular Multilevel Converter based HVDC Systems." (2014).

[73] Sharifabadi, K., Harnefors, L., Nee, H. P., Norrga, S., & Teodorescu, R., "Design, control, and application of modular multilevel converters for HVDC transmission systems," John Wiley & Sons, pp 318-335, 2016.

[74] B. Gemmell, J. Dorn, D. Retzmann and D. Soerangr, "Prospects of multilevel VSC technologies for power transmission," 2008 IEEE/PES Transmission and Distribution Conference and Exposition, Chicago, IL, USA, 2008, pp. 1-16, doi: 10.1109/TDC.2008.4517192.

[75] Andersson, Mats, Rong Cai, and Hailian Xie. "Novel solutions for LCC-HVDC fault ride through," In Proceedings of International High Voltage Direct Current Conference, pp. 32-36. 2016.

[76] S. Aatif, X. Yang, H. Hu, S. K. Maharjan and Z. He, "Integration of PV and Battery Storage for Catenary Voltage Regulation and Stray Current Mitigation in MVDC Railways," in Journal of Modern Power Systems and Clean Energy, doi: 10.35833/MPCE.2019.000155.

[77] T. V. Vu, D. Gonsoulin, D. Perkins, F. Diaz, H. Vahedi and C. S. Edrington, "Predictive energy management for MVDC all-electric ships," 2017 IEEE Electric Ship Technologies Symposium (ESTS), Arlington, VA, USA, 2017, pp. 327-331, doi: 10.1109/ESTS.2017.8069302.